

**Reply to review report of
Evaluating critical rainfall conditions for large-scale landslides by
detecting event times from seismic records**

Hsien-Li Kuo, Guan-Wei Lin*, Chi-Wen Chen, Hitoshi Saito, Ching-Weei Lin,
Hongey Chen, Wei-An Chao

* Correspondence should be addressed to Guan-Wei Lin; gwlin@mail.ncku.edu.tw

This file includes three sections:

1. Reply to the comments of editor
2. Reply to the comments of reviewer #1
3. Reply to the comments of reviewer #2

1. Reply to the comments of editor

We have now received two reviews and two very detailed answers by the authors, along with some modified sections of the manuscript + some possible Annexes. All these support the improvement of the manuscript. We encourage the authors to submit their final revised version of the manuscript assuming also:

- a careful technical review of the grammar (some mix of passive/active voices are used - please homogenize) and figures (some typos errors in some of them) for instance Guezzeti instead of Guzzetti on figure 6, and so on)

- a more in depth discussion on the generosity of the approach used for establishing the EW thresholds in other cases ...

R: The authors deeply appreciate the editor's reviewing and providing valuable suggestions to improve the manuscript. The authors have improved the English writing of the manuscript through a language editing service to make sure that the article is free of grammatical, spelling, and other common errors.

The authors have made a more in-depth discussion on the application of rainfall threshold to Typhoon Soudelor of 2015. All thresholds proposed in the study have been tested in the case study. The illustration has been made in the section 5.1 as follows:

“To verify the usability of the rainfall thresholds proposed in this study, Typhoon Soudelor of 2015 was chosen to demonstrate the early warning performance. Typhoon Soudelor was one of the most powerful storms on record. It generated 1400 mm of rainfall in northeastern Taiwan and almost 1000 mm of rainfall in the southern mountainous area of Taiwan (Wei, 2017; Su et al., 2016). After the seismic signal analytical procedure, the occurrence time, 2015/8/8 18:59:50 (UTC), of a large landslide (named the Putanpunas Landslide) located in southern Taiwan was obtained (Fig. 7). The seismic signal generated by the Putanpunas Landslide was also detected by Chao et al. (2017). The seismic signals generated by this large landslide could be identified from six BATS stations, and the distance error was less than 6 km. The rainfall records of rain gauge station C1V190, which was situated in the same watershed and 14.6 km away from the large landslide, were collected for rainfall analysis. Typhoon Soudelor made landfall in Taiwan on August 7, 2015, and dropped a cumulated rainfall of 546 mm and had a maximum rainfall intensity of 39 mm/h on August 8 at rain gauge station C1V190 (Fig. 8). The rainfall event began at 22:00 August 7 and last for 26 hours, and the Putanpunas Landslide initiated at the 22nd hour. This landslide occurred when the rainfall intensity was on the decline.

Regarding landslide early warning using rainfall thresholds, once the rainfall conditions at a given rainfall station exceed the rainfall thresholds for triggering landslides, the slopes located within the region of the rainfall station will have high potential for failure. Based on the statistically-based $I-D$ threshold for small landslides, a small-landslide warning would have been issued at the sixth hour of the rainfall event (Fig. 8). The long interval of sixteen hours between the warning and the occurrence time of the Putanpunas Landslide could have reduced the reliability of the warning or even caused the warning to be considered a false alarm. Therefore, it is essential to establish different thresholds for landslides of different scales. Using the $I-Rt$ threshold (i.e., $Rt \cdot I = 5,640$), a large-landslide warning would have been issued at the ninth hour of the rainfall event (i.e., thirteen hours before the Putanpunas Landslide occurred). According to the statistically-based $I-D$ threshold for large landslides, a landslide warning would have been issued at the same hour as the $I-Rt$ threshold. In addition, a warning based on the $Rt-D$ threshold (i.e., $Rt \cdot D = 12,773$) would have been issued three hours after the occurrence time of the Putanpunas Landslide. According to the rainfall records and the critical height of water model (i.e. $(I-1.5) \cdot D = 430.2$), a landslide warning would have been issued at 16:00 on August 8, three hours before the occurrence time of the Putanpunas Landslide. Compared to the statistically-based $I-D$ threshold, the $I-Rt$ threshold, and the $Rt-D$ threshold, the critical height of water model had a better early-warning performance for the 2015 Putanpunas Landslide.”

2. Reply to the comments of reviewer #1

Kuo et al., present a landslide catalogue in Taiwan, obtained by remote sensing, from which they extract 62 large landslides that can be accurately timed thanks to seismic detection, and compared to local rainfall gaging data. Then they assess which type of rainfall threshold could be derived for this dataset, including a threshold guided by physical considerations, and compare it to a dataset of smaller landslides in Taiwan. The paper ends with a rather unconvincing or unclear discussion on potential variability of the thresholds and on issues with seismic detection.

Overall, the authors present an interesting, novel dataset (although relatively modest) and do a series of classic (rainfall threshold) and less classic (physically based threshold) analysis that can be worth publishing, but the discussion and some of the analysis need to be improved before that.

R: The authors very much appreciate the reviewer's valuable time, comments and suggestions.

(1) Major comment

1. Timing is an issue but rainfall estimation as well. Notably because rain gage may be far from the landslides and not experiencing similar rainfall especially due to orographic effects. The author explain they only associate landslide with rainfall measured within 100km². I think this is a good start but in the analysis it would be good to indicate (by a color coding?) the horizontal distance from the landslide, as well as to discuss difference in elevation between station and landslide median elevation for example. This would allow the authors to discuss uncertainty and the degree of reliability of rainfall estimates for the landslides.

R: The authors appreciate the reviewer's constructive suggestion. The spatial information (distance and elevation) of each used rain gauge station has been added to supplementary materials as Table S2.

The effect of rain gauge distribution over the accuracy of rainfall has been assessed using gauge observation in a 35 km × 50 km region of south Taiwan (Fig. S2). The amounts of daily rainfall during 2009 Typhoon Morakot (8/6-8/11) recorded at 19 rain gauge stations were selected to validate the accuracy of rainfall. At first, the amounts of daily rainfall were interpolated to 01V040 station using IDW methods. The errors between measurements and interpolated data were smaller than 15 %. It indicates IDW method can be used to interpolate rainfall to a selected location in our study area.

Secondly, the amounts of daily rainfall at the central point of the 35 km × 50 km region were estimated. The errors of daily rainfall between the central point and the nearest rain gauge station (01V040) were smaller than 10 % (0.5%-10% at different date).

Besides, the correlation coefficients would keep at 90% as a distance between the central point and rain gauge stations less than 20 km, and even keep at 98% as a distance less than 10 km (Fig. S3). Therefore, in the study, an upper limit of basin area smaller than 100 km² (10 km × 10 km was adopted to avoid a significant decrease of the accuracy of rainfall.

The influence of topography on rainfall variability has been analyzed in the same 35 km × 50 km region of south Taiwan. The highest station elevation is 1792 m a.s.l. at C1V270, and the lowest station elevation is 105 m a.s.l. at C10830. The standard deviation of station elevation is 561 m. The values of standard deviation of daily rainfall at the 19 stations were calculated, and less than 13% except a high standard deviation, 45%, on August 6 (average daily rainfall less than 2 mm). The results demonstrated that high and even extreme rainfall are less influenced by elevation, while low and medium rainfall events are significantly influenced by elevation variation, with most of the rainfall appearing on high elevations. Similar results have also been reported by some previous studies (Sanchez-Moreno et al., 2014; Ge et al., 2017). Because the study only considered the rainfall events with total cumulated rainfall greater than 500 m, the elevation effect was ignored as selecting rain station. The above illustration has been attached to the supplementary material S3.

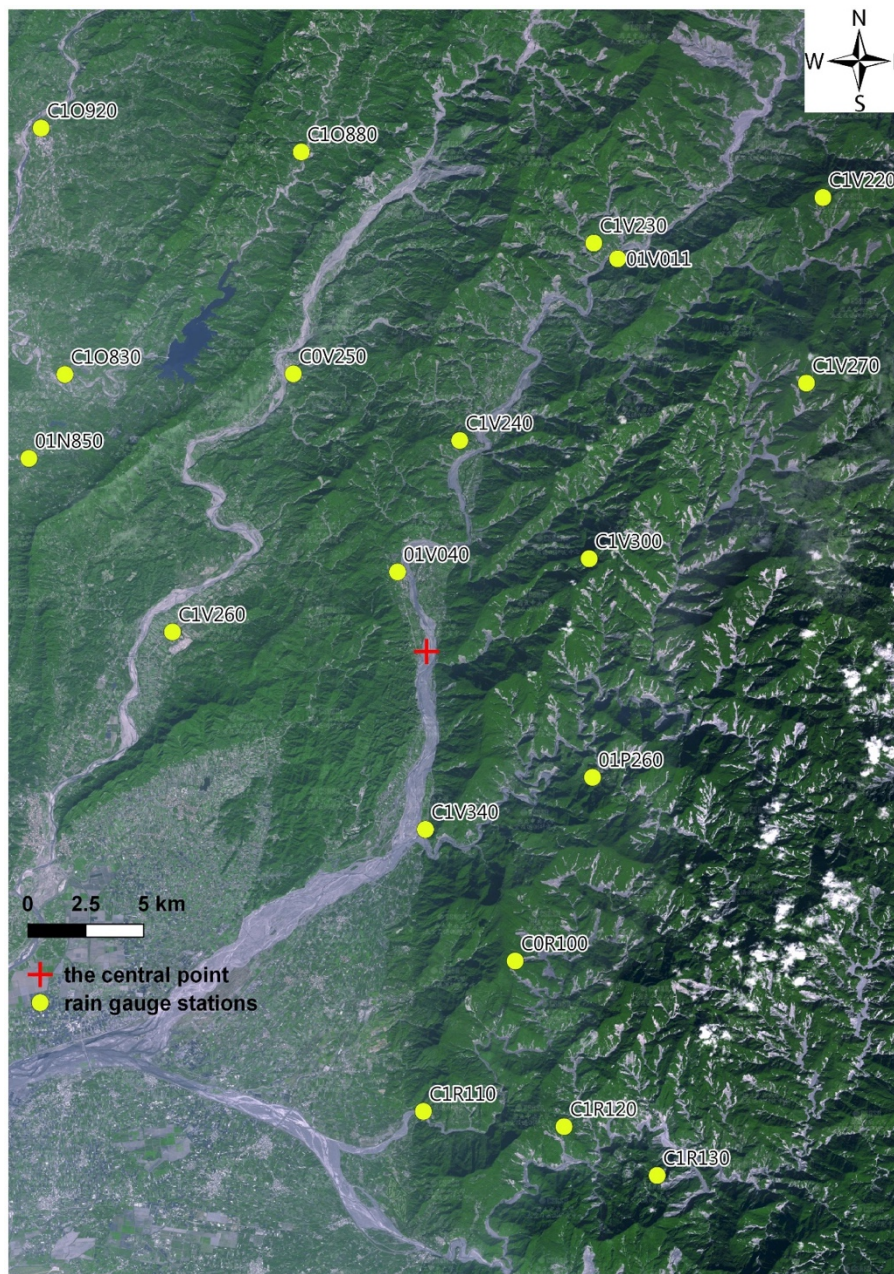


Fig. S2

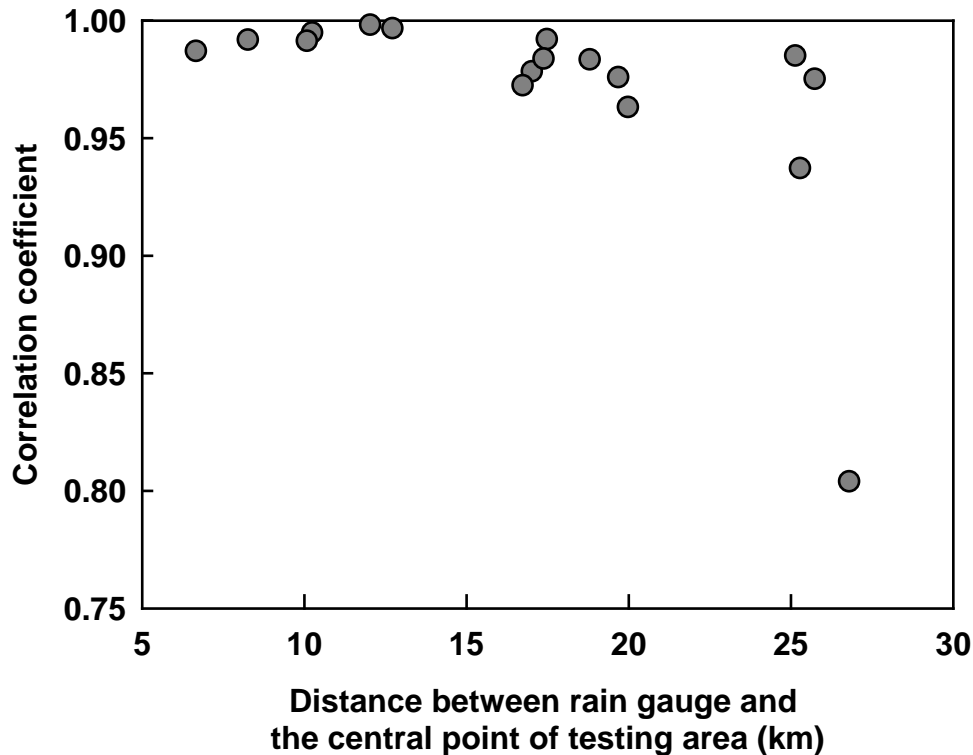


Fig. S3

Reference

- Mishra, A.K. (2013) Effect of rain gauge density over the accuracy of rainfall: a case study over Bangalore, India. SpringerPlus, 2, 311.
- Sanchez-Moreno, J.F., Mannaerts, C.M., and Jetten, V. (2014) Influence of topography on rainfall variability in Santiago Island, Cape Verde. International Journal of Climatology, 34, 1081-1097.
- Ge, G., Shi, Z., Yang, X., Hao, Y., Guo, H., Kossi, F., Xin, Z., Wei, W., Zhang, Z., Zhang, X., Liu, Y., and Liu, J. (2017) Analysis of Precipitation Extremes in the Qinghai-Tibetan Plateau, China: Spatio-Temporal Characteristics and Topography Effects. Atmosphere, 8(7), 127, doi:10.3390/atmos8070127.

2. I think the attempt of the authors to define a threshold based on physical considerations is worth, but insufficient in the present form: the assumption and limit of the model lack validation/discussion, and the practical utility/validity of the model compared to pure empirical ones is poorly demonstrated. I give detailed proposition to test and refine the model, but in any case a more quantitative comparison of the validity of the different threshold seems important if the author want to underline the physical model has a path forward. I think also this part may benefit from being put in perspective compared to other work on physically based threshold. For example:

Salciarini and Tamagni 2013, Physically based rainfall thresholds for shallow landslide initiation at regional scales

Papa et al., 2013, Derivation of critical rainfall thresholds for shallow landslides as a tool for debris flow early warning systems

Alvioli et al., 2014, scaling properties of rainfall induced landslides predicted by a physically based model.

R: The authors appreciate the reviewer's suggestions and agree that the comparison of physically-based and statistically-based thresholds is needed. The study focused on rainfall conditions for triggering landslides in a wide (national scale) study area, a purely physical model may be not suitable. We would like to call it a mixed physically- and statistically-based model. The rainfall threshold using a mixed physically- and statistically-based model in the study will be compare with others using physically-based models. The relative discussion has been added to the text as below.

“In general, physically-based models are easy to understand and have high predictive capabilities (Wilson and Wiczorek, 1995; Salciarini and Tamagni, 2013; Papa et al., 2013; Alvioli et al., 2014). However, they depend on the spatial distribution of various geotechnical data (e.g., cohesion, friction coefficient, and permeability coefficient), which are very difficult to obtain. Statistically-based methods can include conditioning factors that influence slope stability, which are unsuitable for physically-based models. Statistically-based models rely on good landslide inventories and rainfall information. In this study, the Q_C threshold for a large landslide was estimated based on a mixture of physically- and statistically-based methods. Unlike other physically-based $I-D$ thresholds, which are commonly constructed based on artificial rainfall information for shallow landslides (Salciarini et al., 2012; Chen et al., 2013c; Napolitano et al., 2016) (Table S3), the Q_C threshold proposed in this study seemed to be higher and more suitable for large landslides (Fig. 6d).”

“To verify the usability of the rainfall thresholds proposed in this study, Typhoon Soudelor of 2015 was chosen to demonstrate the early warning performance. Typhoon Soudelor was one of the most powerful storms on record. It generated 1400 mm of rainfall in northeastern Taiwan and almost 1000 mm of rainfall in the southern mountainous area of Taiwan (Wei, 2017; Su et al., 2016). After the seismic signal analytical procedure, the occurrence time, 2015/8/8 18:59:50 (UTC), of a large landslide (named the Putanpunas Landslide) located in southern Taiwan was obtained (Fig. 7). The seismic signal generated by the Putanpunas Landslide was also detected by Chao et al. (2017). The seismic signals generated by this large

landslide could be identified from six BATS stations, and the distance error was less than 6 km. The rainfall records of rain gauge station C1V190, which was situated in the same watershed and 14.6 km away from the large landslide, were collected for rainfall analysis. Typhoon Soudelor made landfall in Taiwan on August 7, 2015, and dropped a cumulated rainfall of 546 mm and had a maximum rainfall intensity of 39 mm/h on August 8 at rain gauge station C1V190 (Fig. 8). The rainfall event began at 22:00 August 7 and last for 26 hours, and the Putanpunas Landslide initiated at the 22nd hour. This landslide occurred when the rainfall intensity was on the decline.

Regarding landslide early warning using rainfall thresholds, once the rainfall conditions at a given rainfall station exceed the rainfall thresholds for triggering landslides, the slopes located within the region of the rainfall station will have high potential for failure. Based on the statistically-based I-D threshold for small landslides, a small-landslide warning would have been issued at the sixth hour of the rainfall event (Fig. 8). The long interval of sixteen hours between the warning and the occurrence time of the Putanpunas Landslide could have reduced the reliability of the warning or even caused the warning to be considered a false alarm. Therefore, it is essential to establish different thresholds for landslides of different scales. Using the $Rt-I$ threshold (i.e., $Rt \cdot I = 5,640$), a large-landslide warning would have been issued at the ninth hour of the rainfall event (i.e., thirteen hours before the Putanpunas Landslide occurred). According to the statistically-based I-D threshold for large landslides, a landslide warning would have been issued at the same hour as the $Rt-I$ threshold. In addition, a warning based on the $D-Rt$ threshold (i.e., $D \cdot Rt = 12,773$) would have been issued three hours after the occurrence time of the Putanpunas Landslide. According to the rainfall records and the critical height of water model (i.e. $(I-1.5) \cdot D = 430.2$), a landslide warning would have been issued at 16:00 on August 8, three hours before the occurrence time of the Putanpunas Landslide. Compared to the statistically-based I-D threshold, the $Rt-I$ threshold, and the $D-Rt$ threshold, the critical height of water model had a better early-warning performance for the 2015 Putanpunas Landslide.”

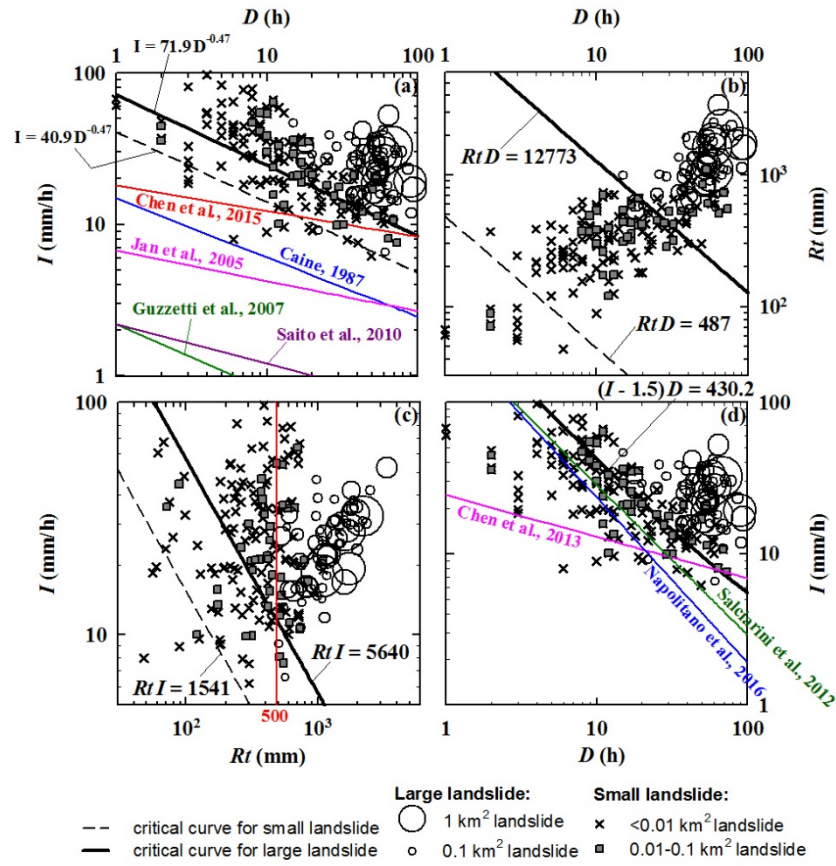


Figure 6

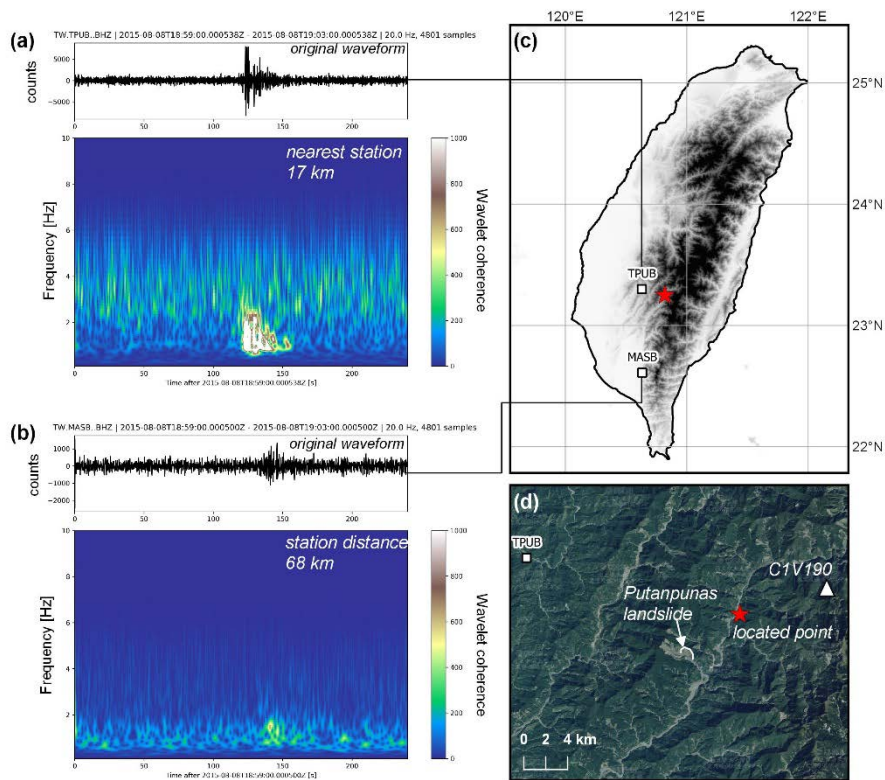


Figure 7

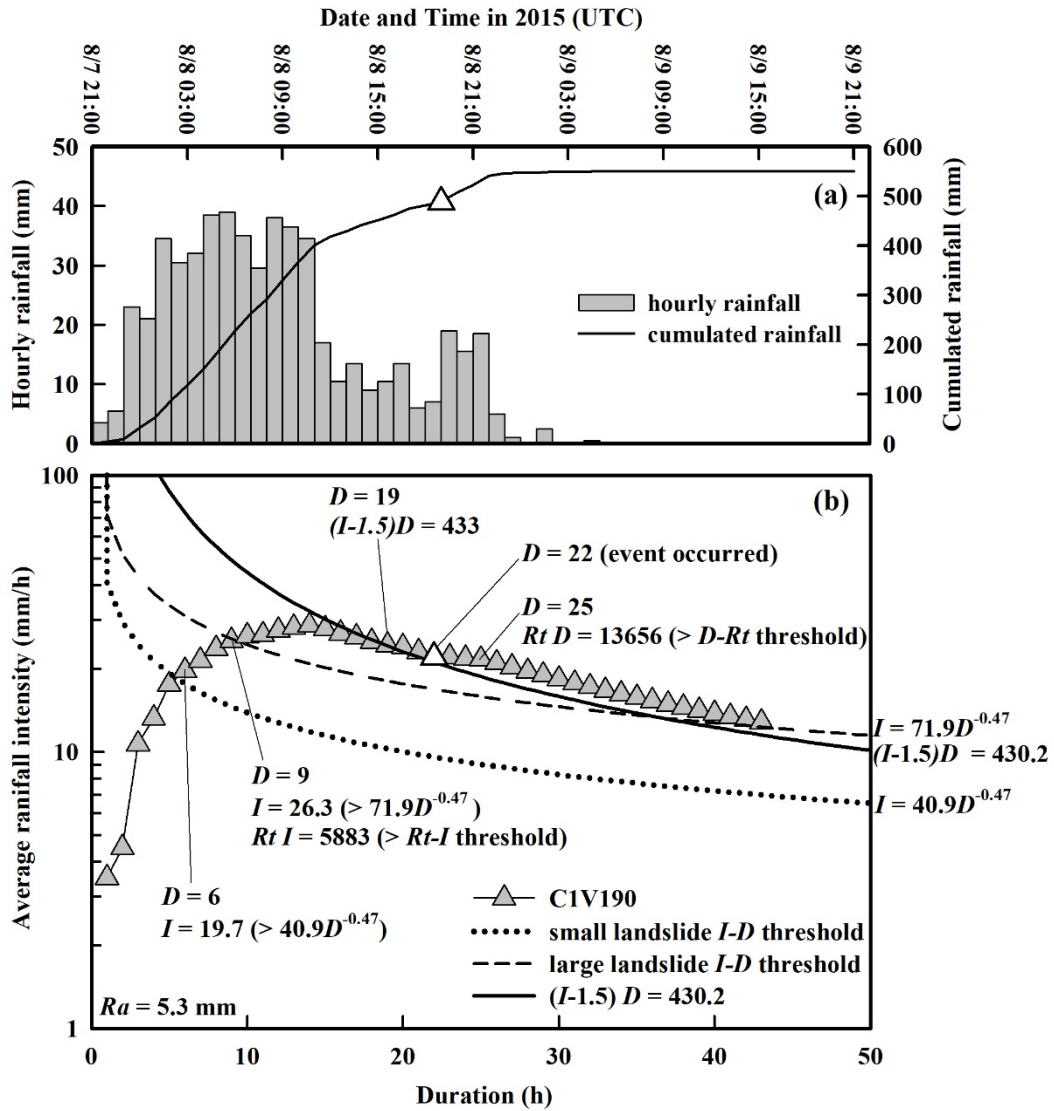


Figure 8

Table S3

Reference	Equation	Study area
1 Salciarini et al. (2012)	$I = 276.2D^{-0.99}$	Model
2 Chen et al. (2013b)	$I = 24.4D^{-0.28}$	Taiwan
3 Napolitano et al. (2016)	$I = 287.8D^{-1.09}$	southern Italy

Reference:

Chen, Y. H., Tan, C. H., Chen, M. M., and Su, T. W. (2013b) Estimation of rainfall threshold for regional shallow landslides in a watershed. Journal of Chinese Soil and Water Conservation, 44(1), 87-96.

- Salciarini, D., Tamagnini, C., Conversini, P., Rapinesi, S. (2012) Spatially distributed rainfall thresholds for the initiation of shallow landslides. *Nat. Hazards* 61, 229–245.
- Napolitano, E., Fusco, F., Baum, R. L., Godt, J. W., and De Vita, P. (2016) Effect of antecedent-hydrological conditions on rainfall triggering of debris flows in ash-fall pyroclastic mantled slopes of Campania (southern Italy). *Landslides*, 13, 967–983.
- Chao, W. A., Wu, Y. M., Zhao, L., Chen, H., Chen, Y. G., Chang, J. M., & Lin, C. M. (2017). A first near real-time seismology-based landslide monitoring system. *Scientific Reports*, 7, 43510.
- Su, Y.F., Chen, W.B., Fu, H. S., Jang, J. H., Chang, C. H. (2016). Application of Rainfall Forecasting to Flood Management --A Case Study of Typhoon Soudelor. *Journal of Disaster Management*, Vol.5, No.2, pp. 1-17 (in Chinese)
- Wei, C. C. (2017). Examining El Niño–Southern Oscillation effects in the subtropical zone to forecast long-distance total rainfall from typhoons: A case study in Taiwan. *Journal of Atmospheric and Oceanic Technology*, 34(10), 2141-2161.

3. I think the discussion needs to be revised significantly. The authors seek to discuss effects on critical threshold that cannot really be assessed with the data they have, while several points are not really discussed: For example 1/ uncertainty on rainfall parameters, 2/ the added value of seismic dating of landslide and its limit (size of landslide distance from stations (currently section 5.3 needs significant clarification) , 3/ The value of the critical rainfall volume : how better compare with other, how to determine or constrain I_0 etc

R: The authors appreciate the reviewer's constructive comment. The section of discussion has been revised significantly. The revision includes:

- 1) The authors agree that uncertainty on rainfall parameters will influence on the distribution of statistically-based rainfall data. In order to constrain the indeterminate variation of rainfall threshold analyses, a consistent process of calculating rainfall data with a standard of station selection has to be constructed. In the study, we tested the accuracy of rainfall data and used a consistent calculation method for rainfall parameters carefully. Therefore, the variation of rainfall parameters (I , D , and Rt) could be under control. The detailed validation of rainfall parameters has been added to the section S3 of the supplementary material.
- 2) The detailed information (position, time, elevation, disturbed area, used rainfall station, activity) of each detected landslide has been added to the supplementary material as Table S2.
- 3) The critical height of water (Q_c) was estimated using the physically-based model proposed by Keefer et al. (1987). Subsequently, the threshold equation, (I -

$I_0 \times D = Q_c$, was adopted to fix the lower boundary of rainfall data in the $I-D$ plot. The value of I_0 was estimated using the same statistically-based method with $I-R_t$ threshold. The value of 1.5 was obtained as the exceeding probability of 5%. We would like to call it a mixed physically- and statistically-based model. The mixed model could recover the limitation while we just used a purely physically-based model or a purely statistically-based model. The comparison of the critical height of water model with other studies has been added in Figure 6, and table S3. The modified illustration has been added to the test as below:

“In this study, the Q_c threshold for a large landslide was estimated based on a mixture of physically- and statistically-based methods. Unlike other physically-based $I-D$ thresholds, which are commonly constructed based on artificial rainfall information for shallow landslides (Salciarini et al., 2012; Chen et al., 2013c; Napolitano et al., 2016) (Table S3), the Q_c threshold proposed in this study seemed to be higher and more suitable for large landslides (Fig. 6d).”

4. Last, I strongly suggest the authors to define variable names for antecedent rainfall (e.g. R_a), cumulated rainfall (e.g. R_c) to later compare with R_t ($R_t = R_c + R_a$) and to be consistent in text and figure when they talk about rainfall amount.

R: Thanks for the suggestion. The variable names have been modified according to the suggestions.

(2) Line by Line comments:

1. P2 L 5: LSL / SSL : this is heavy and makes the draft harder to read. Why not simply use small and large landslide and indicating the boundary is at 0.1km² ?

R: Thanks for the suggestion. The origin term, large-scale landslide and small-scale landslide, have both replaced with “large landslide” and “small landslide”, respectively.

2. P2 L21: State in the text how was estimated the occurrence time. Based on peak rainfall correct? In Fig 1 Caption you say that in general peak rainfall intensity is used. This may go int the main text, with one or two references. Indeed, simple groundwater modelling (e.g. Wilson and Wieczorek, 1995) could estimate soil moisture based on the rainfall data and find a maximal pore pressure after the peak rainfall. Other simple modelling approach or assumption may give different estimation times.

R: Thanks for the suggestions. The authors agree that more and more useful approaches have been developed to get the exact time information of landslide initiation. However, the approaches all depended on in-situ monitoring or other assumptions. So far, the most common and convenient way to assess a factor of rainfall intensity is still based on the peak rainfall intensity. The statement on peak rainfall intensity has been added to text with some references (i.g. Chen et al., 2005; Wei et al., 2006; Staley et al., 2013; Yu et al., 2013; Xue et al., 2016). The study uses the time interval between the timing with peak rainfall intensity and exact landslide timing to explain the misjudgment results of rainfall analysis (Chen et al., 2005). The reference have been added to text as below:

“...In general, if the exact occurrence time of a landslide cannot be investigated, the time point with the maximum hourly rainfall will be conjectured as the occurrence time of the landslide (Chen et al., 2005; Wei et al., 2006; Staley et al., 2013; Yu et al., 2013; Xue et al., 2016).....”

Reference:

Chen, C. Y., Chen, T. C., Yu, F. C., Yu, W. H., and Tseng, C. C. (2005) Rainfall duration and debris-flow initiated studies for real-time monitoring. *Environ Geol*, Vol. 47, 715–724.

Staley, D., Kean, J. W., Cannon, S. H., Schmidt, K. M., and Laber, J. L. (2013) Objective definition of rainfall intensity–duration thresholds for the initiation of post-fire debris flows in southern California. *Landslides*, Vol. 10(5), 547–562.

- Wei, F., Gao, K., Cui, P., Hu, K., Xu, J., Zhang, G., and Bi, B. (2006) Method of debris flow prediction based on a numerical weather forecast and its application. *WIT Transactions on Ecology and the Environment*, Vol. 90, 37-46.
- Xue, X., and Huang, J. (2016) A rainfall and pore pressure thresholds for debris-flow early warning: The Wenjiagou gully case study. *Nat. Hazards Earth Syst. Sci. Discuss.*, doi:10.5194/nhess-2016-149.
- Yu, B., Li, L., Wu, Y., and Chu, S. (2013) A formation model for debris flows in the Chenyulan River Watershed, Taiwan. *Natural Hazards*, Vol. 68(2), 745–762.

3. P2 L34: Fractural geological conditions >> Fractured rock mass

R: Thanks for suggestion. The sentence has been revised based on the suggestion as below.

“... Fractured rock mass coupled with a warm and humid climate, and an average of 3 to 5 typhoon events per year, contribute to the high frequency of slope failures in mountainous areas in Taiwan (Wang and Ho, 2002; Shieh, 2000; Dadson et al., 2004; Chang and Chiang, 2009; Chen, 2011).....”

4. P2 L35: slope disasters >> I would suggest slope failures , more general (here and at other place in the text)

R: Thanks for suggestion. All sentences contained the term “slope disaster” have been replaced with “slope failure” based on the suggestion. For example:

“...The rainfall intensity, however, could not be used effectively to distinguish these two kinds of slope failures.....”

5. P3 L21: By a rainstorm (which one?) or by the Morakot typhoon ? Please clarify.

R: Here refers to landslides caused by heavy rain events, not only by a specific event, we will modify the statement to avoid confuse. The modified text is as follows:

“...Landslides induced specifically by rainstorm events were distinguished by overlaying the pre- and post-event image mosaics.....”

6. P3 L25: end of the sentence unclear. Main factor to separate SSL from LSL or to relate to rainfall triggering? If so how?

R: In the study, the landslide types were divided into large landslide and small landslide based on the size of landslide-disturbed area. The rainfall factors of each landslide were

assessed after classifying. The main purpose in the study is to find the difference of rainfall thresholds between large and small landslides, but not to classify these two types of landslides by rainfall factor or rainfall pattern. The relative sentence will be revised to avoid confuse. The modified text is as follows:

“...Finally, large and small landslides were distinguished and classified according to the criterion of an affected area of 0.1 km². In this study, the types and mechanisms of individual landslides were not investigated, but landslide area was used as the main factor for investigating the different rainfall conditions that trigger large and small landslides.”

7. P3 L 30: Ok the triangular signature is typical, but could you cite and discuss what are other typical properties? I know there are quite some papers discussing how to detect and classify landslides based on various properties of the spectrogram or of the waveform.

R: The authors thank the reviewer’s suggestions. More deeply description on the features of landslide-induced seismic signals will be added to the text as bellows: The modified text is as follows:

“...The seismic wave generated by a landslide can be attributed to the shear force and loading on the ground surface as the mass moves downslope. Many studies have shown that the source mechanism of a landslide is highly complicated, and that its seismic waves mainly consist of surface waves and shear waves, making it difficult to distinguish *P* and *S* waves from station records (Lin et al., 2010; Suwa et al., 2010; Dammeier et al., 2011; Feng, 2011; Hibert et al., 2014). The onset of a landslide seismic signal is generally abrupt. Then the seismic amplitude increases gradually above the ambient noise level to peak ground motion, exhibiting a cigar-shaped envelope. After the peak amplitude, most of the landslide-generated seismic signals have relatively long decay times, on average about 70% of the total signal duration (Norris, 1994; La Rocca et al., 2004; Suriñach et al., 2005; DeParis et al., 2008; Schneider et al., 2010; Dammeier et al., 2011; Allstadt, 2013). In the frequency domain, landslide-induced seismic energy is mainly distributed below 10 Hz, with a triangular signature in a spectrogram, due to an increase over time in high-frequency constituents (Suriñach et al., 2005; Dammeier et al., 2011). The triangular signature in the spectrogram is the distinctive property that readily distinguishes landslide-induced signals from those of earthquakes and other ambient noise.”

Reference:

- Allstadt, K. (2013). Extracting source characteristics and dynamics of the August 2010 Mount Meager landslide from broadband seismograms. *Journal of Geophysical Research: Earth Surface*, 118(3), 1472-1490. doi:10.1002/jgrf.20110.
- Dammeier, F., Moore, J. R., Haslinger, F., and Loew, S. (2011). Characterization of alpine rockslides using statistical analysis of seismic signals. *Journal of Geophysical Research*, 116(F4). doi:10.1029/2011jf002037
- Deparis, J., Jongmans, D., Cotton, F., Baillet, L., Thouvenot, F., and Hantz, D. (2008). Analysis of rock-fall and rock-fall avalanche seismograms in the French Alps. *Bulletin of the Seismological Society of America*, 98(4), 1781-1796. doi:10.1785/0120070082.
- Feng, Z. (2011). The seismic signatures of the 2009 Shiaolin landslide in Taiwan. *Natural Hazards and Earth System Science*, 11(5), 1559-1569. doi:10.5194/nhess-11-1559-2011
- Hibert, C., Ekström, G., and Stark, C. P. (2014). Dynamics of the Bingham Canyon Mine landslides from seismic signal analysis. *Geophysical Research Letters*, 41(13), 4535-4541. doi:10.1002/2014gl060592
- La Rocca, M., Galluzzo, D., Saccorotti, G., Tinti, S., Cimini, G. B., and Del Pezzo, E. (2004). Seismic signals associated with landslides and with a tsunami at Stromboli volcano, Italy. *Bulletin of the Seismological Society of America*, 94(5), 1850-1867. doi:10.1785/012003238.
- Lin, C. H., Kumagai, H., Ando, M., and Shin, T. C. (2010). Detection of landslides and submarine slumps using broadband seismic networks. *Geophysical Research Letters*, 37(22), n/a-n/a. doi:10.1029/2010gl044685
- Norris, R. D. (1994). Seismicity of rockfalls and avalanches at 3 Cascade Range volcanos - Implications for seismic detection of hazardous mass movements. *Bulletin of the Seismological Society of America*, 84(6), 1925-1939.
- Schneider, D., Bartelt, P., Caplan-Auerbach, J., Christen, M., Huggel, C., and McArdell, B. W. (2010). Insights into rock-ice avalanche dynamics by combined analysis of seismic recordings and a numerical avalanche model. *Journal of Geophysical Research*, 115(F4). doi:10.1029/2010jf001734.
- Suriñach, E., Vilajosana, I., Khazaradze, G., Biescas, B., Furdada, G., and Vilaplana, J. M. (2005). Seismic detection and characterization of landslides and other mass movements. *Natural Hazards and Earth System Sciences*, 5, 791-798.
- Suwa, H., Mizuno, T., and Ishii, T. (2010). Prediction of a landslide and analysis of slide motion with reference to the 2004 Ohto slide in Nara, Japan. *Geomorphology*, 124(3-4), 157-163. doi:10.1016/j.geomorph.2010.05.003.

8. P4 L3: Only now we learn that the landslide mapping was done between 2009 and 2014. Please indicate it at the start of the mapping section.

R: Thanks for the suggestion. The modified text is as follows:

“To determine the locations and basic characteristics of large landslides occurring in the years 2005–2014, the landslide areas across the entire island of Taiwan were interpreted using SPOT-4 satellite remote sensing images with a spatial resolution of 10 m in multispectral mode....”

9. P4 L35: Could you give an estimate of how often the location point and landslide maps matched? And what was the maximal acceptable offset from a mapped landslide?

R: Once the seismic signals had the characteristics of landslide-induced ground-motions and were located in mountainous area, exceeding 90% of the signals could be paired with the landslides which were located in the vicinity of seismically-locating points, and the slope aspect were consistent with the direction of the trajectories of seismic signals. The average location error, or the distance between the actual and estimated location, was 10.9 km. The best location estimate was for the ID 40 landslide with an error of 0.5 km, while the worst location estimate was for ID 35 landslide with an error of 49.3 km. The description has been added to Table S2:

“The average location error, or the distance between the actual and estimated location, was 10.9 km. The best location estimate was for the ID 40 landslide with an error of 0.5 km, while the worst location estimate was for ID 35 landslide with an error of 49.3 km. “

10. P5 L 4: Need some reference for that: the track does not necessarily say so much given the size of the diameter of typhoons are sometimes similar to Taiwan island size... And the windward slope is not obvious. If you refer to orographic effects say it clearly, but this also occur at large scale not a fine scale.

R: The authors appreciate the kind suggestions. The statement will be modified based on the suggestions. Some useful reference has be added to text as below:

Chen, C. S., and Chen, Y. L. (2003). The rainfall characteristics of Taiwan. *Monthly Weather Review*, 131(7), 1323-1341.

Sanchez-Moreno, J.F., Mannaerts, C.M., and Jetten, V. (2014) Influence of topography on rainfall variability in Santiago Island, Cape Verde. *International Journal of Climatology*, 34, 1081-1097.

The modified text is as follows:

“...The distribution of precipitation during typhoon events is usually closely related to the typhoon track and the position of the windward slope, also as known as the orographic effect. In addition, the density and distribution of rainfall stations in mountainous areas directly affect the results of rainfall threshold analysis. If the landslide location and the selected rainfall station are located in different watersheds, the rainfall information is unlikely to represent the rainfall conditions for the landslide. In some cases, however, the diameter of the typhoon were so large that the orographic effects could be ignored (Chen and Chen, 2003; Sanchez-Moreno et al., 2014)...”

11. P5 L5-10: Very true indeed. Another important point may be the altitude of the gauging station and of the upper part of the landslide. If the gage is near the river at the outlet of the 100km² catchment possibly 500m or more below slopes where landslide happen the rainfall may be quite different.

R: Thanks for comments. The reply has been addressed as the Q1 of major comment.

12. P5 L 14: Say if this is your definition (we define the beginning of a rain event) or a general one (then cite other studies.)

R: Thanks for comments. The sentence has been revised as follows:

“...In rainfall analysis, the beginning of a rain event is defined as the time point when hourly rainfall exceeds 4 mm, and the rain event ends when the rainfall intensity remains below 4 mm/h for 6 consecutive hours. The critical rainfall condition for a landslide was calculated from the beginning of a rain event to the occurrence time of the landslide (Jan and Lee, 2004; Lee, 2006)...”

Reference:

Jan, C. D., and Lee, M. H. (2004). A debris-flow rainfall-based warning model. *J Chin Soil Water Conserv*, 35(3), 275-285.

Lee, M. H. (2006). The Rainfall threshold and analysis of Debris flows, Doctoral dissertation, National Cheng Kung University, Taiwan, ROC (in Chinese).

13. P5 L18-20: I understand it is hard to choose objectively which time should be considered for antecedent rainfall, but an arbitrary threshold without temporal weighting seems disingenuous... It is fair to use the official definition but what about testing a couple other antecedent rainfall conditions: for example, the cumulated rain over 3 or 5 days. Or a weighted sum over the 10 preceding days (with weight decreasing with time before the event).

R: Thanks for your suggestion. In this study we used a temporal weighting coefficient of 0.7 with weight decreasing with days before the event (Jan and Lee, 2004). The formula can be written as:

$$Ra = \sum_{i=1}^7 0.7^i * R_i$$

We have attached this in a later version. The modified text is as follows:

“...In addition to the three factors mentioned above, the daily rainfall for the seven days preceding the rainstorm was considered as antecedent rainfall (Ra). The antecedent rainfall (Ra) was calculated with a temporal weighting coefficient of 0.7, with the weight decreasing with days before the event. The formula was $Ra = \sum_{i=1}^7 0.7^i \times R_i$, where R_i is the daily rainfall of the i^{th} day before the rainfall event...”

14. P6 L 4-7: How was the occurrence time obtained for SSL ? Not by seismic means? SO how accurate are these times? Are we back to the same uncertainties as shown in Fig 1? Authors should clarify that.

R: The time records of the small landslides used in the study were reported by the disaster investigation report of the Soil and Water Conservation Bureau (SWCB) in Taiwan, but not obtained from seismic records. Most of the small landslides caused disasters and loss of life and property. In some cases, in-situ river steel cable or CCTV could record the time information. The clear illustration on the data source of small landslides will be added to the later version. The modified text is as follows:

“In addition to that of large landslides, the time information of 193 small landslides such as shallow landslides and debris flows from the years 2006–2013 was collected from the annual reports of debris flows investigated by the Soil and Water Conservation Bureau (SWCB) of Taiwan, but it was not extracted from seismic records. Most of the 193 small landslides caused disasters and loss of life and property. In some cases, in-situ steel cables or closed-circuit television

recorded the time information. This information was applied to the rainfall data analysis and then used to compare the rainfall conditions of the large landslides.”

15. P6: Subsection 2.4: missing "I", >> water model ?

R: Thanks for careful reviewing. The mistake has been revised in the text.

16. P6 EQ 1 and 2: ok but the assumption $C' = 0$ maybe quite a big one , especially for large bedrock landslides... Need to be discussed at some point, because Q_c would be larger with none zero C .

R: We thanks reviewer’s recommendation. Well development of detachment plane (e.g., sliding surface between sedimentary layers, connected joints, weathered foliation, etc.) have been widely considered as the geological conditions to occur a large landslide (Agliardi et al., 2001; Tsou et al., 2011). Therefore, in the study, the C' of the detachment plane is simply assumed as the value of zero to behave the critical situation of slope stability. The illustration of C' has been modified to the text.

The modified text is as follows:

“where Z is the vertical depth of the sliding surface, γ_t is the unit weight of the slope material, and θ is the slope angle. Good development of a detachment plane (e.g., sliding surface between sedimentary layers, connected joints, and weathered foliation) has been widely considered as the geological condition under which a large landslide occurs (Agliardi et al., 2001; Tsou et al., 2011). Therefore, in this study, the c' of the detachment plane is simply assumed to be zero to represent the critical situation of slope stability.”

Reference:

Tsou, C. Y., Feng, Z. Y., & Chigira, M. (2011). Catastrophic landslide induced by typhoon Morakot, Shiaolin, Taiwan. *Geomorphology*, 127(3-4), 166-178.

Agliardi, F., Crosta, G., & Zanchi, A. (2001). Structural constraints on deep-seated slope deformation kinematics. *Engineering Geology*, 59(1-2), 83-102.

17. P6 EQ 4: Q_c is actually the height of saturated regolith above the failure plane, in mm. Maybe clearer than calling it a critical volume. Note that in EQ 3 it is a critical height. But in EQ 4 it is simply a height assuming I_0 is correctly estimated.

Another key issue is that this equation does not account for the antecedent rainfall. As I and D are for the triggering storm only, correct? Finally, I do not see why the authors assume a linear drainage. Most hydrological simple model

of soil drainage (backed up by theory and observations) show a non linear drainage rate, where drainage increase with the amount of water in the soil (e.g., Wilson and wieczorek, 1995). I think the authors should discuss this choice here or in discussion. This model is very easy to implement and use to obtain soil water level, only requiring the hourly estimate of rainfall and an assumed drainage parameter. I think it may be an interesting addition to the paper to really make the authors model physical. I note that a number of recent attempt to model physically landslide threshold (cf major comments) should be mentioned and discussed here and/or in discussion these models and how they compare to the author proposition.

R: Thanks for the valuable suggestions. The original naming of Q_c in the manuscript is followed the Keefer (1987). We have revised the naming of Q_c to critical water height. Practically, antecedent rainfall is not considered in the empirical/statistically-based *I-D* method.

18. P7 L5: "their slope angles". Do you mean the mean slope within the landslide body?

R: The slope angles mentioned in the study indicate the mean slope gradient before landslides occurred. The values of slope gradient were utilized to calculate Q_c , therefore they should not be affected by landsliding. The slope angles were estimated with a 40 m digital elevation model (DEM) which was created before 2004. The illustration on slope angles will be modified as below.

“... Most of these large landslides had areas of 0.12 to 0.15 km², and their slope angles before the landslides occurred were concentrated between 30° and 40° (Fig. 4b).....”

19. P7 L7 : " This increase was most likely due to the fact that during the extremely heavy rainfall of Typhoon Morakot in 2009, more than 2,000 mm precipitated in four days, causing numerous landslides on lower slopes and reducing the stability of the steeper slopes in the following years."

I do not think this claim is supported by the data of Fig 4 : First in 2009 Morakot did not seem to be so different from 2005-2008 in terms of slope distribution. 2nd it only affected the southern half of the distribution of 2010-2014. If the hypothesis of the author is true, comparing only pre 2009 and post 2009 in the Morakot area only (i.e. southern half of the dataset) would yield an even more pronounced shift, while the northern half should have no shift. I invite the authors to check and show this to support their claim.

Alternatively they should try to check that statistical uncertainties may not be responsible for shift, and it would be interesting to compute a confidence interval on each histogram. Last point, either if Morakot did perturb the slope distribution the author need to clarify their argument, as it is not obvious how failing gentle slope would weaken steeper slopes (as a start the author could try to demonstrate that failing slopes in 2010-2014 are spatially related to 2009 failures)

R: The authors appreciate reviewer's valuable comments. We agree the original sentence was unclear. The sentence has been revised as below:

“...The number of landslides occurring on slope angles exceeding 40° slightly increased after 2010. Although the increase was quite slight, it was most likely due to the fact that during the extremely heavy rainfall of Typhoon Morakot in 2009, more than 2000 mm precipitated in four days, causing a large number of landslides and exhausting many unstable slopes. Consequently, landslides occurred on steeper slopes in the following years....”

20. P7 L 24-26: Not clear. To clarify.

R: The resultant trace of two horizontal-component signals could be plotted. Comparing the direction of the resultant trace of a given landslide-induced seismic record with the slope aspect in the vicinity of locating point, we could eliminate the irrelevant landslides which have different slope aspects with the signal trajectory. The paragraph has been modified as follows:

“...In addition to distance, the resultant traces of two horizontal-component signals could be plotted. The direction of the resultant trace of a given landslide-induced seismic record with the slope aspect in the vicinity of the located point could be compared so as to eliminate the irrelevant landslides, those which had slope aspects different from the signal traces. The ground motion traces of the signals had to be correlated with the directions of movement of the landslides to reconfirm the matched large landslides. In total, 62 large landslides were paired successfully with seismic record locations (Fig. 2a, Table S2)....”

21. P7 L26: Could you explain with some more details how these 62 LSL were obtained? Is it the combination of near gages and seismic signal quality? Anything else? One sentence for recalling the reader of the criteria used would be helpful

R: After obtaining the signal at the time of the landslide events, we use the locating method proposed by Chen et al. (2013) to locate the vibration source. Once a landslide is close to a locating point of seismic records and the slope aspect of the landslide is consistent with the direction of signal trajectory, the landslide can be considered as the source of the seismic signals.

22. P8 L25: **Interesting, but size is not the only difference with these other thresholds. The fact you focused on large landslides, requiring higher total rainfall, and thus higher I-D lines is likely contributing. However, how much of the difference could be due to seismic dating? To the regional characteristics of the landslide (as some threshold are global, other Taiwanese or Japanese). I think these should be mentioned here or in discussion, because your threshold for SSL is also much larger than most other threshold, and these SSL are more similar in size to past study.**

R: Thanks for suggestions. The study aims to use a seismicity method to get landslide timing for constructing rainfall thresholds, and to discuss which threshold is more suitable to give different warning for small and large landslides. Clearer illustration of the purpose of the study has been added to the introduction section as below:

“This study attempts to determine the occurrence times of landslides by identifying landslide-generated seismic signals to construct rainfall thresholds, and to clarify which thresholds are more suitable for triggering different warnings for small and large landslides....”

23. P9 L 1-2: **it was determined that Rt–D analysis could be used effectively to distinguish SSLs from LSLs. I think it is very interesting to see in Fig 5B that the landslide size groups shift from small for relatively short duration and low rainfall amount to large landslides for long and very large cumulative rainfall.**

R: Thanks for comments. We have added the illustration to the modified manuscript as below:

“The landslide size groups shifted from small landslides for relatively short duration and low effective rainfall to large landslides for long duration and very large effective rainfall.”

24. P9 L8: **"conditions for SSLs included high average rainfall intensity but relatively low cumulated rainfall". You plot Rt that is the total effective rainfall in Fig 5. So do SSL have low cumulated rainfall or low Rt or both (if Ra is**

low...)

In any case this plot is also quite interesting, as it matches well the theoretical expectations (Van asch 1999, Iverson 2000) stating that very large landslides will require high cumulated rainfall (unlikely to accumulate over short timescales) while small landslides may be caused by transient pulse of water accumulation in the shallow regolith relating to very high intensity, but that do not need to cumulate large amount of water.

R: We thanks for comments. The statement has been revised as below:

“...Combining the results of the three kinds of dual-factor rainfall threshold analyses revealed that the critical rainfall conditions for small landslides included high average rainfall intensity but relatively low effective rainfall, while those for large landslides included long rainfall duration and high effective cumulated rainfall. These results corresponded well with the former theoretic expectation (Van Asch et al., 1999; Iverson, 2000).”

25. P9 L14-15: Not only Wieczorek and Glade could cited here. Van asch 1999, Iverson 2000 discussed that earlier.

R: Thank you for your suggestion. The reference, Van Asch (1999) and Iverson (2000), have been cited and added to the modified manuscript.

Reference:

Van Asch, T. W., Buma, J., and Van Beek, L. P. H. (1999). A view on some hydrological triggering systems in landslides. *Geomorphology*, 30(1-2), 25-32.

Iverson, R. M. (2000). Landslide triggering by rain infiltration. *Water resources research*, 36(7), 1897-1910.

The modified text is as follows:

“...However, prolonged rainfall also plays an important role in slow saturation, which in turn influences the groundwater level and soil moisture, and causes large landslides. These facts have been recognized in many studies around the world (Wieczorek and Glade, 2005; Van Asch et al., 1999; Iverson, 2000), but they have been analysed in only a few locations (e.g., a mountainous debris torrent, a shallow landslide event, and an individual rainfall event)....”

26. P9 L20: This seems like a very crude approach. I would strongly encourage the author to have a Compute Qc based on an actual estimation of the landslide slope and the landslide depth: Using Larsen 2010 or a local Area Depth relation

from Taiwanese dataset (Chen 2013) the authors could use A to derive Z and thus obtain a more realistic estimate of Q_c as a function of Z and the mean slope. The effect of small variations in porosity or friction angle could also be computed and shown.

I understand you want a single average threshold to compare to a population. Nevertheless, you can make an almost individual prediction of each large landslide (with Depth and Slope) and compare it to uniquely constrain rainfall information, thanks to your seismic dating. I think it would be worth checking the validity of the model this way, and potentially refining the drainage model that seems critical to really obtain a physically based threshold.

R: Thanks for valuable suggestions. The authors have tried the suggested approaches to recalculate Q_c and to estimate the rainfall threshold. The revised rainfall threshold is $(I - 1.5) D = 430.2$. The relative paragraph and Fig. 6 has been modified in the later version of manuscript.

The modified text is as follows:

“The critical height of water, Q_c , on a sliding surface for each large landslide was estimated based on its slope gradient, depth (estimated by the equation $Z = 26.14A^{0.4}$; Z : depth in m; A : disturbed area in m^2), and the geological material parameters of the study area (Table 1). The Q_c value was inserted into $Q_c = (I - I_0) \cdot D$ to obtain an I_0 value for each large landslide. For the 62 detected landslides, the cumulative probability of 5% of the Q_c and I_0 values was taken as the critical value. The critical value of I_0 was 1.5, the critical Q_c was 430.2, which is more suitable for large than for small landslides, and the threshold curve was rewritten as $(I - 1.5) \cdot D = 430.2$.”

27. P9 L 23 -25: Is this curve allowing to better predict the LSL compared to the other plots in Fig 5 (Especially I – Rt or I-D?) Same question for the separation from SSL/LSL. The authors should provide some statistics confirming that this model is better than a Rt -I for example. Log Log plot is absolutely necessary for all plot. Further, the very low drainage found by the authors, mean their threshold is almost ID ~452 or R~452. And indeed a vertical line in the I -Rt graph at about 500 may be as good...

R: Thank you for your suggestion. The log-log figure will be modified based on suggestions. And a vertical line has been added in the I - Rt graph at Rt of 500m as below:

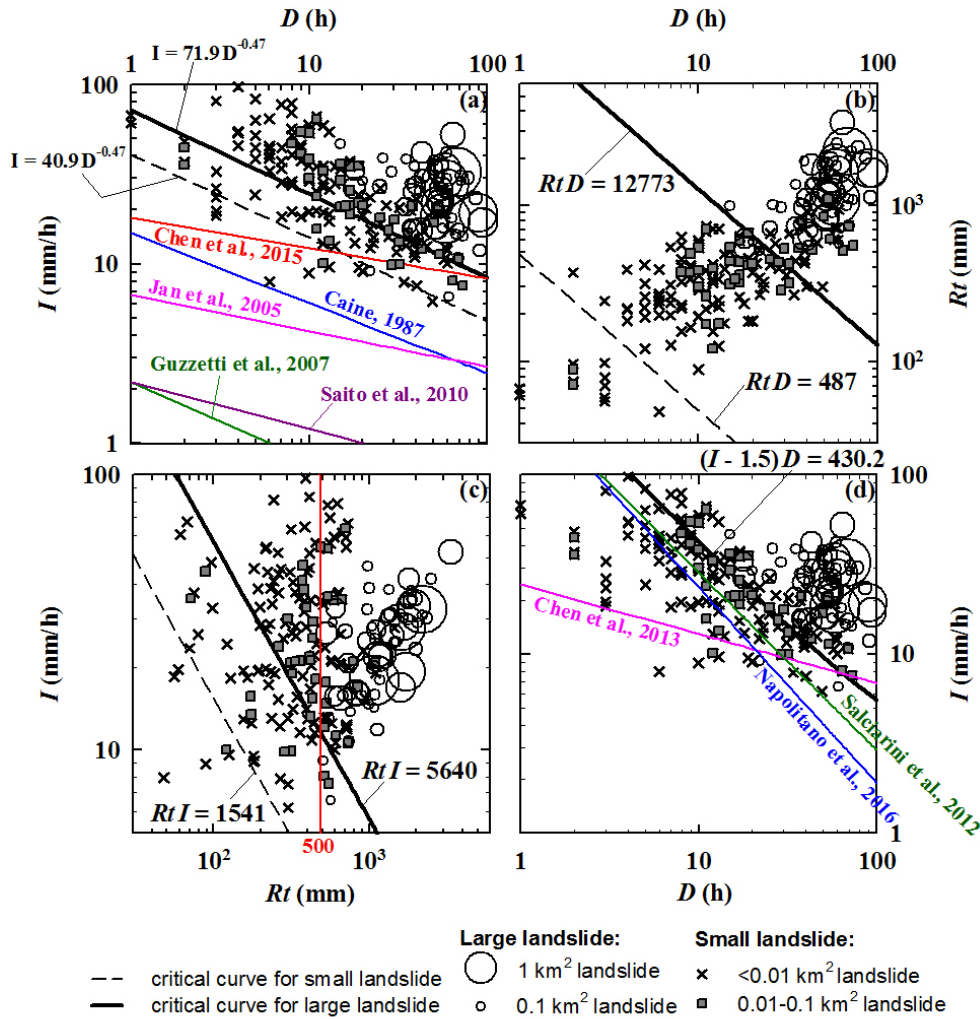


Figure 6

28. P10 L14: If so you should observe a larger fraction of the LSL in 2010-2014 neighbored a 2005-2009 landslide, compare to LSL in 2005-2009 being the reactivation of older landslides. Given the small dataset (62?), I encourage the authors to check each LSL and report the proportion of reactivation before and after 2009. Then they can support and discuss this hypothesis

R: Thank you for the valuable comments. The information on reactivity of 2010-2014 landslides will be provided in table S2. Once a 2010-2014 landslide was on the location of a 2005-2009 landslide, the landslides was classified as a reactivated landslide (marked as “R” in Table S2).

29. P10 Section 5.1 and 5.2 Strange writing: the authors oscillate between presenting new result about shift between threshold for different subset and then concluding that they are insignificant. Based on Fig 7 and 8 I do think the

dataset of the author is insufficient to discuss these two topics and I would strongly suggest the author to remove these two sections (or just mention rapidly that sub dividing the dataset does not give clear difference and send Fig 7 and 8 in Supplement.) and give more space to discussing other points, like their critical rainfall model, or the uncertainties on rainfall.

R: Thanks for comments. The authors agree the conceptual view of reviewer. The discussion needs more solid information and field investigation. Therefore, the part about the influence of rock types and an extreme event has been removed and replaced with in-deep comparison of different rainfall threshold.

30. P11 section 5.3: maybe interesting but Fig 9 is too confusing. So I suspect text and Fig 9 should be clarified a bit.

R: To determine the limits of large landslide detection distance as a function of event volume, we selected the farthest seismic station at which each event was detectable. An event was deemed detectable when we had selected the station for the distance-dependency analysis. The remaining results are shown on a plot of distance versus disturbed area (Fig. 9), where we can observe an upper detection limit described by equation 5. If, for a given event, a station plots in the lower right area below the dashed line (equation (5)), the seismic signal should be detectable. The detection limit also depends on the station signal quality; if the noise level is high, the signal may be obscured, even though a station farther away with a lower noise level will still record it clearly. Similar studies had been reported by Dammeier et al. (2011) and Chen et al. (2013).

31. P11 Eq 5: to discuss validity and limits of EQ 5 it should be made clearer how (empirically?) and with which dataset/environment this relationship was obtained.

R: The authors appreciate reviewer's recommendation. In the study, the lower boundary of detection was determined empirically based on two lowest values of the farthest distance of detection (i.g. 31.0 km and 37.6 km) having the disturbed areas of 1.6×10^5 and $1.2 \times 10^5 \text{ m}^2$. Dammeier et al. (2011) used a similar way to get their equation of the lower boundary of detection. The modification has been added to text as follows:

“...The boundary of detection was determined empirically based on the two lowest values of the farthest distance of detection (i.e., 31.0 km and 37.6 km) having disturbed areas of 1.6×10^5 and $1.2 \times 10^5 \text{ m}^2$. For a given large landslide, if a station is located below the upper detection limit, the seismic signal should be detectable.

However, not all the stations located in detectable regions recorded clear large landslide-induced seismic signals....”

32. Fig 3: closest station is MASB (in the caption) or SGSB (in the map) ? It means 90% of the landslide and seismic signal

R: We deeply thanks for careful inspection. The closest station should be SGSB. The mistake has been revised in Figure 3 of the later version of manuscript.

33. Fig 5: The last panel is not very clear: Cumulated rainfall is the total rainfall in the triggering storm. Antecedent rainfall has no reason to be compared directly with landslide occurrence, but only when summed with the cumulated rainfall. So why not show R_t the total effective rainfall together with R_c the cumulative rainfall (Given that $R_t \geq R_c$ it should be easy to visualize).

R: Thanks for the constructive suggestion. The last panel in Figure 5 has been revised to display R_t and R_c . The revised Figure 5 is as below:

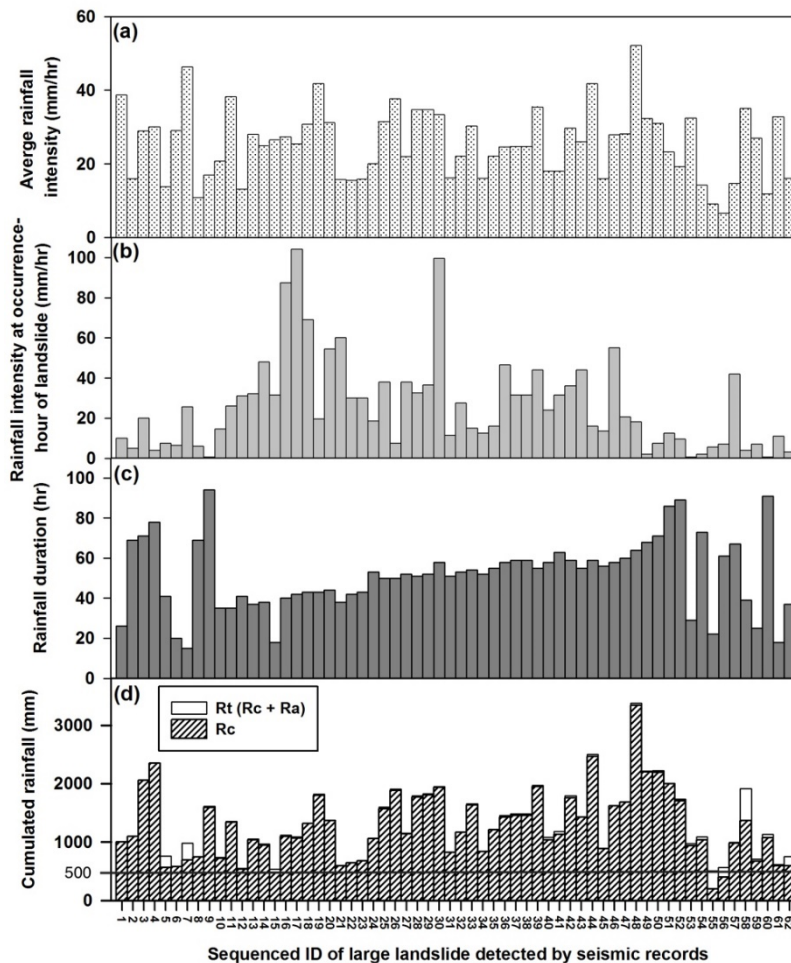


Figure 5

34. Fig 6: Log Log scale is needed on all panel. Right now we do not see clearly the position of the different data points.

R: Thanks for the constructive suggestion. All sub-figures in Figure 6 have been transferred to log-log scale as follows:

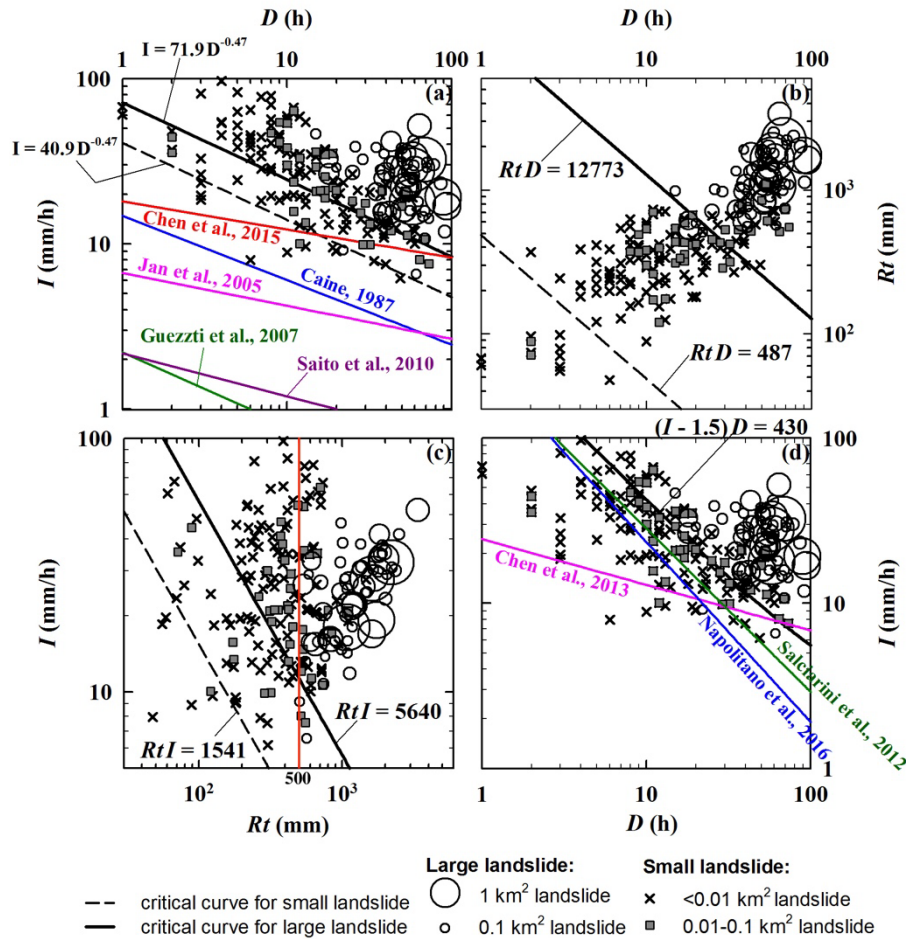


Figure 6

35. Fig 7 and 8: I do not believe any of the subset can be significantly distinguished. What is driving the (small) difference in threshold curve is only 1 or 2 points out of each subset (that seems to be 15-25 points). These low points shift the threshold while the bulk of each population do not seem different in any way. I am convinced this can only be due to chance and not to a shift of the whole population. I am even surprised that the curves are so low because if they are the 5% exceedance probability ~1 point should be left out in subset of ~20...

R: We appreciate the valuable comments, and decided to remove this section. Meanwhile, we added a section to illustrate the validation of the rainfall thresholds mentioned in the study and other previous studies.

36. Fig 9: I really tried, but did not understand it... I got that the line, is an empirical estimation of the distance at which station should be able to detect a landslide of a given size. What are the points? The 62 LSL? If yes, why are they all above the line? Does that mean only distant station detect the slides? I can believe for some but not the whole dataset, and this seems contradictory with Fig 3

R: This detection limit line is estimated empirically based on distribution of data which represented the farthest distance that landslide signal was detected. This result indicate that the distance between a station and a landslide below this line must be detected, but if it exceeds this line, it would probably be missed.

To determine the limits of large landslide detection distance as a function of event volume, we selected the farthest seismic station at which each event was detectable. An event was deemed detectable when we had selected the station for the distance-dependency analysis. The remaining results are shown on a plot of distance versus disturbed area (Fig. 9), where we can observe an upper detection limit described by equation 5. If, for a given event, a station plots in the lower right area below the dashed line (equation (5)), the seismic signal should be detectable. The detection limit also depends on the station signal quality; if the noise level is high, the signal may be obscured, even though a station farther away with a lower noise level will still record it clearly.

In total, 62 data points in Fig. 9. Each data point represents the distance between landslide location and the farthest detectable station as well as landslide-disturbed area. In the order words, it indicate that landslide signals can be detectable as the distance between landslide and seismic station shorter than the value of data. Therefore, to determine a lower boundary of these data can demarcate an effectively detectable region. The illustration of section 5.2 has been modified as follows:

“The number of large landslides detected from seismic records, 62, comprised only nine percent of the total large landslides in 2005–2014 in Taiwan. This low percentage indicates that the vast majority of large landslides were not well identified from seismic records. If this limitation can be surmounted, more time information on large landslide occurrences can be used to develop rainfall thresholds. The average interstation spacing of the Broadband Array in Taiwan for Seismology is around 30 km. A higher density of seismic stations would improve

the detection function. In addition, to determine the limitation of large landslide detection distance as a function of large landslide-disturbed area, the most distant seismic station where large landslide signals were visible was selected. Some previous studies have applied similar approaches to probe the detection limit (Dammeier et al., 2011; Chen et al., 2013). The relationship between the maximum distance of detection and the large landslide-disturbed area shows a limitation of the detection distance due to the large landslide's magnitude (Fig. 9). In Figure 9, each data point represents the distance between a landslide location and the most distant seismic station detecting it, as well as the landslide-disturbed area. In other words, when the distance between a seismic station and a landslide that has the same given landslide-disturbed area as the data is shorter than the value of the data, seismic signals induced by the landslide can be interpreted from the records of the seismic station. Therefore, a lower boundary of these data can be determined to demarcate an effective detectable region. As a large landslide's area increases, the maximum distance between the large landslide location and seismic detection increases. A detection limit can be described by

$$\log(\text{distance}) = 0.5069 \times \log(\text{area}) - 1.3443, \quad (5)$$

The boundary of detection was determined empirically based on the two lowest values of the farthest distance of detection (i.e., 31.0 km and 37.6 km) having disturbed areas of 1.6×10^5 and 1.2×10^5 m². For a given large landslide, if a station is located below the upper detection limit, the seismic signal should be detectable. However, not all the stations located in detectable regions recorded clear large landslide-induced seismic signals. One of the possible reasons is that the environmental background noise affected the signal to noise ratio of the seismic records during heavy rainfall events. Therefore, the detection limit may also depend on the signal quality at each station.”

37. References not used in the manuscript

-- **Wilson and Wieczorek 1995, Rainfall thresholds for the initiation of debris flows at La Honda, California**

-- **Iverson, 2000, Landslide triggering by rain infiltration**

-- **Van Asch et al., 1999, A view on some hydrological triggering systems in landslides**

Larsen et al., 2010, Landslide erosion controlled by hillslope material

R: Thanks for reviewing. The reference list has been overhauled completely before resubmitted.

Reference

- Wilson, R. C., and Wieczorek, G. F. (1995). Rainfall thresholds for the initiation of debris flows at La Honda, California. *Environmental & Engineering Geoscience*, 1(1), 11-27.
- Iverson, R. M. (2000). Landslide triggering by rain infiltration. *Water resources research*, 36(7), 1897-1910.
- Van Asch, T. W., Buma, J., and Van Beek, L. P. H. (1999). A view on some hydrological triggering systems in landslides. *Geomorphology*, 30(1-2), 25-32.
- Larsen, I. J., Montgomery, D. R., and Korup, O. (2010). Landslide erosion controlled by hillslope material. *Nature Geoscience*, 3(4), 247.

3. Reply to the comments of reviewer #2

The paper “Evaluating critical rainfall conditions for large-scale landslides by detecting event times from seismic records” is a very interesting paper with original approach. The combination of the tools and methods to define rainfall threshold to landsliding is interesting and the several steps of the analysis are presented. However, the reader can be lost in the used databases, in particular between what concerns the 2009 typhoon analysis and the rest of the chronical. The results can be discussed (detection of only 62 landslides, thresholds between 500/300mm...), or justified by figures completed (see below comments on the figures).

R: The authors appreciate the constructive feedback of the reviewer – it has certainly helped the authors improve this manuscript. The reply is summarized as below:

- 1) Some confusing statements (e.g. landslide number, topic event, study period, etc.) will be modified in the revised manuscript.
- 2) The authors will provide and modify the description of data sources, quality, and accuracy (including rainfall information, satellite image, and seismic records).
- 3) More in-deep discussion on results will be added in the modified version.
- 4) The suggested modification of methods and figures will be done in the manuscript.

Specific comments:

1. P2 L21: the event of 2009 is the only one mentioned, for the moment we can think that the research only focus on this event.

R: The authors appreciate the reminding. We agree that the current manuscript may confuse readers due to many examples belonging to Typhoon Morakot. In the study, totally nineteen rainstorm events (seventeen typhoon-induced events and two heavy rainfall events) in the period of 2005-2014 were selected to examine the seismic records, but not only one event. The modified manuscript will clearly describe the targets in the section of introduction and study materials. The list of selected typhoons and heavy rainfall events will be added to the modified version (Table S1).

In the original manuscript, Typhoon Morakot was mentioned many times because it was one of the most tragic event in Taiwan in the past 20 years (more than 20,000 landslides, and more than four hundred large landslides with the disturbed area larger than 0.1 km²), and therefore many good examples can be shown. In the modified version, the examples of other events have been provided in the supplementary material.

Table S1

	Event	Date (year/month/date)
1	Haitang	2005/07/16-07/20
2	Talim	2005/08/30-09/01
3	0609 Rain	2006/06/09
4	Bilis	2006/07/12-07/15
5	0604 Rain	2007/06/04
6	Kalmaegi	2008/07/16-07/18
7	Fung-Wong	2008/07/26-07/29
8	Sinlaku	2008/09/11-09/16
9	Morakot	2009/08/05-08/10
10	Fanapi	2010/09/17-09/20
11	Megi	2010/10/21-10/23
12	Nanmadol	2011/08/27-08/31
13	Talim	2012/06/19-06/21
14	Saola	2012/07/31-08/03
15	Tembin	2012/08/21-08/25
16	Soulik	2013/07/11-07/13
17	Trami	2013/08/20-08/22
18	Matmo	2014/07/21-07/23
19	Fung-Wong	2014/09/19-09/22

The modified text is as follows:

“...In this study, a total of nineteen rainstorm events (seventeen typhoon-induced events and two heavy rainfall events) in the years 2005–2014 were selected to examine the seismic records (Table S1). The seismic data during typhoons and heavy rainfall events having cumulated rainfall exceeding 500 mm from 2005 to 2014 were collected....”

2. P3 L8: Date of the images? Number? Mapping only for the 2009 event.

R: Thanks for comments. The date and number of used SPOT-4 satellite images have been listed in Table S2. Landslide mapping was conducted for nineteen rainstorm events (seventeen typhoon-induced events and two heavy rainfall events).

3. P3 L23: Why 0.1km² Is it the limit of the automatic detection based on SPOT images? How many landslides were detected?

R: Based on the definition and characteristic of deep-seated gravitational slope deformation (DSGSD) and description of large-scale landslides (Lin et al., 2013a; Lin

et al., 2013b), a large-scale landslide should have three characteristics, including 1) a depth larger than 10 m, 2) a volume greater than 1000,000 m³, and 3) a speedy movement velocity. In practice, it is difficult to get these three characteristics without in-situ investigation and geodetic survey. Therefore, we chose the disturbed area of 100,000 m² (0.1 km², volume/depth) as the indicator to sort large-scale landslides from other types of slope failure. Landslide interpretation with satellite imagery is the fastest way to classify large-scale landslides. Actually, more than three hundred seismic signals having the seismic characteristics of landslide-induced ground motions, however, only 62 signals having clear landslide-signal signatures were detected by at least three seismic stations. Therefore, we just could locate the possible locations of these 62 signals and paired the locating points with landslides. Although the successful detection and locating rate may be less than 20 % in the period of 2005-2014, we believe that the 62 landslides still provide many valuable time information.

Reference:

- Lin, C. W., Tseng, C. M., Tseng, Y. H., Fei, L. Y., Hsieh, Y. C., and Tarolli, P. (2013). Recognition of large scale deep-seated landslides in forest areas of Taiwan using high resolution topography. *Journal of Asian Earth Sciences*, 62, 389-400.
- Lin, M. L., Chen, T. W., Lin, C. W., Ho, D. J., Cheng, K. P., Yin, H. Y., and Chen, M. C. (2013). Detecting large-scale landslides using LiDar data and aerial photos in the Namasha-Liuoguey area, Taiwan. *Remote Sensing*, 6(1), 42-63.

The modified text is as follows:

“...Landslides induced specifically by rainstorm events were distinguished by overlaying the pre- and post-event image mosaics. Based on the definition and description of deep-seated gravitational slope deformation (DSGSD) and large landslides (Lin et al., 2013a; Lin et al., 2013b), a large landslide should possess three characteristics: 1) a depth larger than 10 m, 2) a volume greater than 1,000,000 m³, and 3) a high velocity. In practice, it is difficult to confirm these three characteristics without in-situ investigation and geodetic survey. Therefore, a disturbed area of 100,000 m² was determined as an accommodating indicator to sort large landslides from small landslides. Finally, large and small landslides were distinguished and classified according to the criterion of an affected area of 0.1 km². In this study, the types and mechanisms of individual landslides were not investigated, but landslide area was used as the main factor for investigating the different rainfall conditions that trigger large and small landslides.”

4. P3 L26: How we consider the progressive instability and the signal before the

main failure?

R: The authors agree that investigation of progressive instability is quite important. We believe that even slight displacement of materials on slope can stir energy transfer and induce seismic signals. However, the seismic signals generated by the processes of progressive deformation/displacement of material on slope do not contain enough energy to be recorded by remote seismic stations. Therefore, we did not try to monitor creeping processes by seismicity-approaches.

5. P4 L3: Now we don't care about 2009 event. Why 2005-2014? What was the aim of 2009?

R: Due to a large number of large landslides in 2009, the seismicity method for landslide-generated signals was successfully used. The study attempt to use the seismicity method for a longer period. Besides, the quality of seismic records of Taiwan's broadband seismic network had been significantly enhanced after 2005. The study period was decided to begin in 2005. In addition, identification of landslide-induced signals was conducted manually in the study. Therefore, identification cost a lot of time, and so far we finished the identification until 2014. So the study period during 2005-2004 was determined. It can be expected that more landslide signals will be found in the future.

6. P4 L11: "only events with obvious signature", do you mean the 62 landslides in the fig.1? can you develop the characteristics of the signal that you can highlight with these 62 events?

R: The sentence maybe not clear. The revision is as below:

“...To reduce the uncertainty caused by manual identification, events with obvious triangular signatures in the spectrograms (e.g. Fig. S1) were used to examine rainfall statistics in this study.”

The in-deep description of the characteristics of landslide-induced seismic signals has been added to text as follows:

“...The seismic wave generated by a landslide can be attributed to the shear force and loading on the ground surface as the mass moves downslope. Many studies have shown that the source mechanism of a landslide is highly complicated, and that its seismic waves mainly consist of surface waves and shear waves, making it difficult to distinguish *P* and *S* waves from station records (Lin et al., 2010; Suwa et al., 2010; Dammeier et al., 2011; Feng, 2011; Hibert et al., 2014). The

onset of a landslide seismic signal is generally abrupt. Then the seismic amplitude increases gradually above the ambient noise level to peak ground motion, exhibiting a cigar-shaped envelope. After the peak amplitude, most of the landslide-generated seismic signals have relatively long decay times, on average about 70% of the total signal duration (Norris, 1994; La Rocca et al., 2004; Suriñach et al., 2005; Deparis et al., 2008; Schneider et al., 2010; Dammeier et al., 2011; Allstadt, 2013). In the frequency domain, landslide-induced seismic energy is mainly distributed below 10 Hz, with a triangular signature in a spectrogram, due to an increase over time in high-frequency constituents (Suriñach et al., 2005; Dammeier et al., 2011). The triangular signature in the spectrogram is the distinctive property that readily distinguishes landslide-induced signals from those of earthquakes and other ambient noise.”

Reference:

- Allstadt, K. (2013). Extracting source characteristics and dynamics of the August 2010 Mount Meager landslide from broadband seismograms. *Journal of Geophysical Research: Earth Surface*, 118(3), 1472-1490. doi:10.1002/jgrf.20110.
- Dammeier, F., Moore, J. R., Haslinger, F., and Loew, S. (2011). Characterization of alpine rockslides using statistical analysis of seismic signals. *Journal of Geophysical Research*, 116(F4). doi:10.1029/2011jf002037
- Deparis, J., Jongmans, D., Cotton, F., Baillet, L., Thouvenot, F., and Hantz, D. (2008). Analysis of rock-fall and rock-fall avalanche seismograms in the French Alps. *Bulletin of the Seismological Society of America*, 98(4), 1781-1796. Doi:10.1785/0120070082.
- Feng, Z. (2011). The seismic signatures of the 2009 Shiaolin landslide in Taiwan. *Natural Hazards and Earth System Science*, 11(5), 1559-1569. Doi:10.5194/nhess-11-1559-2011
- Hibert, C., Ekström, G., and Stark, C. P. (2014). Dynamics of the Bingham Canyon Mine landslides from seismic signal analysis. *Geophysical Research Letters*, 41(13), 4535-4541. Doi:10.1002/2014gl060592
- La Rocca, M., Galluzzo, D., Saccorotti, G., Tinti, S., Cimini, G. B., and Del Pezzo, E. (2004). Seismic signals associated with landslides and with a tsunami at Stromboli volcano, Italy. *Bulletin of the Seismological Society of America*, 94(5), 1850-1867. Doi:10.1785/012003238.
- Lin, C. H., Kumagai, H., Ando, M., and Shin, T. C. (2010). Detection of landslides and submarine slumps using broadband seismic networks. *Geophysical Research Letters*, 37(22), n/a-n/a. doi:10.1029/2010gl044685

- Norris, R. D. (1994). Seismicity of rockfalls and avalanches at 3 Cascade Range volcanos – Implications for seismic detection of hazardous mass movements. *Bulletin of the Seismological Society of America*, 84(6), 1925-1939.
- Schneider, D., Bartelt, P., Caplan-Auerbach, J., Christen, M., Huggel, C., and McArdell, B. W. (2010). Insights into rock-ice avalanche dynamics by combined analysis of seismic recordings and a numerical avalanche model. *Journal of Geophysical Research*, 115(F4). Doi:10.1029/2010jf001734.
- Surinach, E., Vilajosana, I., Khazaradze, G., Biescas, B., Furdada, G., and Vilaplana, J. M. (2005). Seismic detection and characterization of landslides and other mass movements. *Natural Hazards and Earth System Sciences*, 5, 791-798.
- Suwa, H., Mizuno, T., and Ishii, T. (2010). Prediction of a landslide and analysis of slide motion with reference to the 2004 Ohto slide in Nara, Japan. *Geomorphology*, 124(3-4), 157-163. Doi:10.1016/j.geomorph.2010.05.003.

7. P4 L19: how can you consider the lag time between rainfall / soil saturation... and failure?

R: Thanks for the valuable comments. This study used seismic signals to find out landslide occurrence time, and undoubtedly this time information could help to study the infiltration of rainfall or the relationship between soil saturation and landslides. However, this study currently focused on constructing and compare the rainfall thresholds for landslide warning, the traditionally statistical methods to estimate rainfall threshold were chosen. Time lag between rainfall history and soil saturation process was not considered in the study.

8. P4 L29: I think the chosen method can be shortly developed here.

R: Thanks for t your suggestion. The detailed content of locating method has been added to the text as follows:

“.... Locations were estimated with a cross-correlation method that could maximize tremor signal coherence among the seismic stations. The criteria of the stations chosen were their geographic distribution and tremor signal-to-noise ratios. The interpreted signals were treated with an envelope function to process cross-correlations analysed from different station pairs. Centroid location estimates were obtained by cross-correlating all station pairs and performing the Monte Carlo grid search method (Wech and Creager, 2008). While traditional methods seek the source location that minimizes the horizontal time difference between predicted travel time and peak lag time, this method seeks to minimize the vertical correlation distance between the peak correlation value and the

predicted correlation value.”

Reference:

Wech, A. G., and Creager, K. C. (2008). Automated detection and location of Cascadia tremor. *Geophysical Research Letters*, 35(20).

9. P4 L35: there is only Xiaolin landslide in this figure. So you focus on 2009 events? do you compared all the landslides detected by remote sensing (fig.1 is it landslides detected by seismic signal of remote sensing; to clarify) (how many by remote sensing?) with the seismic signal? an example of signal related to a smaller event than Xiaolin would be interesting (fig.3). Do the SSLs have a significant signal also?

R: Thanks for the comments. In the figure 2c, five matched landslides (including Xiaolin) were visible. Each orange circle means a successfully-paired landslide. The outline of each paired landslide will be added to the figure. Theoretically, the seismic signal induced by a small landslide could be found if there is a seismic station very close to it. In practice, the seismic signals generated by small landslides do not contain enough energy to be recorded by remote seismic stations. Therefore, we do not try to examine small landslides by seismicity approaches. Besides, the signal and spectrogram of a 2005 large landslide smaller than Xiaolin will be provided and added to supplementary material as below:

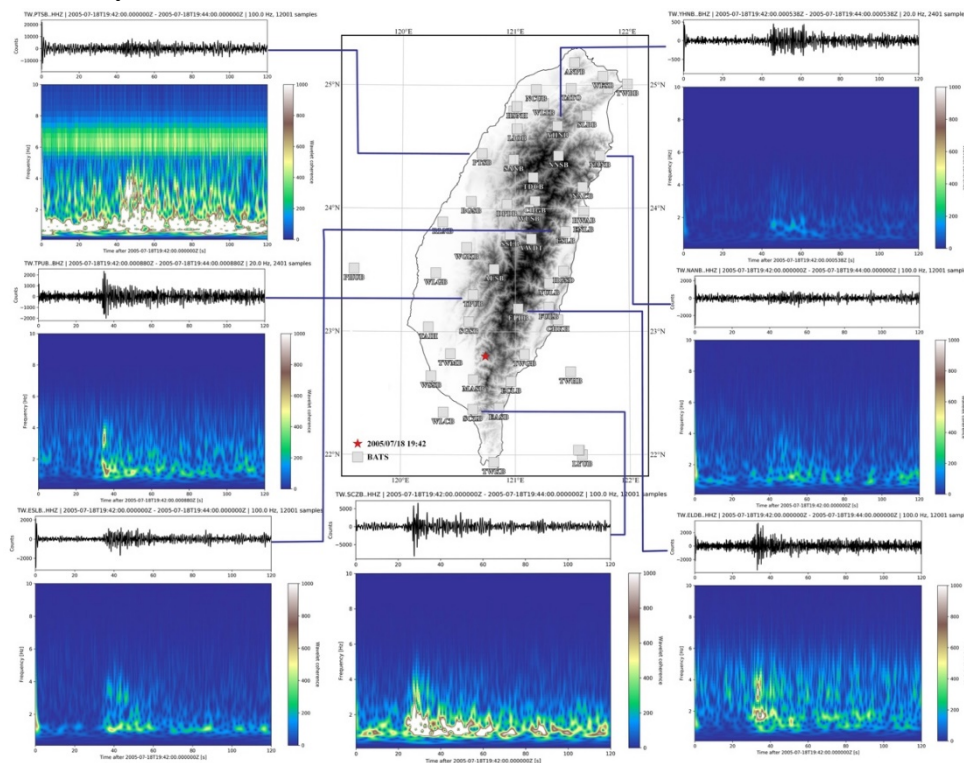


Fig. S1

10. P5 L3: Now you are studying events between 2005-2014? It is a little bit confusing. How many typhoon events? don't you consider previous smaller rainfall events that could affect the mechanical properties of the slopes?

R: In the study, totally seventeen typhoon events and two heavy rainfall events occurring in the period of 2005-2014 were chosen to examine the seismic records and identify landslide-induced signals. The list of selected events has been provided in Table S1.

In the study, seven-days antecedent rainfall was considered as a rainfall parameter. The effect of antecedent rainfall should decay with time. Therefore, decay rate of antecedent rainfall with day was used to estimate effective rainfall. According to the decay rate, 0.7, the effect of antecedent rainfall with counting days longer than 7 days is slight. In the study, we adopt seven-days antecedent rainfall to estimate effective rainfall.

Table S1

	Event	Date (year/month/date)
1	Haitang	2005/07/16-07/20
2	Talim	2005/08/30-09/01
3	0609 Rain	2005/06/09
4	Bilis	2005/07/12-07/15
5	0604 Rain	2006/06/04
6	Kalmaegi	2006/07/16-07/18
7	Fung-Wong	2008/07/26-07/29
8	Sinlaku	2008/09/11-09/16
9	Morakot	2009/08/05-08/10
10	Fanapi	2010/09/17-09/20
11	Megi	2010/10/21-10/23
12	Nanmadol	2011/08/27-08/31
13	Talim	2012/06/19-06/21
14	Saola	2012/07/31-08/03
15	Tembin	2012/08/21-08/25
16	Soulik	2013/07/11-07/13
17	Trami	2013/08/20-08/22
18	Matmo	2014/07/21-07/23
19	Fung-Wong	2014/09/19-09/22

11. P5 L6: How can you consider the topographic, orographic effects?

R: We appreciate the comments. We tested the rainfall data used in the study to validate the influence of distance and topographic effect on rainfall distribution. The effect of rain gauge distribution over the accuracy of rainfall has been assessed using gauge observation in a 35 km × 50 km region of south Taiwan (Fig. S2). The amounts of daily rainfall during 2009 Typhoon Morakot (8/6-8/11) recorded at 19 rain gauge stations were selected to validate the accuracy of rainfall. The influence of topography on rainfall variability has been analyzed in the same 35 km × 50 km region of south Taiwan. The highest station elevation is 1792 m a.s.l. at C1V270, and the lowest station elevation is 105 m a.s.l. at C10830. The standard deviation of station elevation is 561 m. The values of standard deviation of daily rainfall at the 19 stations were calculated, and less than 13% except a high standard deviation, 45%, on sixth August (average daily rainfall less than 2 mm). The results demonstrated that high and even extreme rainfall are less influenced by elevation, while low and medium rainfall events are significantly influenced by elevation variation, with most of the rainfall appearing on high elevations. Similar results have also been reported by some previous studies (Sanchez-Moreno et al., 2014; Ge et al., 2017). Because the study only considered the rainfall events with total cumulated rainfall greater than 500 m, the elevation effect was ignored as selecting rain station.

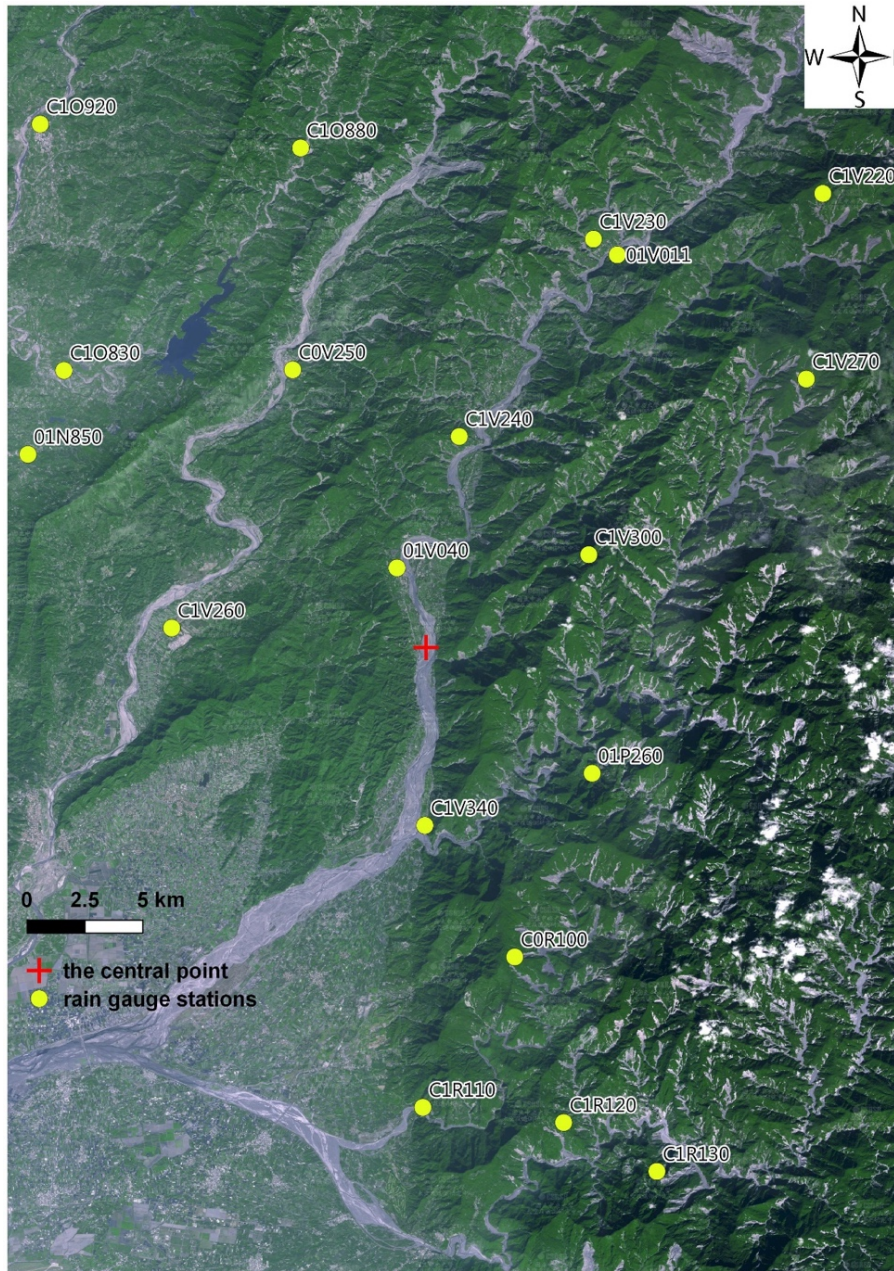


Fig. S2

Reference:

- Sanchez-Moreno, J.F., Mannaerts, C.M., and Jetten, V. (2014) Influence of topography on rainfall variability in Santiago Island, Cape Verde. *International Journal of Climatology*, 34, 1081-1097.
- Ge, G., Shi, Z., Yang, X., Hao, Y., Guo, H., Kossi, F., Xin, Z., Wei, W., Zhang, Z., Zhang, X., Liu, Y., and Liu, J. (2017) Analysis of Precipitation Extremes in the Qinghai-Tibetan Plateau, China: Spatio-Temporal Characteristics and Topography Effects. *Atmosphere*, 8(7), 127, doi:10.3390/atmos8070127.

12. P5 L10: 100km² is already large catchment.

R: The effect of station distance has been tested to variation of rainfall. The errors of daily rainfall between the central point and the nearest rain gauge station (01V040) were smaller than 10 % (0.5%-10% at different date). Besides, the correlation coefficients would keep at 90% as a distance between the central point and rain gauge stations less than 20 km, and even keep at 98% as a distance less than 10 km (Fig. S3). Therefore, in the study, an upper limit of basin area smaller than 100 km² (10 km × 10 km) was adopted to avoid a significant decrease of the accuracy of rainfall. Because the density of rainfall stations in mountainous area would significantly decrease, the number of usable rainfall stations may be limited. The size of catchment area of 100km² is the upper limit for choose rainfall station. In practice, we chose the closest rainfall station.

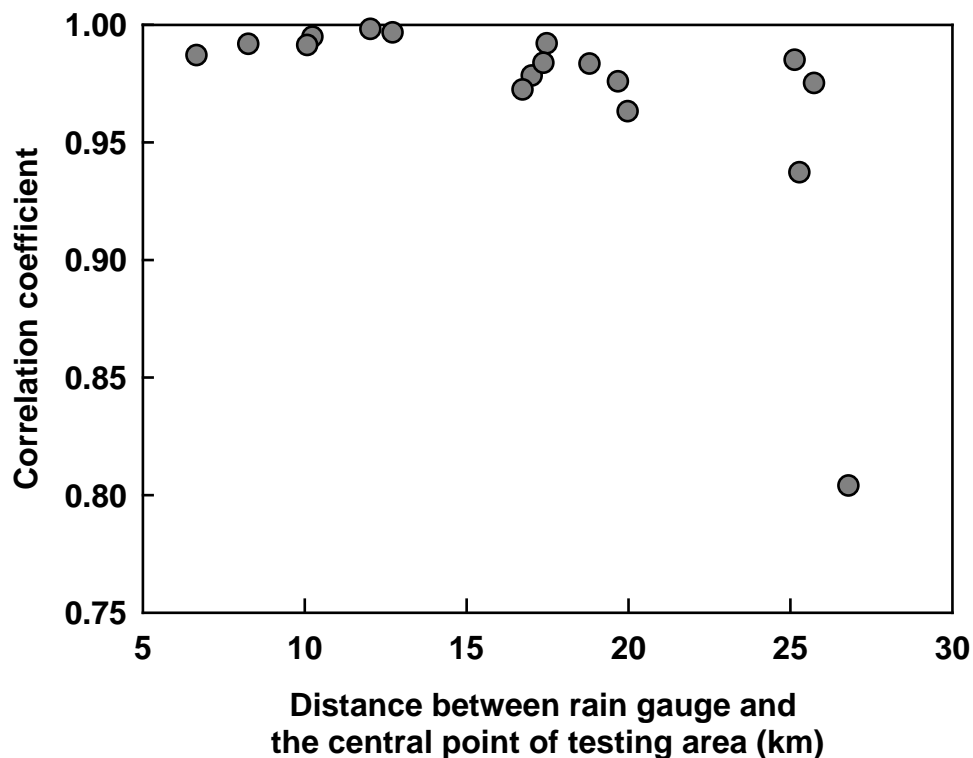


Fig. S3

13. P5 L2: rain event = typhoon?

R: Yes. The sentence has been revised as below.

“In the study, hourly rainfall data were collected from the records of rain gauge stations (Fig. 2a). The major rainfall events analysed in the study were typhoon events. The distribution of precipitation during typhoon events is usually closely related to the typhoon track and the position of the windward slope, also as known

as the orographic effect....”

14. P6 L4: 193 small landslides for which period?

R: The 193 small landslides were investigated by SWBC during 2006-2014. The illustration on the small landslides has been improved in the later version of manuscript as below.

“In addition to that of large landslides, the time information of 193 small landslides such as shallow landslides and debris flows from the years 2006–2013 was collected from the annual reports of debris flows investigated by the Soil and Water Conservation Bureau (SWCB) of Taiwan, but it was not extracted from seismic records. Most of the 193 small landslides caused disasters and loss of life and property. In some cases, in-situ steel cables or closed-circuit television recorded the time information. This information was applied to the rainfall data analysis and then used to compare the rainfall conditions of the large landslides”

15. P6 L15: EQ1 cohesion here is only considered for a discontinuity ($C = 0$)? Or for the specific material?

R: We thanks reviewer’s recommendation. Well development of detachment plane (e.g., sliding surface between sedimentary layers, connected joints, weathered foliation, etc.) have been widely considered as one important geological condition to induce a large landslide. Therefore, in the study, the C' of the detachment plane is simply assumed as the value of zero to behave the critical situation of slope stability. Cohesion in equation (1) is not considered for a specific material. The illustration of C' has been modified in the text as below.

“...Good development of a detachment plane (e.g., sliding surface between sedimentary layers, connected joints, and weathered foliation) has been widely considered as the geological condition under which a large landslide occurs (Agliardi et al., 2001; Tsou et al., 2011). Therefore, in this study, the c' of the detachment plane is simply assumed to be zero to represent the critical situation of slope stability.”

Reference:

- Tsou, C. Y., Feng, Z. Y., & Chigira, M. (2011). Catastrophic landslide induced by typhoon Morakot, Shiaolin, Taiwan. *Geomorphology*, 127(3-4), 166-178.
- Agliardi, F., Crosta, G., & Zanchi, A. (2001). Structural constraints on deep-seated slope deformation kinematics. *Engineering Geology*, 59(1-2), 83-102.

16. P7 L9/22: lower slopes VS steeper slopes... upslope VS downslope? Can you explain it? Is it a regressive erosion of the slope?

R: Thanks for the important reviewing. The sentence should be revised as below:

“...Although the increase was quite slight, it was most likely due to the fact that during the extremely heavy rainfall of Typhoon Morakot in 2009, more than 2000 mm precipitated in four days, causing a large number of landslides and exhausting many unstable slopes. Consequently, landslides occurred on steeper slopes in the following years....”

17. P7 L9/24 & 26: landslides for 2009 event? Or the detection of 62 landslides grounded on seismic signal among 686 inventoried landslides? What is the landslide seismic magnitude?

R: In this section, the topographic analysis was for 686 large landslides during 2005-2014. The paragraph will be modified to avoid confusion. We did not calculate landslide seismic magnitude in the study due to the lack of a standard method for estimating landslide seismic magnitude so far.

18. P8 L4: what about SSL?

R: Most of the small landslides have strong instantaneous rainfall intensity. This means that a short duration and heavy rainfall can easily trigger small landslides.

Discussion:

The discussion is interesting because it puts the results in perspective. Nevertheless, some points have to be clarify.

19. 5.1. The authors highlight the fact that critical rainfall to trigger landslides has decreased since 2010 (500mm to 300mm) according to the results fig. 7. How many events the threshold is based on? The figure 7 is not so evident.

To explain these results, the authors question the Morakot typhoon. Was it an exceptional hydro-climatic event? The other solution is that instabilities induced by the 2009 typhoon are responsible of recent landslides. This idea should be developed here, and maybe associated to a map of the landslides scars (delineation of the departure areas) and differentiated according to the periods of the triggering...

R: Thanks for comments. The authors agree the conceptual view of reviewer. The discussion needs more solid information and field investigation. Therefore, the part

about the influence of rock types and an extreme event will be removed and replaced with in-deep comparison of different rainfall threshold.

20. 5.2. The authors mention the fact that landslides occurred several types of rocks with different geotechnical behaviors, but the chosen geotechnical parameters (table 1) are identical. Why?

R: The main research purpose of this study was to establish a rainfall warning threshold which is applicable for large landslides, so a relatively simple but effective method was adopted. In this method, Keefer (1987) assumes that there is a potential sliding surface for these landslides, and the depth of the large-scale landslides are often deep to the strata. Therefore, although the movements of the soil material are not completely the same, under this assumption, it can still reach a considerable good effect.

In order to improve the Q_c threshold, the critical volume of water, Q_c , for each large landslide was estimated based on its slope gradient and depth (estimated by the equation: $Z = 26.14A^{0.4}$; Z : depth, m; A : disturbed area, m^2). Following the equation (4), the drainage rate, I_0 , for each landslide can be calculated. For the 62 detected landslide, the cumulative probability of 5% of Q_c and I_0 values was taken as the critical values in the mixing physically- and statistically-based threshold. The critical value of I_0 was 1.5, and the critical Q_c was 430.2. The paragraph has been modified as follows:

“The critical height of water, Q_c , on a sliding surface for each large landslide was estimated based on its slope gradient, depth (estimated by the equation $Z = 26.14A^{0.4}$; Z : depth in m; A : disturbed area in m^2), and the geological material parameters of the study area (Table 1). The Q_c value was inserted into $Q_c = (I - I_0) \cdot D$ to obtain an I_0 value for each large landslide. For the 62 detected landslides, the cumulative probability of 5% of the Q_c and I_0 values was taken as the critical value. The critical value of I_0 was 1.5, the critical Q_c was 430.2, which is more suitable for large than for small landslides, and the threshold curve was rewritten as $(I - 1.5) \cdot D = 430.2$.”

21. Effective rainfall, and rainfall duration thresholds according to the rock types are not clear in the figure 8, could another statistical analysis put the conclusion of the authors in obvious fact?

R: Thank you for your suggestion. The figure has been removed.

Figure:

22. Fig. 2. Add legend for the detected landslide: Is it detected by seismic signal

analysis? Is the point, the centroid of the landslide? Why not the delineation of the landslide body? Dates of the both satellite images here.

R: Thank you for your suggestion. The figure has been modified based on suggestions.

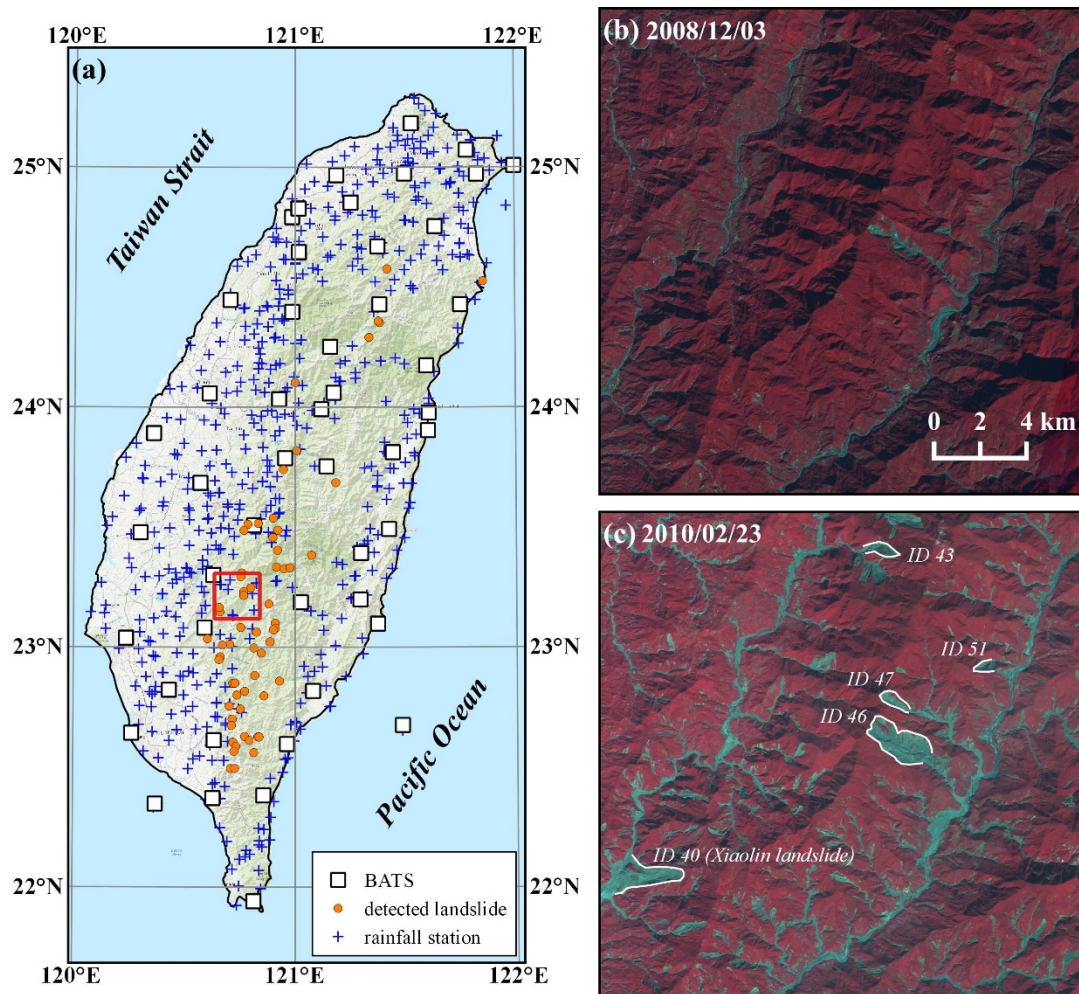


Figure 2

23. Fig. 3. Location of the detected landslides in 2009? Is there other spectrogram for previous landslides? Or after 2009? or associated to another landslide triggered in 2009: X spectrogram for 1 landslide. The star is the location defined with which seismic station?

R: This events, the Xioulin landslide, is one of the most tragic event during Typhoon Morakot, 2009. The other 61 detected landslides also have the triangle-shape characteristic patterns in their spectrograms. The star is the location defined with all the stations which could detect the signals from the Xioulin landslide. We provided one example of spectrograms of a landslide in 2005 in supplementary materials (Fig. S1) and one example of a 2015 landslide in Figure 7.

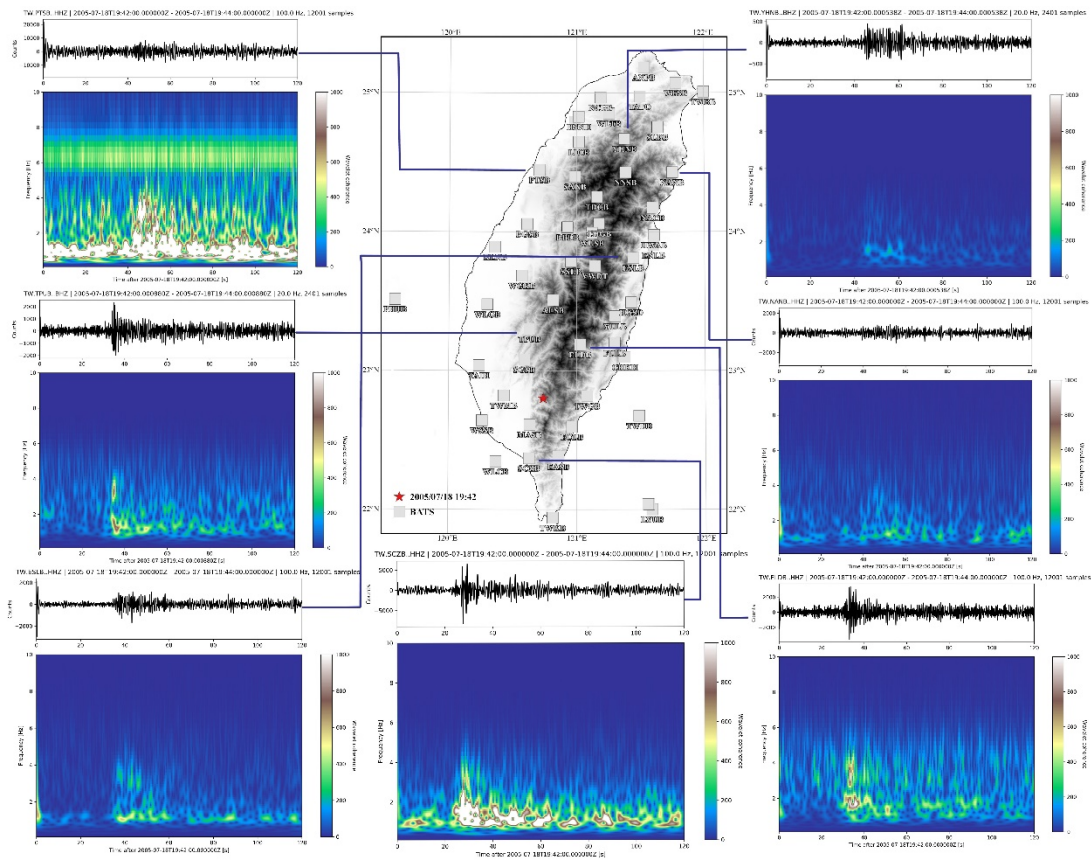


Fig. S1

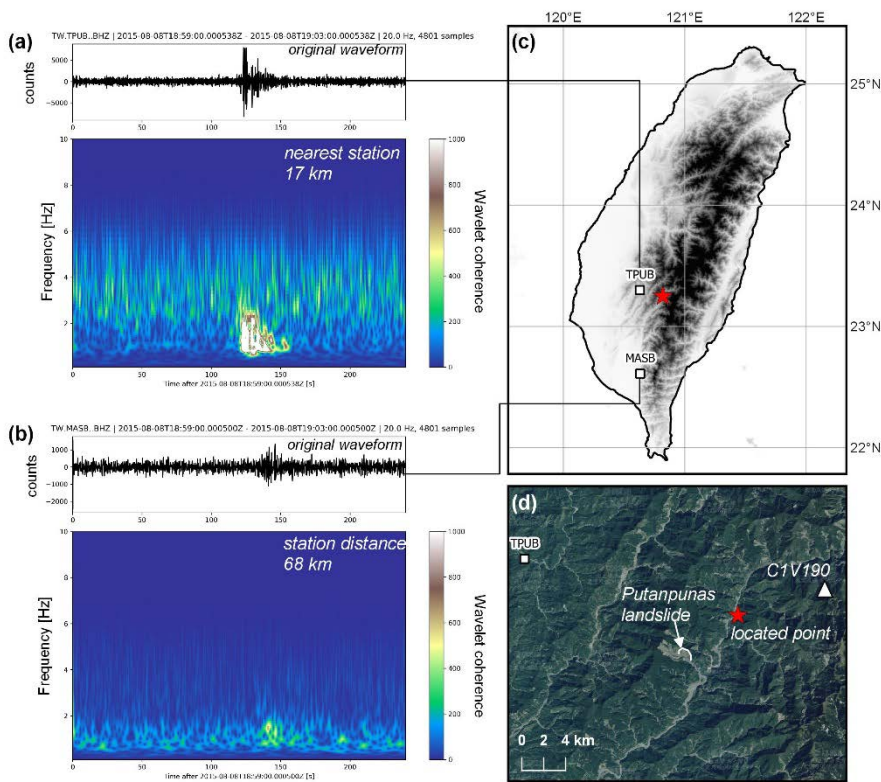


Figure 7

24. Fig. 4. Maybe with the topography visible on the map?

R: Thank you for your suggestion. We had tried added topography in the fig. 4a. However, so many information made visually chaotic.

25. Fig. 7. A) Is there only 1 event for the lowest limit?

R: Yes. The figure will be removed in modified version.

Certificate of Editing

This is to certify that the academic paper

Evaluating critical rainfall conditions for large-scale landslides by detecting event times from seismic records

by the authors

Hsien-Li Kuo¹, Guan-Wei Lin^{1,*}, Chi-Wen Chen², Hitoshi Saito³, Ching-Weei Lin¹, Hongey Chen^{2,4}, Wei-An Chao⁵

¹ Department of Earth Sciences, National Cheng Kung University, No. 1, University Road, Tainan City, 70101, Taiwan

² National Science and Technology Center for Disaster Reduction, No. 200, Sec. 3, Beixin Road, Xindian District, New Taipei City, 23143, Taiwan

³ College of Economics, Kanto Gakuin University, 1-50-1 Mitsuura-higashi, Kanazawa-ku, Yokohama, 236-8501, Japan

⁴ Department of Geosciences, National Taiwan University, No.1, Section 4, Roosevelt Road, Taipei, 10617, Taiwan

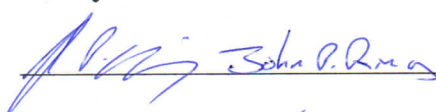
⁵ Department of Civil Engineering, National Chiao Tung University, No. 1001, Daxue Rd., Hsinchu, 30010, Taiwan

has been proofread and edited by a native speaker of English.

The editor, Mr. John Pearson Ring, is an established freelance science editor with twenty years of experience. He was born and raised in Brunswick, Maine, USA, and earned a Bachelor of Arts degree at Hamilton College in Clinton, New York, USA. He is currently the Head Coordinator at the Language Training and Testing Center, Taipei, Taiwan (<https://www.lttc.ntu.edu.tw/>), and was formerly a freelance editor for the Academic Writing Education Center at National Taiwan University, Taipei, Taiwan (<http://www.awec.ntu.edu.tw/>).

Signed and dated by the editor described above:

Signature:

 _____

Date:

 _____

Contact Information:

John P. Ring

Email: johnringintaiwan@yahoo.com

Mobile: (+886) 939 647 451

Evaluating critical rainfall conditions for large-scale landslides by detecting event times from seismic records

Hsien-Li Kuo¹, Guan-Wei Lin^{1,*}, Chi-Wen Chen², Hitoshi Saito³, Ching-Weei Lin¹, Hongey Chen^{2,4}, Wei-An Chao⁵

5 ¹ Department of Earth Sciences, National Cheng Kung University, No. 1, University Road, Tainan City, 70101, Taiwan

² National Science and Technology Center for Disaster Reduction, No. 200, Sec. 3, Beixin Road, ~~Xindian~~Xindian District, New Taipei City, 23143, Taiwan

³ College of Economics, Kanto Gakuin University, 1-50-1 Mitsuura-higashi, Kanazawa-ku, Yokohama, 236-8501, Japan

⁴ Department of Geosciences, National Taiwan University, No.1, Section 4, Roosevelt Road, Taipei, 10617, Taiwan

10 ⁵ Department of Civil Engineering, National Chiao Tung University, No. 1001, Daxue Rd., Hsinchu, 30010, Taiwan

*Correspondence to: Guan-Wei Lin (gwlin@mail.ncku.edu.tw)

Abstract. One of the purposes of ~~slope-disaster~~landslide research is to establish an early warning method for rainfall-induced landslides. The insufficient ~~observational-records~~observations of the past, however, have inhibited the analysis of critical rainfall conditions. This dilemma may be resolved by extracting the times of landslide occurrences from the seismic signals recorded by adjacent seismic stations. In this study, the seismic records of the Broadband Array in Taiwan for Seismology (~~BATS~~) were examined to identify the ground motion triggered by large-scale landslides occurring from 2005 to 2014. ~~After the signals from local and teleseismic earthquakes were eliminated,~~A total of 62 landslide-induced seismic signals were identified. The seismic signals provided the occurrence times of the landslides for assessment of the rainfall conditions, including rainfall intensity (I , mm/h), duration (D , h), and ~~accumulated~~effective rainfall (R , mm/Rt). Comparison of three common rainfall threshold models ($I-D$, $I-R$, and $R-R$) revealed duration and ~~accumulated~~effective rainfall to be the crucial factors in developing a forecast warning model. In addition, a critical ~~volume~~height of water model, ~~$(I-1.04) \cdot D = 452$ mm~~, combining ~~physical and statistical and deterministic~~ approaches, ~~$(I-1.5) \cdot D = 430.2$~~ , was established through analysis of rainfall information from the 62 large-scale landslides that occurred. ~~The critical height of water model was applied to Typhoon Soudelor of 2015 and successfully issued a large landslide warning for southern Taiwan.~~

25 Key words: large-scale landslide, seismic signal, rainfall threshold, forecast

1. Introduction

In recent years, the frequency of extreme rainfall events has increased globally, as has the number of large-scale natural disasters (Tu and Chou, 2013; Saito et al., 2014). These large-scale natural disasters (e.g., landslides, floods, etc.) cause both huge economic losses and human casualties. In mountainous areas, large-scale landslides (~~L~~LSLs) can change the landscape and erosion processes as well. Several previous studies have reported that the characteristics of a large-scale landslide may include (1) extremely rapid mass movement, (2) huge landslide volume, and (3) deep-seated excavation into rock formations (Chigira and Kiho, 1994; Lin et al., 2006). However, the discrimination of large-scale and non-large-scale landslides is still ~~indistinct~~challenging. In practice, the velocity of mass movement and depth of excavation are both difficult to measure, so the landslide area is commonly regarded as an indicator of the scale of a landslide. Although the occurrence frequency of ~~L~~LSLs is lower than that of non-large-scale landslides, known as small-scale landslides (~~S~~SSLs), ~~L~~LSLs, large landslides cause rapid changes in the landscape, and the scale of ~~L~~LSL-induced disasters ~~induced by large landslides~~ is greater than that of ~~S~~SSLs. Therefore, in this study, a landslide that disturbed an area larger than 0.1 km² is considered a large-scale landslide, while one not meeting this criterion is considered a small-scale landslide. It is well known that rainfall plays a significant role in the occurrence of landslides, so thorough understanding of the influences of different rainfall factors

is necessary. To reduce losses, the critical rainfall conditions that trigger ~~LSLs~~large landslides must be identified so that a rainfall threshold can be used as a forecast model to execute disaster prevention and mitigation measures.

In past research, it was difficult to estimate the threshold of precipitation convincingly due to the lack of accurate information on the occurrence times of landslides. Recent studies in geophysics (Kanamori et al., 1984; Suriñach et al., 2005; Lin et al., 2010; Ekström and Stark, 2013; Chao et al., 2016; Chao et al., 2017) have suggested that the mass movement of large-scale landslides may generate ground motion. If such ground motion is recorded by seismic stations, the occurrence times of large-scale landslides can be extracted from the records. In one case study, the rainfall that triggered the Xiaolin landslide, a giant landslide in southern Taiwan that disturbed an area of ~2.6 km² and resulted in more than 400 deaths in August 2009, was examined. ~~It was found that if the occurrence time of the landslide was unknown,~~In general, if the exact occurrence time of a landslide cannot be investigated, the time point with the maximum hourly rainfall will be conjectured as the occurrence time of the landslide (Chen et al., 2005; Wei et al., 2006; Staley et al., 2013; Yu et al., 2013; Xue et al., 2016). It was found that the time error between the conjectured and exact times would be 13 hours, which would result in an erroneous cumulated rainfall measurement of 513.5 mm (Fig. 1). However, with the assistance of seismic records, the time information for estimating critical rainfall can be acquired.

~~This study attempts to determine the occurrence times of landslides by identifying landslide-generated seismic signals to construct rainfall thresholds, and to clarify which thresholds are more suitable for triggering different warnings for small and large landslides.~~ By applying various rainfall factors into statistical analysis, a statistical threshold can be built to explore the critical rainfall conditions of landslide occurrences, such as using rainfall intensity and duration to define rainfall threshold curves (Caine, 1980; Guzzetti et al., 2008; Saito et al., 2010; Chen et al., 2015). Those rainfall thresholds provide valuable information for disaster prevention and mitigation. In this study, ~~we used~~ seismic data recorded by the network of the Broadband Array in Taiwan for Seismology (BATS) (Fig. 2a) and landslide maps generated from satellite images ~~were used~~ to obtain the exact occurrence times and locations of ~~LSLs~~large landslides. From these, ~~we developed~~ the rainfall threshold for ~~LSLs~~large landslides in Taiwan ~~was developed~~. Moreover, located at the junction of the Eurasian plate and the Philippine Sea plate, Taiwan has frequent tectonic activity (Ho, 1986; Yu et al., 1997; Willett et al., 2003). ~~Fractural-geological conditions~~Fractured rock mass coupled with a warm and humid climate, and an average of 3 to 5 typhoon events per year, contribute to the high frequency of slope ~~disasters~~failures in mountainous areas in Taiwan (Wang and Ho, 2002; Shieh, 2000; Dadson et al., 2004; Chang and Chiang, 2009; Chen, 2011). The high coverage of the seismic network and rain gauge stations in Taiwan, coupled with the high occurrence frequency of landslides, make the island a suitable area for examining the use of seismic observations to identify landslide occurrence times and thus the rainfall factors contributing to landslide events.

2. Study Method

2.1 Large-scale landslide mapping

To determine the locations and basic characteristics of ~~LSLs~~large landslides occurring in the years 2005–2014, the landslide areas across the entire island of Taiwan were interpreted using SPOT-4 satellite remote sensing images with a spatial resolution of 10 m in multispectral mode. Images with minimal cloud cover were selected from pre- and post-typhoon and heavy rainfall events. All images were orthorectified to a standard base image and checked manually using fixed visible markers to ensure spatial consistency over time. Figures 2b and 2c show synthetic SPOT images that were used to identify landslides triggered by Typhoon Morakot in 2009. Bare areas are visibly distinguishable in the SPOT images.

40

The Normalized Difference Vegetation Index (NDVI) was used to conduct a preliminary classification of bare areas (Lin et al., 2004). The exact NDVI thresholds for bare areas differed from one image to another and were determined by tuning the cut-off value based on visible contrasts. After image interpretation, classified areas were clustered based on slope using a digital elevation model with a resolution of 40 m to identify bare areas not associated with landslides (e.g., roads and buildings).

5 The results of the interpretation were compared with a 1:5000 topographic map to exclude areas of interpretation misjudgement, such as fallow farmland or alluvial fans. Landslides induced specifically by ~~a~~-rainstorm ~~event~~events were distinguished by overlaying the pre- and post-event image mosaics. Based on the definition and description of deep-seated gravitational slope deformation (DSGSD) and large landslides (Lin et al., 2013a; Lin et al., 2013b), a large landslide should possess three characteristics: 1) a depth larger than 10 m, 2) a volume greater than 1,000,000 m³, and 3) a high velocity. In practice, it is difficult to confirm these three characteristics without in-situ investigation and geodetic survey. Therefore, a disturbed area of 100,000 m² was determined as an accommodating indicator to sort large landslides from small landslides. Finally, ~~LSL~~large and ~~SSL~~small landslides were distinguished and classified according to the criterion of an affected area of 0.1 km². In this study, the types and mechanisms of individual landslides were not investigated, but landslide area was used as the main factor for investigating the different rainfall conditions that trigger LSLlarge and small landslides.

15 **2.2 Interpretation of ground motions induced by large-scale landslides**

The movement of a landsliding mass has several different motion processes, such as sliding, falling, rotation, saltation, rolling and impacting. These complex motion processes act on the ground surface to generate ground motion (Kanamori et al., 1984; Ekström and Stark, 2013). When this ground motion is recorded by adjacent seismic stations, the landslide-related pattern in a spectrogram develops a triangular time/frequency signature in the 1–10 Hz frequency band (Suriñach et al. 2005; Chen et al. 2013).The seismic wave generated by a landslide can be attributed to the shear force and loading on the ground surface as the mass moves downslope. Many studies have shown that the source mechanism of a landslide is highly complicated, and that its seismic waves mainly consist of surface waves and shear waves, making it difficult to distinguish *P* and *S* waves from station records (Lin et al., 2010; Suwa et al., 2010; Dammeier et al., 2011; Feng, 2011; Hibert et al., 2014). The onset of a landslide seismic signal is generally abrupt. Then the seismic amplitude increases gradually above the ambient noise level to peak ground motion, exhibiting a cigar-shaped envelope. After the peak amplitude, most of the landslide-generated seismic signals have relatively long decay times, on average about 70% of the total signal duration (Norris, 1994; La Rocca et al., 2004; Suriñach et al., 2005; Deparis et al., 2008; Schneider et al., 2010; Dammeier et al., 2011; Allstadt, 2013). In the frequency domain, landslide-induced seismic energy is mainly distributed below 10 Hz, with a triangular signature in a spectrogram, due to an increase over time in high-frequency constituents (Suriñach et al., 2005; Dammeier et al., 2011). The triangular signature in the spectrogram is the distinctive property that readily distinguishes landslide-induced signals from those of earthquakes and other ambient noise.

In this study, a total of nineteen rainstorm events (seventeen typhoon-induced events and two heavy rainfall events) in the years 2005–2014 were selected to examine the seismic records (Table S1). The seismic data during typhoons and heavy rainfall events having cumulated rainfall exceeding 500 mm from 2005 to 2014 were collected, and the seismic signals of local earthquakes, regional earthquakes, and teleseismic earthquakes were excluded based on the earthquake catalogues maintained by the United States Geological Survey and the Central Weather Bureau, Taiwan. After the removal of instrument response, mean, and linear trends, a multitaper method (Percival and Walden, 1993; Burtin et al., 2009) was employed for spectral analysis of the continuous seismic records. A 5-min moving window with 50% overlap of the seismic records provided a good spectrogram in the frequency range of 1–10 Hz. Eventually, landslide-related triangular signatures in the spectrograms were manually identified to find the characteristic signals generated by landslides (Fig. 3a, 3b). To reduce the uncertainty caused by

the artificial method of manual identification, only events with very obvious triangular signatures in the spectrograms (e.g. Fig. S1) were used to examine rainfall statistics in this study.

The detection of the occurrence time of landslide-induced ground motion is a substantial key to this study. In seismology, many methods can be used to detect the appearance of the seismic signals of earthquakes, and one of the most widely used methods is the STA/LTA ratio (Allen, 1978). For landslides, the duration of landslide-induced signals usually ranges from tens to hundreds of seconds (Helmstetter and Garambois, 2005; Chen et al., 2013, 2013a). As compared with the current widely-used rainfall data recorded once per hour, the duration of landslide-induced seismic signals is significantly short. Thus, to avoid misjudgements caused by different signal-detection methods or manual interpretation, this study adopted the time of the maximum amplitude of the envelope of the vertical-component signal recorded in the station closest to the landslide as the occurrence time of the landslide. Considering the transmission speed of seismic waves, a time difference of several seconds to several tens of seconds was negligible with respect to the sampling rate of rainfall records.

To determine which landslides generated ground motion, it was necessary to locate the seismic sources of the signals. However, the arrival times of the *P*- and *S*-waves of landslide-induced ground motion could not be clearly distinguished. As a result, a locating approach proposed by Chen et al. (2013, 2013a) and Chao et al. (2016) was adopted in this study to locate the landslide-induced signals. The locations were estimated with a cross-correlation method that could maximize tremor signal coherence among the seismic signals received by different seismic stations. The criteria of the stations chosen were their geographic distribution and subsequently the seismic sources were located with tremor signal-to-noise ratios. The interpreted signals were treated with an envelope function to process cross-correlations analysed from different station pairs. Centroid location estimates were obtained by cross-correlating all station pairs and performing the Monte Carlo grid search method (Wech and Creager, 2008). While traditional methods seek the source location that minimizes the horizontal time difference between predicted travel time and peak lag time, this method seeks to minimize the vertical correlation distance between the peak correlation value and the predicted correlation value.

Finally, the location results of landslide-induced seismic signals were compared with the exact locations of LSL large landslides interpreted from satellite images (Fig. 3c, 3d). If the locations matched, the occurrence times of the landslides could be obtained, and the time information could be applied to rainfall data analysis.

2.3 Analysis methods of statistically-based rainfall threshold for landslides

In the study, hourly rainfall data were collected from the records of rain gauge stations (Fig. 2a). The major rainfall events analysed in the study were typhoon events. The distribution of precipitation during typhoon events is usually closely related to the typhoon track and the position of the windward slope, also as known as the orographic effect. In addition, the density and distribution of rainfall stations in mountainous areas directly affect the results of rainfall threshold analysis. If the landslide location and the selected rainfall station are located in different watersheds, the rainfall information is unlikely to represent the rainfall conditions for the landslide. In some cases, however, the diameter of the typhoon was so large that the orographic effects could be ignored (Chen and Chen, 2003; Sanchez-Moreno et al., 2014). Therefore, in this study, the selection criteria for a rainfall station were that the rainfall station must be located within the same watershed as the landslide, and at the shortest straight distance from the landslide; moreover, the watershed must be smaller than 100 km² in area to ensure that the records at rain gauge stations were sufficient to represent the rainfall at the landslide locations.

These criteria were established after testing the influences of distance and topographic effects on rainfall distribution (see supporting information S3). In rainfall analysis, the beginning of a rain event is defined as the time point when hourly rainfall

exceeds 4 mm, and the rain event ends when the rainfall intensity remains below 4 mm/h for 6 consecutive hours. The critical rainfall condition for a landslide was calculated from the beginning of a rain event to the occurrence time of the landslide. (Jan and Lee, 2004; Lee, 2006). In this way, average rainfall intensity (mm/h), cumulated rainfall (mm), and rainfall duration (h) for each LSL large landslide could be used as the factors in the rainfall threshold analysis. In addition to the three factors mentioned above, the daily rainfall for the seven days preceding the rainstorm was considered as antecedent rainfall- (*Ra*). The antecedent rainfall (*Ra*) was calculated with a temporal weighting coefficient of 0.7, with the weight decreasing with days before the event. The formula was $Ra = \sum_{i=1}^7 0.7^i \times R_i$, where R_i is the daily rainfall of the i^{th} day before the rainfall event. The sum of antecedent rainfall and principal event rainfall was regarded as the total effective rainfall (*Rt*). This definition of a rain event has been officially adopted in Taiwan (Jan and Lee, 2004). The use of different definitions of a rain event would result in differences in statistical rainfall conditions, but the statistical criteria used in this study ensured the consistency of data processing in the critical rainfall analysis.

Based on different rainfall factors, three common rainfall threshold analysis methods were used in the study. The first method was the *I-D* method, with the power law curve, $I = aD^{-b}$, where *a* is the scaling parameter (the intercept) of the threshold curve and *b* is the slope (the scaling exponent) (Caine, 1980; Wieczorek, 1987; Keefer et al., 1987). In this study, the *I-D* rainfall threshold curve at 5% exceedance probability was estimated by the method proposed by Brunetti et al. (2010). This threshold was expected to leave 5% of the data points below the threshold line. The second method was the rainfall-based warning model proposed by Jan and Lee (2004), which is based on the *Rt* and *I* product values. With the *I-Rt-I* method, rainfall intensity and cumulated rainfall were plotted and used to calculate the cumulative probability of the product value of *I* and *Rt* by the Weibull distribution method (Jan and Lee, 2004). The cumulative probability of 5% of *Rt* and *I* product values was taken as the *I-Rt-I* rainfall threshold. The third method was the *Rt-D* method (Aoki, 1980; Fan et al., 1999). In the *Rt-D* method, the 5% cumulative probability of the product value of *Rt* and *D* by the Weibull distribution method was taken as the *Rt-D* rainfall threshold.

In addition to that of LSL large landslides, the time information of 193 small-scale landslides, such as shallow landslides and debris flows, from the years 2006–2014 was collected from the annual reports of debris flows investigated by the Soil and Water Conservation Bureau (SWCB) of Taiwan, but it was not extracted from seismic records. Most of the 193 small landslides caused disasters and loss of life and property. In some cases, in-situ steel cables or closed-circuit television recorded the time information. This information was applied to the rainfall data analysis and then used to compare the rainfall conditions of the LSL large landslides.

2.4 Critical volume height of water model

Whether a given slope will produce a landslide depends on the balance between the shear strength of the slope material and the downslope component of the gravitational force imposed by the weight of the slope material above a potential slip surface. A critical volume height of water model proposed by Keefer et al. (1987) was used in this study to construct a rainfall threshold. The model was derived from existing slope stability theory with some simplifying assumptions. The shear strength of the material at a point within a slope is expressed as:

$$s = c' + (p - u_w) \tan \phi' \quad \text{Eq. (1)}$$

where *c'* is effective cohesion of material, *p* is total stress perpendicular to the potential sliding surface, *u_w* is pore water pressure, and *φ'* is effective friction angle of slope material. The main cause of a slope disaster failure is the infiltration of rainfall into the slope and accumulation above the impermeable layer, which increases the pore water pressure of the slope

material. As the pore water pressure (u_w) increases, the shear strength (s) decreases, eventually leading to slope failure. A critical value of pore water pressure u_{wc} exists in each slope, assuming an infinite slope composed of a non-cohesive sliding surface ($c=0$). The pore water pressure threshold can be calculated as:

$$5 \quad u_{wc} = Z \cdot \gamma_t [1 - (\tan \theta / \tan \phi')] \quad \text{Eq. (2)}$$

where Z is the vertical depth of the sliding surface, γ_t is the unit weight of the slope material, and θ is the slope angle. Good development of a detachment plane (e.g., sliding surface between sedimentary layers, connected joints, and weathered foliation) has been widely considered as the geological condition under which a large landslide occurs (Agliardi et al., 2001; Tsou et al., 2011). Therefore, in this study, the c' of the detachment plane is simply assumed to be zero to represent the critical situation of slope stability.

As the pore water pressure u_w increases to the pore water pressure threshold u_{wc} , a critical ~~volume~~height of water Q_C is retained above the sliding surface until the initiation of slope failure. The Q_C is calculated as:

$$15 \quad Q_C = (u_{wc} / \gamma_w) \cdot n_{ef} \quad \text{Eq. (3)}$$

where u_{wc} is the critical value of pore water pressure, γ_w is the unit weight of water, and n_{ef} is the effective porosity, which is the residual porosity of the slope material under free gravity drainage. The drainage rate of a saturated zone is represented by the average value I_0 , the unit of which is mm/h. In a heavy rainfall event, the critical quantity of water for causing a slope ~~disaster~~failure is defined as:

$$25 \quad Q_C = (I - I_0) \cdot D \quad \text{Eq. (4)}$$

3. Results

3.1 Topographic features of large-scale landslides

30 The satellite imagery interpretation showed that, from 2005 to 2014, a total of 686 landslide events with areas greater than 0.1 km² occurred in mountainous areas of Taiwan (Fig. 4a). Most of these ~~LSLs~~large landslides had areas of 0.12 to 0.15 km², and their slope angles before the landslides occurred were concentrated between 30° and 40° (Fig. 4b). The number of landslides occurring on slope angles exceeding 40° slightly increased after 2010. ~~This~~Although the increase was quite slight, it was most likely due to the fact that during the extremely heavy rainfall of Typhoon Morakot in 2009, more than ~~2,000~~2000 mm precipitated in four days, causing ~~numerous a large number of~~ landslides ~~on lower~~and exhausting many unstable slopes ~~and reducing the stability of the~~ (Chen et al., 2013b). Consequently, landslides occurred on steeper slopes in the following years. The ~~LSLs~~large landslides were primarily concentrated on slopes with elevations ranging from 500 m to 2000 m (Fig. 4c), but the distributions of the highest and lowest elevations of these ~~LSLs~~large landslides showed that ~~the~~their average vertical displacement ~~of these LSLs~~ was greater than 500 m.

40

The location information of the 193 small-scale landslides investigated by the SWCB was used to obtain the topographic features of the [SSLs-small landslides](#) as well. The distribution of the slope angles of ~~the SSLs~~[these landslides](#) was similar to that of the [LSLs-large landslides](#). However, the distribution of the elevations of the [SSLs-small landslides](#) was quite different from that of the [LSLs-large landslides](#). Unlike ~~those of~~ the [LSLs-large landslides](#), a large portion of the elevations of [SSLs-small landslides](#) was concentrated at about 1000 m. Although the difference in elevation distribution between [LSLs-large](#) and [SSLs-small landslides](#) seems to indicate that the topographic features of [LSLs-large landslides](#) were relatively more widespread than those of [SSLs-small landslides](#), the situation should be attributed to the limited *in-situ* investigations of the SWCB. Currently, the vast majority of landslides still cannot be investigated in the field.

3.2 The critical rainfall conditions for triggering [LSLs-large landslides](#)

Comparison of the location solutions of seismic signals and the landslide distribution map revealed that the matched [LSLs-large landslides](#) had deviations in distance of 0 to 20 ~~kilometers~~[kilometres](#). In addition to distance, the [resultant traces of two horizontal-component signals could be plotted. The direction of the resultant trace of a given landslide-induced seismic record with the slope aspect in the vicinity of the located point could be compared so as to eliminate the irrelevant landslides, those which had slope aspects different from the signal traces.](#) The ground motion traces of the signals ~~were also~~[had to be](#) correlated with the directions of movement of the landslides to reconfirm the matched [LSLs-large landslides](#). In total, 62 [LSLs-large landslides](#) were paired successfully with seismic record locations (Fig. 2a, [Table S2](#)). These 62 [LSLs-large landslides](#) were distributed in watersheds with high cumulated rainfall during heavy rainfall events. In addition, the 62 [LSLs-large landslides](#) were verified by satellite images from multiple years to guarantee that the shapes and positions were highly credible. Subsequently, the occurrence times of these 62 [LSLs-large landslides](#) were obtained from seismic signals.

The time information was used to implement rainfall analysis. About two-thirds (41) of the [LSLs-large landslides](#) occurred when the total effective rainfall exceeded 1000 mm (Fig. 5). The statistical results of rainfall intensities at the times of [LSL-large landslide](#) occurrences showed that more than half of the [LSLs-large landslides](#) occurred when the rainfall intensity was less than 20 mm/h. Only seven of the [LSLs-large landslides](#) occurred when the rainfall duration was less than 24 hours, and the rainfall durations of these seven events all exceeded 10 hours. The results of single rainfall-factor analysis indicated that the effects of rainfall duration and cumulated rainfall were much more remarkable for [LSLs-large landslides](#) than for [SSLs-small landslides](#), and that the rainfall intensity at the time of landslide occurrence was not the main factor influencing [LSLs-large landslides](#). Therefore, the average rainfall intensity was adopted for the following multi-factorial analyses.

4. Rainfall thresholds for [LSLs-large landslides](#)

4.1 Dual rainfall-factor analysis of *I-D*, *I-Rt*, and *Rt-D* thresholds

The single rainfall-factor analysis indicated that there was no significant correlation between landslides and rainfall intensity at the time of [LSL-large landslide](#) occurrences. In the dual rainfall-factor analysis, the *I-D* rainfall threshold was assessed by using the average values of rainfall intensity and rainfall duration. The obtained *I-D* rainfall threshold was $I = 71.9D^{-0.47}$ ($D > 24$ h) (Fig. 6a). ~~We also compared the~~[The](#) rainfall information obtained from [SSLs-small landslides](#) that were reported by the SWCB from 2006 to 2014 [was also compared](#), and the *I-D* rainfall threshold curve for [LSLs-large landslides](#) also fit the lower boundary of the rainfall conditions of [SSLs-small landslides](#). In addition, the distribution of the rainfall durations indicated that the [SSLs-small landslides](#) were distributed evenly from 3 to 70 hours, while the [LSLs-large landslides](#) were mostly distributed above 20 hours. The rainfall intensity, however, could not be used effectively to distinguish these two kinds of slope ~~disasters~~[failures](#). Even under the same rainfall duration, the rainfall intensities of many [SSLs-small landslides](#) were higher than those of [LSLs-large landslides](#). This result sufficiently demonstrated that rainfall intensity could not be used to distinguish

between [SSLs:small landslides](#) and [LSLs:large landslides](#). Therefore, the $I-D$ rainfall threshold may not allow assessment of the landslide scale. It was also found that most of the [LSLs:large landslides](#) with larger areas were concentrated in rainfall durations of more than 50 hours, but the average rainfall intensity was not well-correlated with landslide area. The average rainfall intensity of the [SSLs:small landslides](#) was very high for short durations, but the average duration of the [SSLs:small landslides](#) was much lower than that of [LSLs:large landslides](#). Therefore, continuous high-intensity rainfall incurs a high likelihood of [LSL:large landslide](#) occurrence.

~~We also compared the~~The $I-D$ rainfall thresholds obtained in the study ~~were also compared~~ with those of previous studies that focused on shallow landslides or debris flows. This comparison revealed that the $I-D$ threshold curve for [LSLs:large landslides](#) was much higher than the threshold curves for shallow landslides or debris flows.

Based on the analysis of the relationship between total effective rainfall (Rt) and rainfall duration (D), the product of Rt and D for [LSLs:large landslides](#) with a cumulative probability of 5% was 12,773 mm·h (Fig. 6b), and the rainfall threshold was also much higher than the 5% cumulative probability of [SSLs:small landslides](#) (487 mm·h). Total effective rainfall differed considerably between [LSLs:large](#) and [SSLs:small landslides](#). Most [SSLs:small landslides](#) had a total effective rainfall below 500 mm, ~~while~~and only a few [SSLs](#) occurred when total effective rainfall exceeded 1000 mm. ~~The landslide size groups shifted from small landslides for relatively short duration and low effective rainfall to large landslides for long duration and very large effective rainfall.~~ As a result of the disparity in the $Rt-D$ threshold curves for [LSLs:large](#) and [SSLs:small landslides](#), it was determined that $Rt-D$ analysis could be used effectively to distinguish [SSLs:small landslides](#) from [LSLs:large landslides](#).

The analysis of the relationship between average rainfall intensity (I) and total effective rainfall (Rt) revealed that the product value of both factors for 5% cumulative probability was 5,640 mm²/h (Fig. 6c). The $Rt-I$ threshold curve for [LSLs:large landslides](#) was not much higher than that for [SSLs:small landslides](#) (1,541 mm²/h). Combining the results of the three kinds of dual-factor rainfall threshold analyses revealed that the critical rainfall conditions for [SSLs:small landslides](#) included high average rainfall intensity but relatively low ~~cumulated~~[effective](#) rainfall, while those for [LSLs:large landslides](#) included long rainfall duration and high effective cumulated rainfall. ~~These results corresponded well with the former theoretic expectation (Van Asch et al., 1999; Iverson, 2000).~~

The main mechanism of shallow landslides is heavy rainfall along with rapid infiltration, causing soil saturation and a temporary increase in pore-water pressure. However, prolonged rainfall also plays an important role in slow saturation, which in turn influences the groundwater level and soil moisture, and causes [LSLs:large landslides](#). These facts have been recognized in many studies around the world (Wieczorek and Glade, 2005; Van Asch et al., 1999; Iverson, 2000), but they have been analysed in only a few locations (e.g., a mountainous debris torrent, a shallow landslide event, and an individual rainfall event). Using the regional dataset of landslides and the times information, this study identified the critical rainfall conditions for [LSLs:large](#) and [SSLs:small landslides](#) in Taiwan.

4.2 The critical ~~volume~~[height](#) of water model for ~~forecasting~~ [LSL:large landslides](#)

The ~~critical height of water, Q_c , on a sliding surface for each large landslide was estimated based on its slope gradient, depth (estimated by the equation $Z = 26.14A^{0.4}$; Z: depth in m; A: disturbed area in m²), and the geological material parameters of the study area (Table 1)~~~~were used to calculate the critical volume of water Q_c on the sliding surface, which was found to be 452 mm.~~ The Q_c value was inserted into $Q_c = (I - I_0) \cdot D$ to obtain an I_0 value ~~for each large landslide. For the 62 detected landslides, the cumulative probability of 5% of the Q_c and I_0 values was taken as the critical value. The critical value~~

of I_0 was 1.04 mm/h , the critical Q_c was 430.2, which is more suitable for LSLs large than for SSLs small landslides, and the threshold curve was rewritten as $(I - 1.04) \cdot D = 452430.2$. The application of this threshold curve to average rainfall intensity and rainfall duration showed that almost all the LSLs large landslides could have been forecasted. This application demonstrated a good function as a LSL large landslide forecast model (Fig. 6d). In addition, the threshold curve can be used to distinguish LSLs large landslides and SSLs small landslides clearly. This advantage can prevent or reduce false forecasts. The critical volume/height of water model combines statistical and deterministic approaches for the assessment of critical rainfall. Therefore, the parameters used to calculate Q_c can be adjusted based on regional geologic and topographic environments within a specific area. The Q_c model illustrates the importance of the cumulative volume of water and rainfall duration to LSLs large landslides and takes into account the effects of both infiltration of water and average rainfall intensity. The critical hydrological conditions for LSLs large landslides, a long duration and a high amount of cumulated rainfall, can be determined as well.

In general, physically-based models are easy to understand and have high predictive capabilities (Wilson and Wieczorek, 1995; Salciarini and Tamagni, 2013; Papa et al., 2013; Alvioli et al., 2014). However, they depend on the spatial distribution of various geotechnical data (e.g., cohesion, friction coefficient, and permeability coefficient), which are very difficult to obtain. Statistically-based methods can include conditioning factors that influence slope stability, which are unsuitable for physically-based models. Statistically-based models rely on good landslide inventories and rainfall information. In this study, the Q_c threshold for a large landslide was estimated based on a mixture of physically- and statistically-based methods. Unlike other physically-based I - D thresholds, which are commonly constructed based on artificial rainfall information for shallow landslides (Salciarini et al., 2012; Chen et al., 2013c; Napolitano et al., 2016) (Table S3), the Q_c threshold proposed in this study seemed to be higher and more suitable for large landslides (Fig. 6d).

Although the geological and rainfall conditions in Taiwan and in other countries are not the same, seismic records can be used to obtain the time information of landslide occurrences for rainfall threshold analysis in other countries. For countries with geological and rainfall conditions similar to those of Taiwan (e.g., Japan and the Philippines) (Saito and Oguchi, 2005; Yoshimatsu and Abe, 2006; Evans et al., 2007; Yumul et al., 2011), the results of this study may serve as a useful reference for the development of a forecast model for rainfall-triggered landslides.

5. Discussion

5.1 Influence Application of Typhoon Morakot in 2009 on the rainfall thresholds for LSLs

A previous study has pointed out that because Typhoon Morakot in 2009 was an extreme rainfall event that resulted in 486 large-scale landslides in Taiwan, the surface erosion caused by the typhoon was equivalent to 20 years of accumulated erosion (Chen et al., 2013). Comparison of the data on the rainfall that triggered the LSLs in 2005–2008 with that in 2010–2014 (To verify the usability of the rainfall thresholds proposed in this study, Typhoon Soudelor of 2015 was chosen to demonstrate the early warning performance. Typhoon Soudelor was one of the most powerful storms on record. It generated 1400 mm of rainfall in northeastern Taiwan and almost 1000 mm of rainfall in the southern mountainous area of Taiwan (Wei, 2017; Su et al., 2016). After the seismic signal analytical procedure, the occurrence time, 2015/8/8 18:59:50 (UTC), of a large landslide (named the Putanpunas Landslide) located in southern Taiwan was obtained (Fig. 7). The seismic signal generated by the Putanpunas Landslide was also detected by Chao et al. (2017). The seismic signals generated by this large landslide could be identified from six BATS stations, and the distance error was less than 6 km. The rainfall records of rain gauge station C1V190, which was situated in the same watershed and 14.6 km away from the large landslide, were collected for rainfall analysis. Typhoon Soudelor made landfall in Taiwan on August 7, 2015, and dropped a cumulated rainfall of 546 mm and had a

maximum rainfall intensity of 39 mm/h on August 8 at rain gauge station C1V190 (Fig. 8). The rainfall event began at 22:00 August 7 and last for 26 hours, and the Putanpunas Landslide initiated at the 22nd hour. This landslide occurred when the rainfall intensity was on the decline.

5 Regarding landslide early warning using rainfall thresholds, once the rainfall conditions at a given rainfall station exceed the rainfall thresholds for triggering landslides, the slopes located within the region of the rainfall station will have high potential for failure. Based on the statistically-based $I-D$ threshold for small landslides, a small-landslide warning would have been issued at the sixth hour of the rainfall event (Fig. 8). The long interval of sixteen hours between the warning and the occurrence time of the Putanpunas Landslide could have reduced the reliability of the warning or even caused the warning to be considered
10 a false alarm. Therefore, it is essential to establish different thresholds for landslides of different scales. Using the $I-Rt$ threshold (i.e., $Rt/I= 5,640$), a large-landslide warning would have been issued at the ninth hour of the rainfall event (i.e., thirteen hours before the Putanpunas Landslide occurred). According to the statistically-based $I-D$ threshold for large landslides, a landslide warning would have been issued at the same hour as the $I-Rt$ threshold. In addition, a warning based on the $Rt-D$ threshold (i.e., $Rt-D = 12,773$) would have been issued three hours after the occurrence time of the Putanpunas Landslide. According to
15 the rainfall records and the critical height of water model (i.e. $(I-1.5) \cdot D=430.2$), a landslide warning would have been issued at 16:00 on August 8, three hours before the occurrence time of the Putanpunas Landslide. Compared to the statistically-based $I-D$ threshold, the $I-Rt$ threshold, and the $Rt-D$ threshold, the critical height of water model had a better early-warning performance for the 2015 Putanpunas Landslide.

~~Fig. 7) revealed that the critical rainfall to trigger a LSL after 2010 was slightly less than it was before 2009. The critical value of Rt decreased from 500 mm for the 2005–2008 LSLs to 300 mm for the 2010–2014 LSLs. After Typhoon Morakot, the rainfall threshold for LSLs declined. One possible reason may be that the stability of potential slopes was affected by the excessive rainfall of Typhoon Morakot, which led to a decrease in the rainfall threshold after 2009. The other possible reason may be that some of the SSLs that occurred in 2005–2009 disturbed adjacent slopes, leaving old landslides prone to expansion. However, due to the limited amount of LSL rainfall data, the slight difference in rainfall thresholds is still difficult to view as~~
20 ~~solid evidence in support of the decline in critical rainfall conditions for triggering LSLs.~~
25

5.2 Rainfall thresholds for different rock types

Among the 62 LSLs, 23 LSLs were located in slate, 23 LSLs occurred in schist, 11 LSLs occurred in interbedded sedimentary rocks, and 5 LSLs were located in meta sandstone. From the relationship between total effective rainfall and rainfall duration (Fig. 8), it was found that the critical Rt for schist was the lowest. Schist is a kind of foliated metamorphic rock that is prone
30 to abundant crack propagation along with sudden loss of cohesion. The cracks in the rock mass become both a path for water infiltration and the interface of rock mass separation or collapse. By contrast, the critical value of Rt for metamorphic sandstone is relatively higher. LSLs on meta sandstone occurred only when Rt exceeded 500 mm. In comparison, schist LSLs occurred when Rt was lower than 500 mm. In general, meta sandstone has a compact texture, which leads to high strength.

35 The main path of water infiltration into the ground is usually dense cracks generated in rocks. However, the differences in the critical values of Rt for LSLs in different rock types are limited (Fig. 8). In addition, the rainfall data that could be used for developing rainfall thresholds for LSLs in each rock type are insufficient. Although we would like to discuss the influences of rock types on the occurrence of LSLs, it is obvious from the current data that the differences in critical rainfall between different rock types are not significant.

5.32 Limitation of seismic detection for LSLs large landslides

The number of LSLs large landslides detected from seismic records, 62, comprised only nine percent of the total LSLs large landslides in 2005–2014 in Taiwan. This low percentage indicates that the vast majority of LSLs large landslides were not well identified from seismic records. If this limitation can be surmounted, more time information on LSLs large landslide occurrences can be used to develop rainfall thresholds. The average interstation spacing of the Broadband Array in Taiwan for Seismology is around 30 km. A higher density of seismic stations would improve the detection function. In addition, to determine the limitation of LSLs large landslide detection distance as a function of LSLs large landslide-disturbed area, the most distant seismic station where LSLs large landslide signals were visible was selected. Some previous studies have applied similar approaches to probe the detection limit (Dammeier et al., 2011; Chen et al., 2013, 2013a). The relationship between the maximum distance of detection and the LSLs large landslide-disturbed area shows a limitation of the detection distance due to the LSLs large landslide's magnitude (Fig. 9). In Figure 9, each data point represents the distance between a landslide location and the most distant seismic station detecting it, as well as the landslide-disturbed area. In other words, when the distance between a seismic station and a landslide that has the same given landslide-disturbed area as the data is shorter than the value of the data, seismic signals induced by the landslide can be interpreted from the records of the seismic station. Therefore, a lower boundary of these data can be determined to demarcate an effective detectable region. As a LSLs large landslide's area increases, the maximum distance between the LSLs large landslide location and seismic detection increases. An upper detection limit can be described by

$$\log(\text{distance}) = 0.5069 \times \log(\text{area}) - 1.3443 \quad \text{Eq. (5)}$$

For a given LSLs

The boundary of detection was determined empirically based on the two lowest values of the farthest distance of detection (i.e., 31.0 km and 37.6 km) having disturbed areas of 1.6×10^5 and 1.2×10^5 m². For a given large landslide, if a station is located below the upper detection limit, the seismic signal should be detectable. However, not all the stations located in detectable regions recorded clear LSLs large landslide-induced seismic signals. One of the possible reasons is that the environmental background noise affected the signal to noise ratio of the seismic records during heavy rainfall events. Therefore, the detection limit may also depend on the signal quality at each station.

6. Conclusion

In this study, seismic signals recorded by a broadband seismic network were used to determine the exact times of occurrence of large-scale landslides (LSLs), and the rainfall threshold for LSLs large landslides was assessed statistically based on the time information. Based on the rainfall information of 62 LSLs large landslides that occurred from 2005 to 2014 in Taiwan, the rainfall conditions for triggering LSLs large landslides include total effective rainfall of more than 1000 mm and rainfall duration of more than 24 hours. After the rainfall thresholds were analysed by the *I-D*, *Rt-D*, and *I-Rt-I* methods, the rainfall thresholds based on different dual factors for triggering LSLs large landslides were obtained. Furthermore, a critical water model combining statistical and deterministic approaches was developed to figure out a three-factor threshold for LSLs large landslides. The rainfall information and geologic/topographic parameters finally were applied to obtain the threshold curve, $(I-1.045) \cdot D = 452430.2$, where average rainfall intensity *I* is in mm/h and rainfall duration *D* is in h. This new critical model can be used to improve the forecasting of LSLs large landslides and will not lead to confusion between SSLs small landslides and LSLs large landslides. The influences of extreme rainstorm events and rock types on the rainfall threshold were also investigated. However, the changes in the rainfall thresholds for LSLs large landslides either before or after an extreme event or in different rock types were not notable.

Acknowledgement

The authors gratefully acknowledged the financial support of the Ministry of Science and Technology of Taiwan and the Soil and Water Conservation Bureau, Council of Agriculture, Executive Yuan of Taiwan. The source of all seismic and rainfall information included in this paper was the Institute of Earth Sciences, Academia Sinica of Taiwan, and the Seismology Center, Central Weather Bureau (CWB), Taiwan.

Supplementary Material

The supplementary material contains five sections (S1–S5), including three supplementary figures (Fig. S1–S3) and three supplementary tables (Tables S1–S3). Nineteen selected rainfall events occurring in the years 2005–2014 are listed in Table S1. A sequence of spectrograms of seismic signals induced by the ID 1 landslide of 2005 is displayed in Fig. S1. The validation of the rainfall data used in the study is explained in section S3, which includes Fig. S2 and S3. Detailed information on the 62 detected landslides is shown in Table S2. The equations of three physically-based I-D thresholds reported in previous studies are listed in Table S3.

References

- 10 [Agliardi, F., Crosta, G., and Zanchi, A.: Structural constraints on deep-seated slope deformation kinematics, *Engineering Geology*, 59\(1-2\), 83-102, 2001.](#)
- Allen, R. V.: Automatic earthquake recognition and timing from single traces, *Bulletin of the Seismological Society of America*, 68(5), 1521-1532, 1978.
- [Allstadt, K.: Extracting source characteristics and dynamics of the August 2010 Mount Meager landslide from broadband seismograms, *Journal of Geophysical Research: Earth Surface*, 118\(3\), 1472-1490. doi:10.1002/jgrf.20110, 2013.](#)
- 15 Aoki, S.: Critical rainfall triggering debris-flow disaster, National Research Institute for Earth Science and Disaster Prevention, 38, 22-26, (in Japanese), 1980.
- Brunetti, M. T., Peruccacci, S., Rossi, M., Luciani, S., Valigi, D., and Guzzetti, F.: Rainfall thresholds for the possible occurrence of landslides in Italy, *Natural Hazards and Earth System Sciences*, 10, 447-458, 2010.
- Burtin, A., Bollinger, L., Cattin, R., Vergne, J., and Nabelek, J. L.: Spatiotemporal sequence of Himalayan debris flow from analysis of high-frequency seismic noise, *Journal of Geophysical Research*, 114, F4, 2009.
- 20 Caine, N.: The rainfall intensity: duration control of shallow landslides and debris flows, *Geografiska Annaler. Series A. Physical Geography*, 62, 23-27, 1980.
- Chang, K. and Chiang, S.: An integrated model for predicting rainfall-induced landslides, *Geomorphology*, 105, 366–373, 2009.
- 25 Chao, W. A., Zhao, L., Chen, S. C., Wu, Y. M., Chen, C. H. and Huang, H. H.: Seismology-based early identification of dam-formation landquake events, *Scientific reports*, 6, 19259, 2016.
- [Chao, W. A., Wu, Y. M., Zhao, L., Chen, H., Chen, Y. G., Chang, J. M., & Lin, C. M.: A first near real-time seismology-based landquake monitoring system, *Scientific Reports*, 7, 43510, 2017](#)
- Chen, C. H., Chao, W. A., Wu, Y. M., Zhao, L., Chen, Y. G., Ho, W. Y., Lin, T. L., Kuo, K. H., and Chang, J. M.: A seismological study of landquakes using a real-time broad-band seismic network, *Geophysical Journal International*, 30 194(2), 885-898, ~~2013~~2013a.
- [Chen, C. S., and Chen, Y. L.: The rainfall characteristics of Taiwan, *Monthly Weather Review*, 131\(7\), 1323-1341, 2003.](#)
- Chen, C. W., Saito, H., and Oguchi, T.: Rainfall intensity–duration conditions for mass movements in Taiwan, *Progress in Earth and Planetary Science*, 2, 1-13, 2015.
- 35 Chen, J. C.: Variability of impact of earthquake on debris-flow triggering conditions: case study of Chen-Yu-Lan watershed, Taiwan, *Environmental Earth Sciences*, 64(7), 1787–1794, 2011.
- Chen, Y. C., Chang, K. T., Chiu, Y. J., Lau, S. M., and Lee, H. Y.: Quantifying rainfall controls on catchment-scale landslide erosion in Taiwan, *Earth Surface Processes and Landforms*, 38, 372-382, ~~2013~~2013b.
- [Chen, Y. H., Tan, C. H., Chen, M. M., and Su, T. W.: Estimation of rainfall threshold for regional shallow landslides in a watershed, *Journal of Chinese Soil and Water Conservation*, 44\(1\), 87-96, 2013c.](#)
- 40

- Chigira, M., and Kiho, K.: Deep-seated rockslide-avalanches preceded by mass rock creep of sedimentary rocks in the Akaishi Mountains, central Japan, *Engineering Geology*, 38(3-4), 221-230, 1994.
- Dadson, S. J., Hovius, N., Chen, H., Dade, W. B., Lin, J. C., Hsu, M. L., Lin, C. W., Horng, M. J., Chen, T. C., Milliman, J., and Stark, C. P.: Earthquake triggered increase in sediment delivery from an active mountain belt, *Geology*, 32, 733–736, 2004.
- 5 Dammeier, F., Moore, J. R., Haslinger, F., and Loew, S.: Characterization of alpine rockslides using statistical analysis of seismic signals, *Journal of Geophysical Research*, 116, F04024, 2011.
- [Deparis, J., Jongmans, D., Cotton, F., Baillet, L., Thouvenot, F., and Hantz, D.: Analysis of rock-fall and rock-fall avalanche seismograms in the French Alps, *Bulletin of the Seismological Society of America*, 98\(4\), 1781-1796, doi:10.1785/0120070082, 2008.](#)
- 10 Ekström, G., and Stark, C. P.: Simple scaling of catastrophic landslide dynamics, *Science*, 339, 1416-1419, 2013.
- Evans, S. G., Guthrie, R. H., Roberts, N. J., and Bishop, N. F.: The disastrous 17 February 2006 rockslide-debris avalanche on Leyte Island, Philippines: a catastrophic landslide in tropical mountain terrain, *Natural Hazards and Earth System Science*, 7(1), 89-101, 2007.
- 15 Fan, J. C., Wu, M. F., and Peng, G. T.: The Critical Rainfall Line of Debris Flow Occurrence at Feng-Chiou, *Sino-Geotechnics*, 74, 39-46, 1999.
- [Feng, Z.: The seismic signatures of the 2009 Shiaolin landslide in Taiwan, *Natural Hazards and Earth System Science*, 11\(5\), 1559-1569, doi:10.5194/nhess-11-1559-2011, 2011.](#)
- [Ge, G., Shi, Z., Yang, X., Hao, Y., Guo, H., Kossi, F., Xin, Z., Wei, W., Zhang, Z., Zhang, X., Liu, Y., and Liu, J.: Analysis of Precipitation Extremes in the Qinghai-Tibetan Plateau, China: Spatio-Temporal Characteristics and Topography Effects, *Atmosphere*, 8\(7\), 127, 2017.](#)
- 20 Guzzetti, F., Peruccacci, S., Rossi, M., and Stark, C. P.: Rainfall thresholds for the initiation of landslides in central and southern Europe, *Meteorology and atmospheric physics*, 98(3), 239-267, 2007.
- Guzzetti, F., Peruccacci, S., Rossi, M., and Stark, C. P.: The rainfall intensity–duration control of shallow landslides and debris flows: an update, *Landslides*, 5(1), 3-17, 2008.
- 25 Handin, J., and Hager Jr, R. V.: Experimental deformation of sedimentary rocks under confining pressure: Tests at room temperature on dry samples, *AAPG Bulletin*, 41(1), 1-50, 1957.
- Handin, J., Hager Jr, R. V., Friedman, M., and Feather, J. N.: Experimental deformation of sedimentary rocks under confining pressure: pore pressure tests, *AAPG Bulletin*, 47(5), 717-755, 1963.
- 30 Helmstetter, A., and Garambois, S.: Seismic monitoring of Séchilienne rockslide (French Alps): Analysis of seismic signals and their correlation with rainfalls, *Journal of Geophysical Research: Earth Surface*, 115(F3), 2010.
- [Hibert, C., Ekström, G., and Stark, C. P. : Dynamics of the Bingham Canyon Mine landslides from seismic signal analysis, *Geophysical Research Letters*, 41\(13\), 4535-4541, doi:10.1002/2014gl060592, 2014.](#)
- Ho, C. S.: A synthesis of the geologic evolution of Taiwan, *Tectonophysics*, 125, 1–16, 1986.
- 35 [Iverson, R. M.: Landslide triggering by rain infiltration, *Water resources research*, 36\(7\), 1897-1910, 2000.](#)
- Jan, C. D., and Lee, M. H.: A Debris-Flow Rainfall-Based Warning Model, *Journal of Chinese Soil and Water Conservation*, 35, 275-285, 2004.
- Jan, C. D., and Chen, C. L.: Debris flows caused by Typhoon Herb in Taiwan, In *Debris-Flow Hazards and Related Phenomena*, Springer Berlin Heidelberg, 539-563, 2005.
- 40 Kanamori, H., Given, J. W., and Lay, T.: Analysis of seismic body waves excited by the Mount St. Helens eruption of May 18, 1980, *Journal of Geophysical Research: Solid Earth*, 89, 1856-1866, 1984.
- Keefer, D. K., Wilson, R. C., Mark, R. K., Brabb, E. E., Brown, W. M., Ellen, S. D., and Zatkun, R. S.: Real-time landslide warning during heavy rainfall, *Science*, 238, 921-925, 1987.

- La Rocca, M., Galluzzo, D., Saccorotti, G., Tinti, S., Cimini, G. B., and Del Pezzo, E.: Seismic signals associated with landslides and with a tsunami at Stromboli volcano, Italy, *Bulletin of the Seismological Society of America*, 94(5), 1850-1867. doi:10.1785/012003238, 2004.
- 5 [Larsen, I. J., Montgomery, D. R., and Korup, O.: Landslide erosion controlled by hillslope material, *Nature Geoscience*, 3\(4\), 247, 2010.](#)
- [Lee, M. H.: The Rainfall threshold and analysis of Debris flows, Doctoral dissertation, National Cheng Kung University, Taiwan, ROC \(in Chinese\), 2006.](#)
- [Lin, C. H., Kumagai, H., Ando, M., and Shin, T. C.: Detection of landslides and submarine slumps using broadband seismic networks, *Geophysical Research Letters*, 37\(22\), 2010.](#)
- 10 [Lin, C. W., Liu, S. H., Lee, S. Y., and Liu, C. C.: Impacts of the Chi-Chi earthquake on subsequent rainfall-induced landslides in central Taiwan, *Engineering Geology*, 86\(2\), 87-101, 2006.](#)
- [Lin, C. W., Shieh, C. L., Yuan, B. D., Shieh, Y. C., Liu, S. H. and Lee, S. Y.: Impact of Chi-Chi earthquake on the occurrence of landslides and debris flows: Example from the Chenyulan River watershed, Nantou, Taiwan, *Engineering geology*, 71, 49-61, 2004.](#)
- 15 [Lin, C. W., Tseng, C. M., Tseng, Y. H., Fei, L. Y., Hsieh, Y. C., and Tarolli, P.: Recognition of large scale deep-seated landslides in forest areas of Taiwan using high resolution topography, *Journal of Asian Earth Sciences*, 62, 389-400, 2013a,](#) ~~[Kumagai, H., Ando, M., and Shin, T.: Detection of landslides and submarine slumps using broadband seismic networks, *Geophysical Research Letters*, 37, L22309, 1-5, 2010.](#)~~
- [Lin, M. L., Chen, T. W., Lin, C. W., Ho, D. J., Cheng, K. P., Yin, H. Y., and Chen, M. C.: Detecting large-scale landslides using LiDar data and aerial photos in the Namasha-Liuoguey area, Taiwan, *Remote Sensing*, 6\(1\), 42-63, 2013b.](#)
- 20 [Lin, C., Kumagai, H., Ando, M., and Shin, T.: Detection of landslides and submarine slumps using broadband seismic networks, *Geophysical Research Letters*, 37, L22309, 1-5, 2010.](#)
- [Mishra, A.K.: Effect of rain gauge density over the accuracy of rainfall: a case study over Bangalore, India, *SpringerPlus*, 2, 311, 2013.](#)
- 25 [Napolitano, E., Fusco, F., Baum, R. L., Godt, J. W., and De Vita, P.: Effect of antecedent-hydrological conditions on rainfall triggering of debris flows in ash-fall pyroclastic mantled slopes of Campania \(southern Italy\), *Landslides*, 13, 967-983, 2016.](#)
- [Norris, R. D.: Seismicity of rockfalls and avalanches at 3 Cascade Range volcanos - Implications for seismic detection of hazardous mass movements, *Bulletin of the Seismological Society of America*, 84\(6\), 1925-1939, 1994.](#)
- 30 [Percival, D. B., and Walden, A. T.: Spectral analysis for physical applications: Multitaper and conventional univariate techniques, Cambridge Univ. Press, Cambridge, U. K, 1993.](#)
- [Saito, H., Nakayama, D., and Matsuyama, H.: Relationship between the initiation of a shallow landslide and rainfall intensity—duration thresholds in Japan, *Geomorphology*, 118\(1\), 167-175, 2010.](#)
- 35 [Saito, H., Korup, O., Uchida, T., Hayashi, S., and Oguchi, T.: Rainfall conditions, typhoon frequency, and contemporary landslide erosion in Japan, *Geology*, 42\(11\), 999-1002, 2014.](#)
- [Saito, K., and Oguchi, T.: Slope of alluvial fans in humid regions of Japan, Taiwan and the Philippines, *Geomorphology*, 70\(1\), 147-162, 2005.](#)
- [Salciarini, D., Tamagnini, C., Conversini, P., Rapinesi, S.: Spatially distributed rainfall thresholds for the initiation of shallow landslides, *Nat. Hazards* 61, 229-245, 2012.](#)
- 40 [Sanchez-Moreno, J.F., Mannaerts, C.M., and Jetten, V.: Influence of topography on rainfall variability in Santiago Island, Cape Verde, *International Journal of Climatology*, 34, 1081-1097, 2014.](#)

- Schneider, D., Bartelt, P., Caplan-Auerbach, J., Christen, M., Huggel, C., and McArdell, B. W.: Insights into rock-ice avalanche dynamics by combined analysis of seismic recordings and a numerical avalanche model, *Journal of Geophysical Research*, 115(F4). doi:10.1029/2010jf001734, 2010.
- Shieh, S. L.: User's Guide for Typhoon Forecasting in the Taiwan Area (VIII), Central Weather Bureau, Taipei Aman, 2000.
- 5 [Staley, D., Kean, J. W., Cannon, S. H., Schmidt, K. M., and Laber, J. L.: Objective definition of rainfall intensity–duration thresholds for the initiation of post-fire debris flows in southern California, *Landslides*, Vol. 10\(5\), 547–562, 2013.](#)
- Suriñach, E., Vilajosana, I., Khazaradze, G., Biescas, B., Furdada, G., and Vilaplana, J.: Seismic detection and characterization of landslides and other mass movements, *Natural Hazards and Earth System Science*, 5, 791-798, 2005.
- 10 [Su, Y.F., Chen, W.B., Fu, H. S., Jang, J. H., Chang, C. H.: Application of Rainfall Forecasting to Flood Management --A Case Study of Typhoon Soudelor, *Journal of Disaster Management*, Vol.5, No.2, pp. 1-17 \(in Chinese\), 2016.](#)
- [Suwa, H., Mizuno, T., and Ishii, T.: Prediction of a landslide and analysis of slide motion with reference to the 2004 Ohto slide in Nara, Japan, *Geomorphology*, 124\(3-4\), 157-163, 2010.](#)
- [Tsou, C. Y., Feng, Z. Y., and Chigira, M.: Catastrophic landslide induced by typhoon Morakot, ShiaoLin, Taiwan, *Geomorphology*, 127\(3-4\), 166-178, 2011.](#)
- 15 Tu, J. Y., and Chou, C.: Changes in precipitation frequency and intensity in the vicinity of Taiwan: typhoon versus non-typhoon events, *Environmental Research Letters*, 8, 1-7, 2013.
- Wang, B., and Ho, L.: Rainy season of the Asian-Pacific summer monsoon, *J. Climate*, 15, 386–398, 2002.
- [Wech, A. G., and Creager, K. C.: Automated detection and location of Cascadia tremor, *Geophysical Research Letters*, 35\(20\), 2008.](#)
- 20 West, T. R.: *Geology applied to engineering*. Prentice Hall, Inc., Simon/Schuster Company, Englewood Cliffs, New Jersey, 07632, 541, 1995.
- [Wei, C. C.: Examining El Niño–Southern Oscillation effects in the subtropical zone to forecast long-distance total rainfall from typhoons: A case study in Taiwan, *Journal of Atmospheric and Oceanic Technology*, 34\(10\), 2141-2161, 2017.](#)
- [Wei, F., Gao, K., Cui, P., Hu, K., Xu, J., Zhang, G., and Bi, B.: Method of debris flow prediction based on a numerical weather forecast and its application, *WIT Transactions on Ecology and the Environment*, Vol. 90, 37-46, 2006.](#)
- 25 Wieczorek, G. F.: Effect of rainfall intensity and duration on debris flows in central Santa Cruz Mountains, California, *Reviews in Engineering Geology*, 7, 93-104, 1987.
- Wieczorek, G., and Glade, T.: Climatic Factors Influencing Occurrence of Debris Flows. In: Jakob, M. and Hungr, O., Eds., *Debris-Flow Hazards and Related Phenomena*, Springer, Berlin, 325-362, 2005.
- 30 [Wilson, R. C., and Wieczorek, G. F.: Rainfall thresholds for the initiation of debris flows at La Honda, California, *Environmental & Engineering Geoscience*, 1\(1\), 11-27, 1995.](#)
- Willett, S. D., Fisher, D., Fuller, C., Yeh, E.C., and Lu, C. Y.: Erosion rates and orogenic wedge kinematics in Taiwan inferred from apatite fission track thermochronometry, *Geology*, 31, 945–948, 2003.
- [Xue, X., and Huang, J.: A rainfall and pore pressure thresholds for debris-flow early warning: The Wenjiagou gully case study, *Nat. Hazards Earth Syst. Sci. Discuss.*, doi:10.5194/nhess-2016-149, 2016](#)
- 35 Yoshimatsu, H., and Abe, S.: A review of landslide hazards in Japan and assessment of their susceptibility using an analytical hierarchic process (AHP) method, *Landslides*, 3(2), 149-158, 2006.
- Yu, B., Li, L., Wu, Y., and Chu, S.: A formation model for debris flows in the Chenyulan River Watershed, Taiwan, *Natural Hazards*, Vol. 68(2), 745–762, 2013.
- 40 [Yu, S. B., Chen, H. Y., and Kuo, L. C.: Velocity field of GPS stations in the Taiwan area, *Tectonophysics*, 274, 41–59, 1997.](#)
- Yumul, G. P., Cruz, N. A., Servando, N. T., and Dimalanta, C. B.: Extreme weather events and related disasters in the Philippines, 2004–08: a sign of what climate change will mean, *Disasters*, 35(2), 362-382, 2011.

Table 1. Parameters for calculating critical ~~volume~~height of water $Q_c - Q_c$

vertical depth of sliding surface, Z Parameters	10-m Value	Reference
unit weight of slope material, γ_t	2.65 t/m ²	
average slope angle, θ		32°
effective friction angle, ϕ'	37°	<u>Handin et al. (1957, 1963)</u>
effective porosity, n_{ef}	0.1	<u>West (1995)</u>

*The vertical depth of a sliding surface of 10 m is adopted according to the definition of LSLs. The average slope angle is the average slope degree of the 62 detected LSLs. The ϕ' value is quoted from

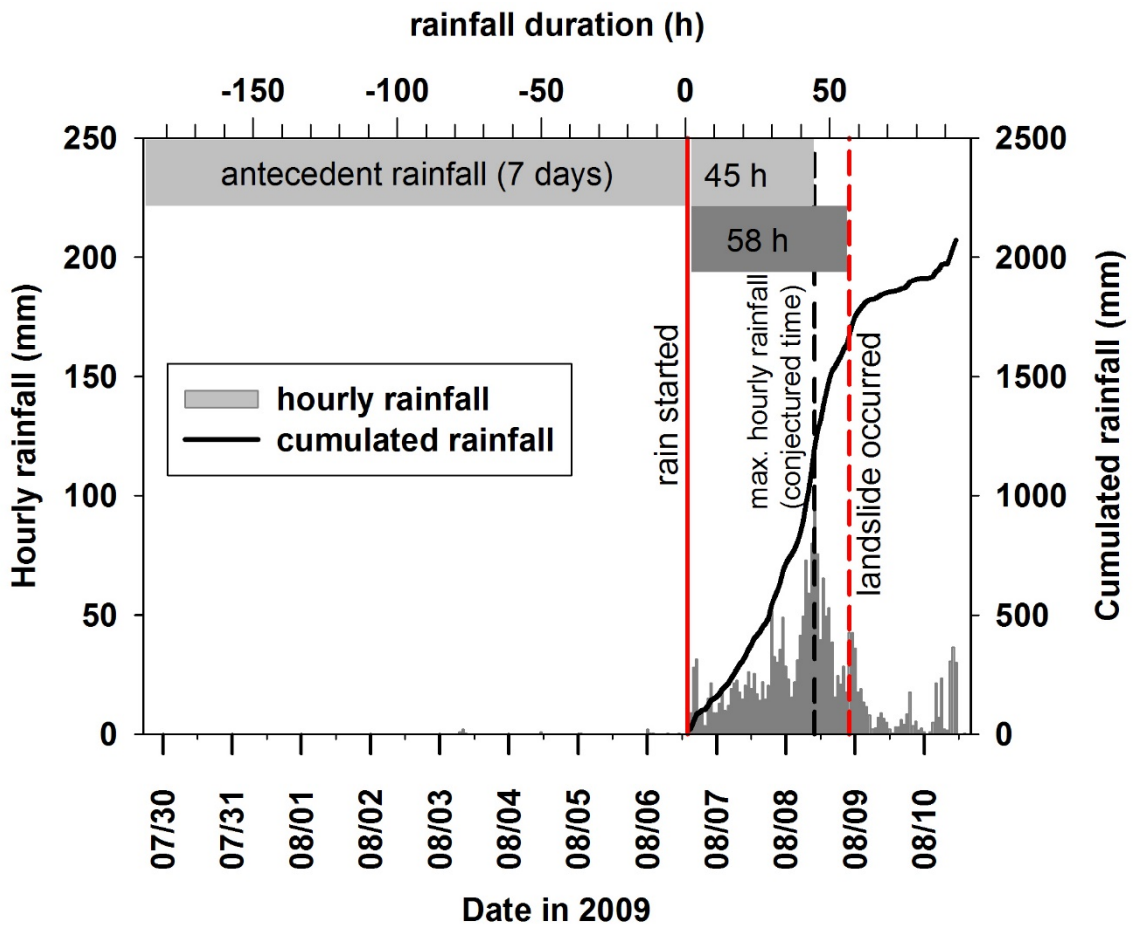


Figure Handin et al. (1957, 1963). The n_{ef} value is a median value according to experimental data reported by West (1995).

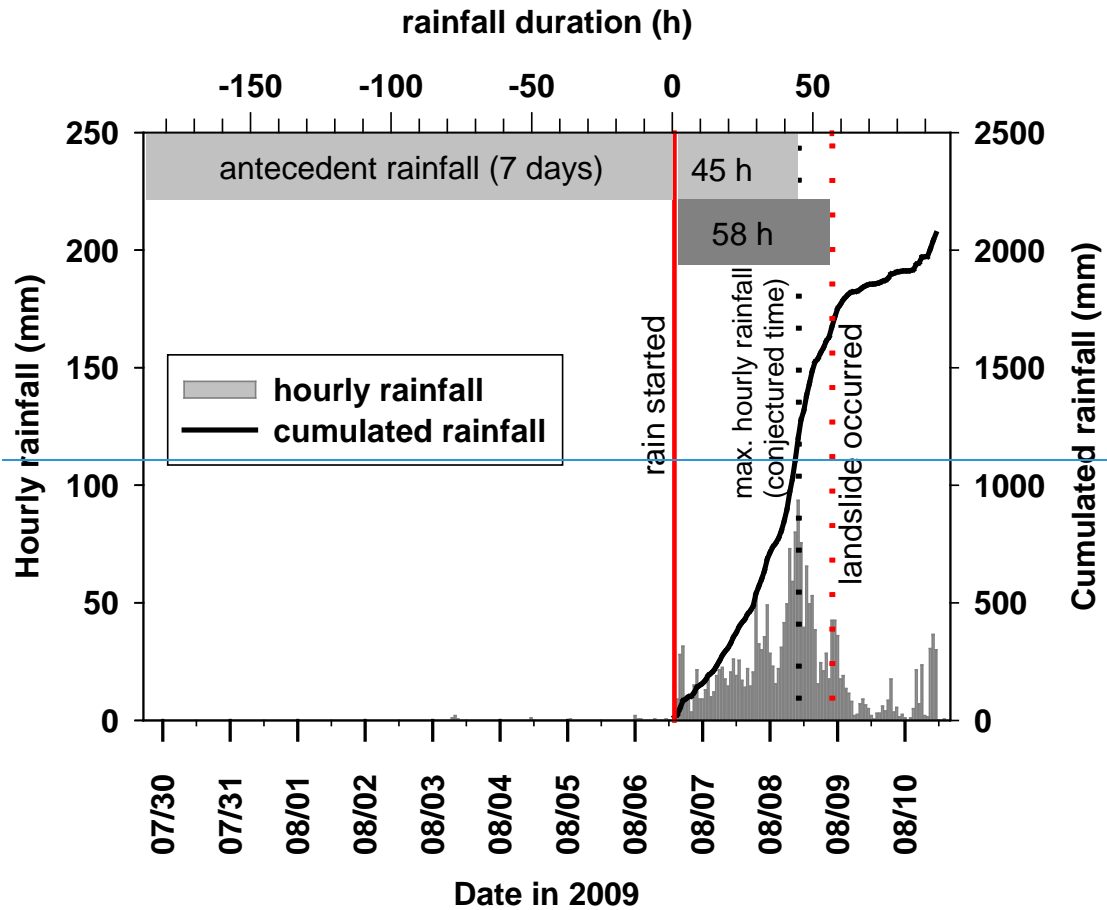


Fig. 1: Time series of hourly rainfall and cumulative rainfall from July 29 to August 10, 2009. Rainfall data were collected from the CWB C0V250 rainfall gauge station, which is 12 km from the Xiaolin landslide. The Xiaolin landslide occurred at UTC 22:16 on August 8, 2009. The rainfall event induced by Typhoon Morakot in 2009 started at UTC 14:00 on August 6, when hourly rainfall exceeded 4 mm. The maximum hourly rainfall was at UTC 10:00 on August 8. In general, if the exact time of landslide occurrence cannot be investigated, the time point with the maximum hourly rainfall will be conjectured as the occurrence time of the landslide. (Chen et al., 2005).

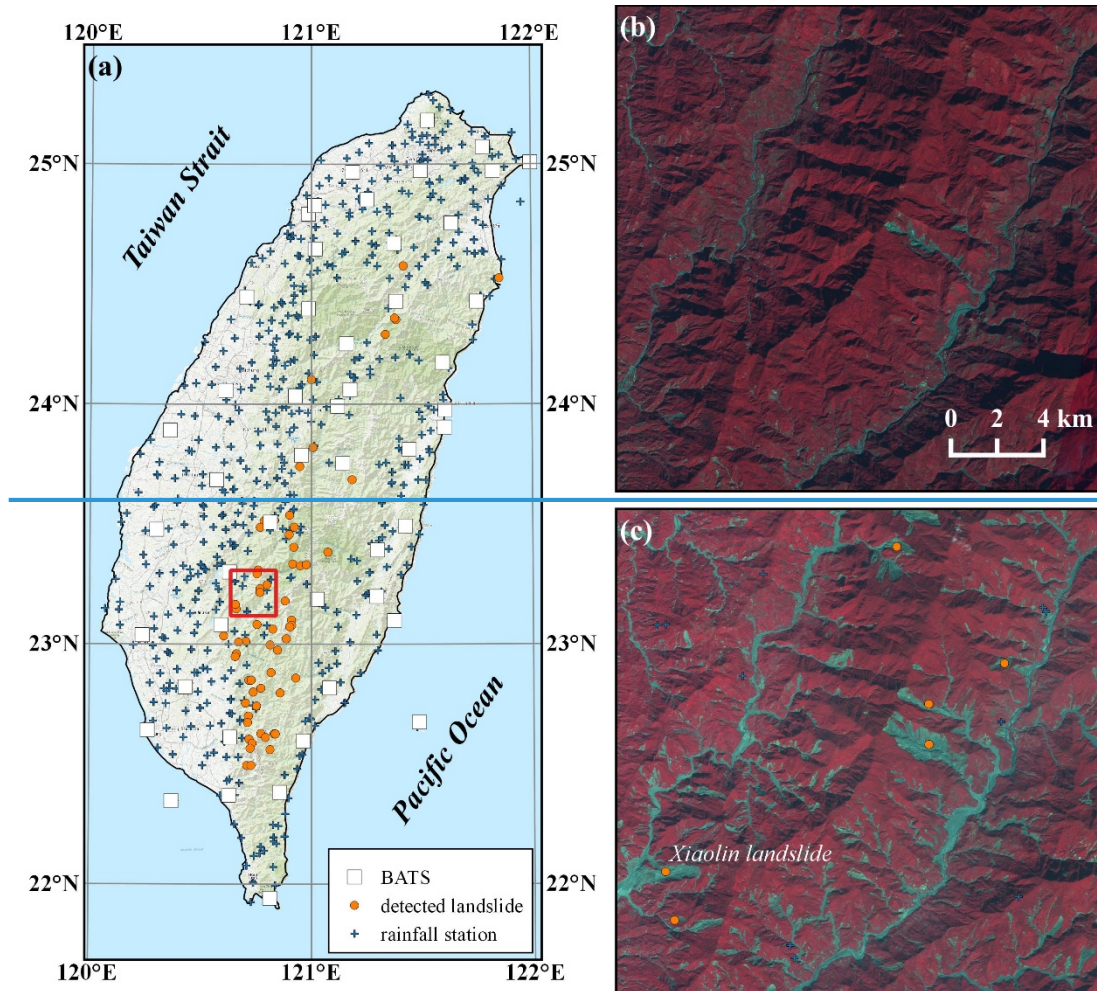


Fig.

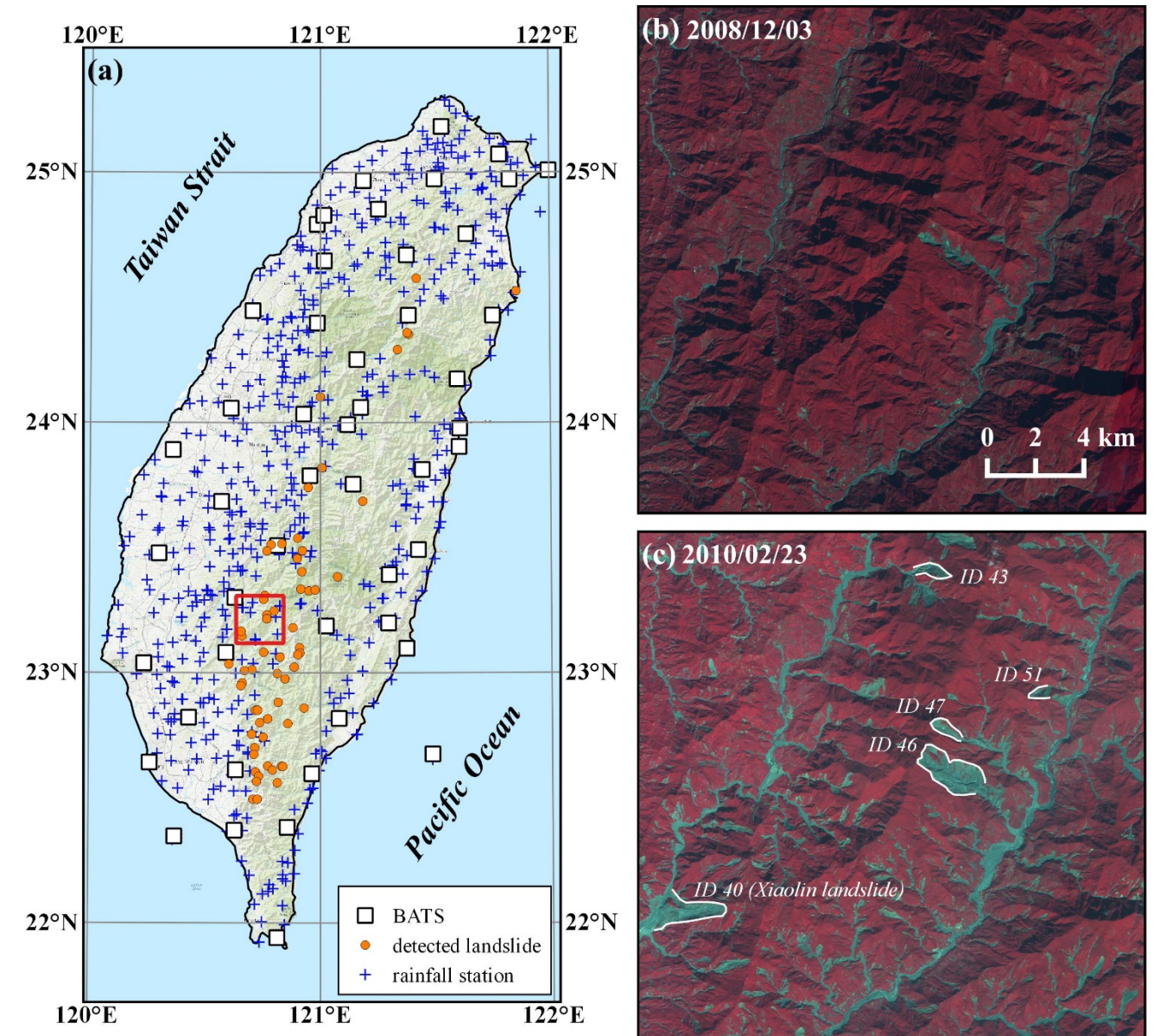
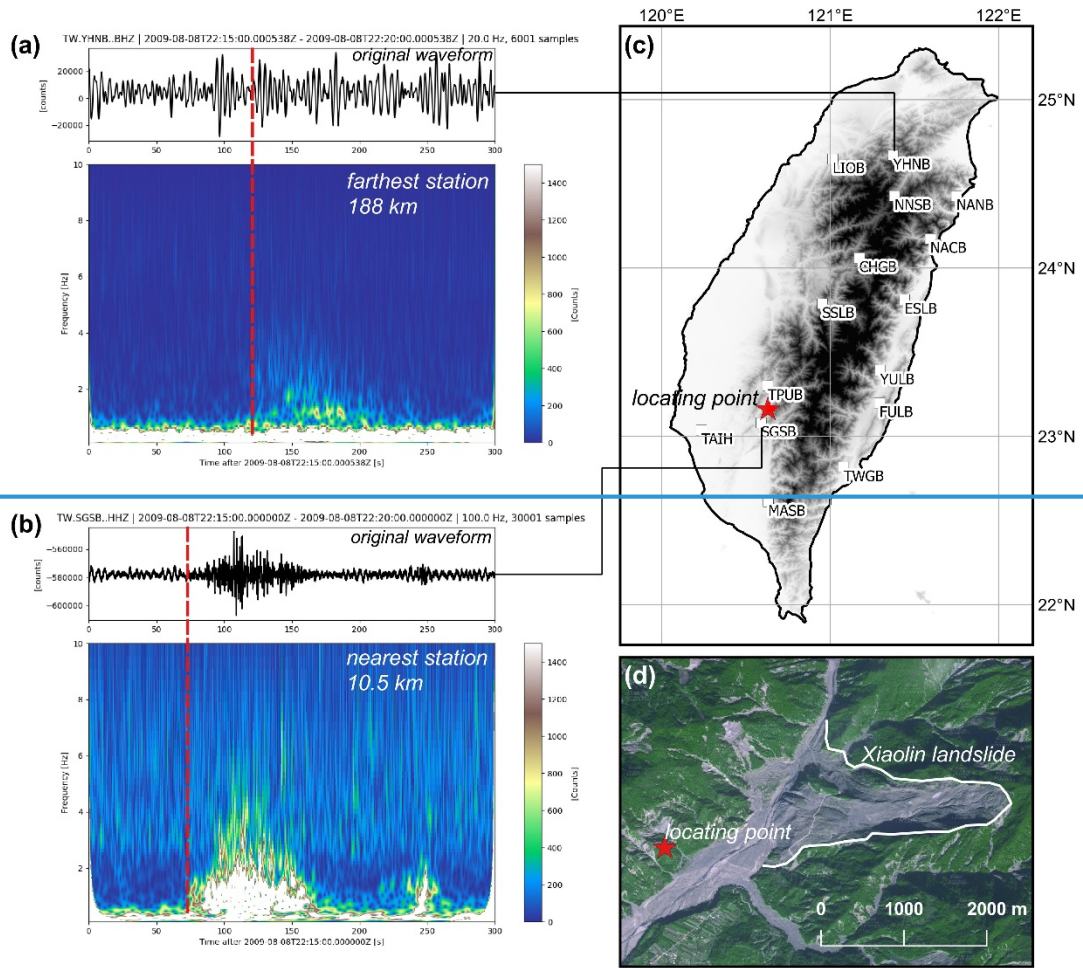


Figure 2-: Comparison of satellite images pre- and post-Typhoon Morakot. (a) Overview map of Taiwan and distribution of rainfall gauge stations. The red frame denotes the areas displayed in (b) and (c). (b) SPOT image taken [between January and June 2009 on December 3, 2008](#). (c) SPOT image taken [between September and December 2009 on February 23, 2010](#).



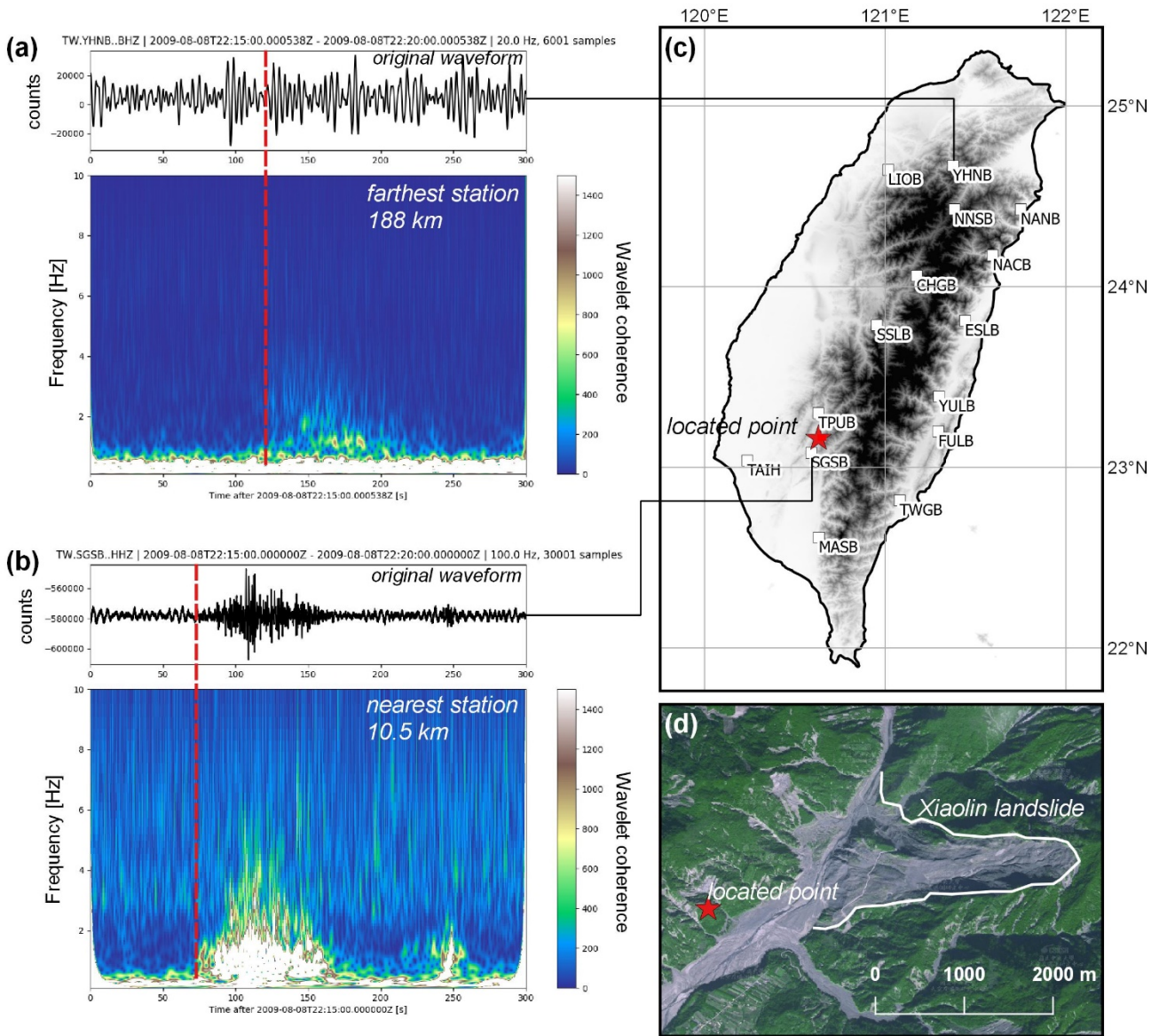
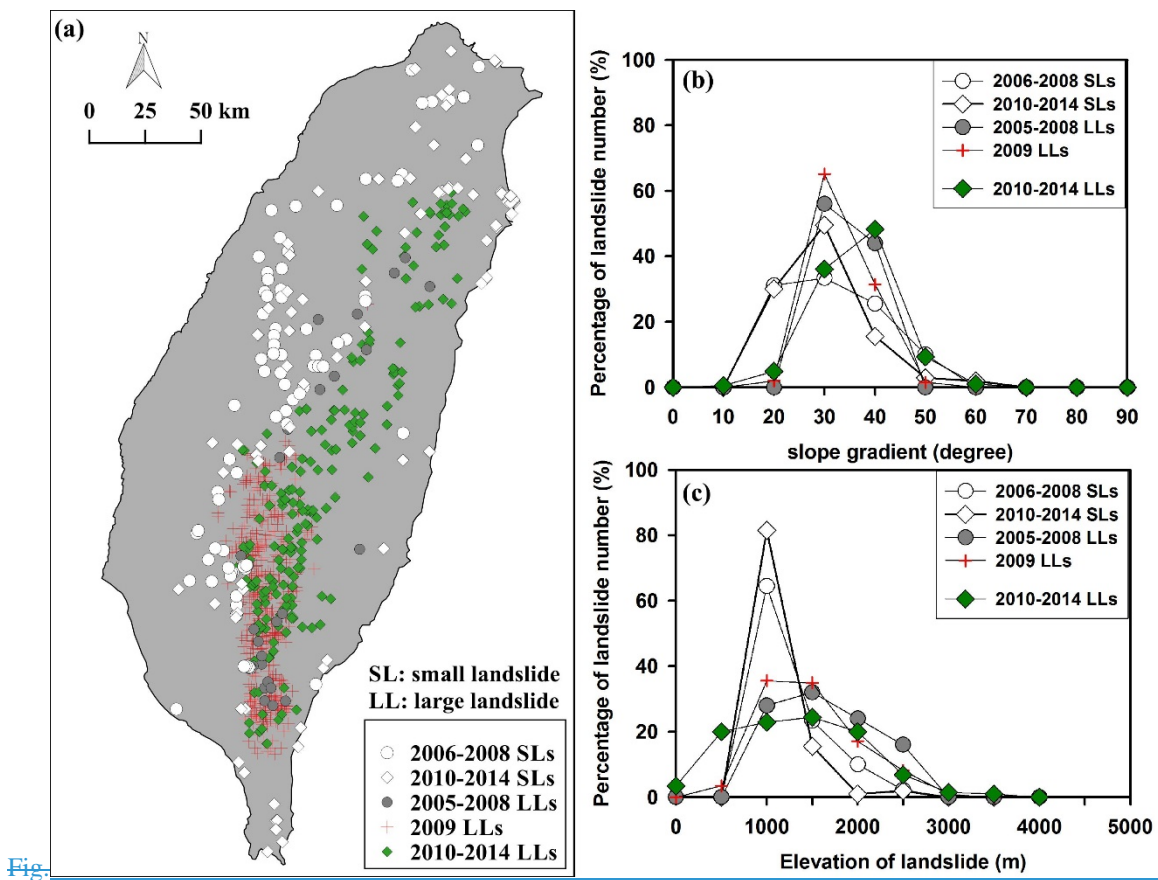
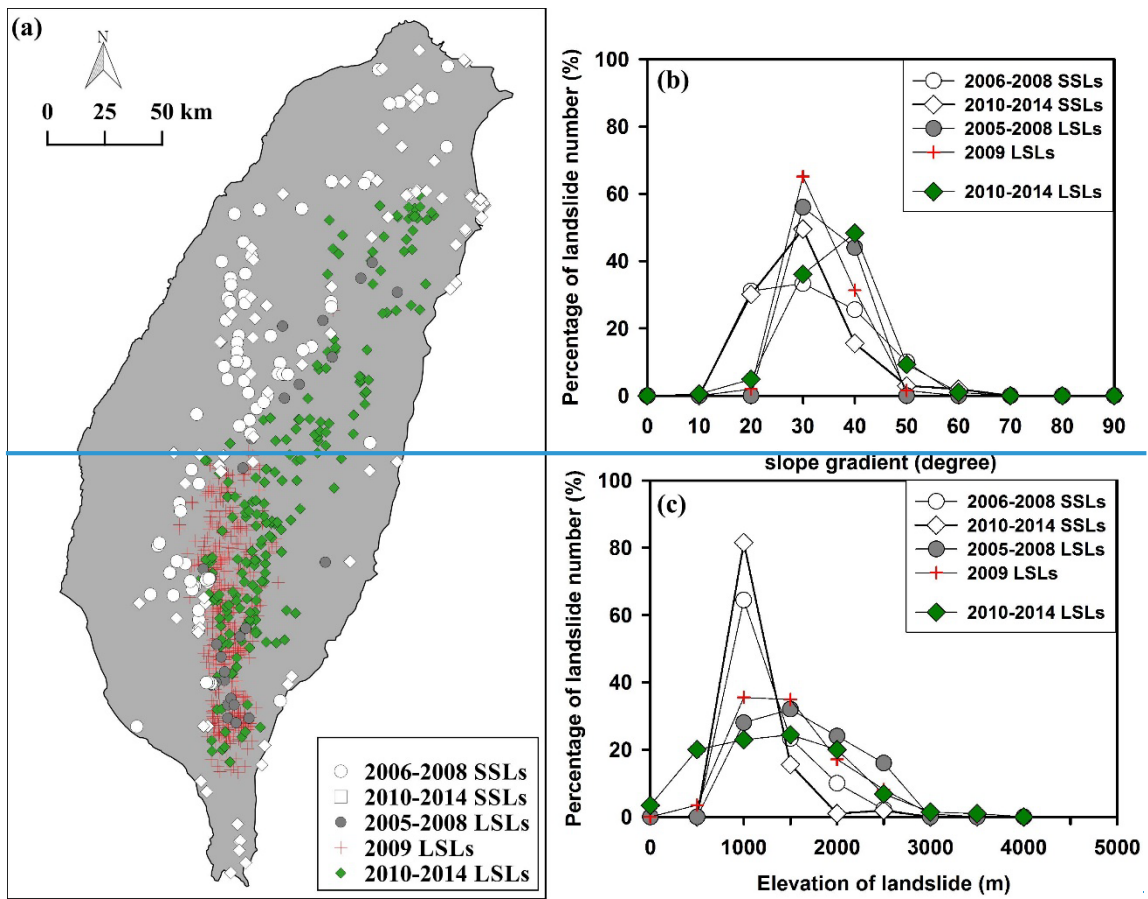
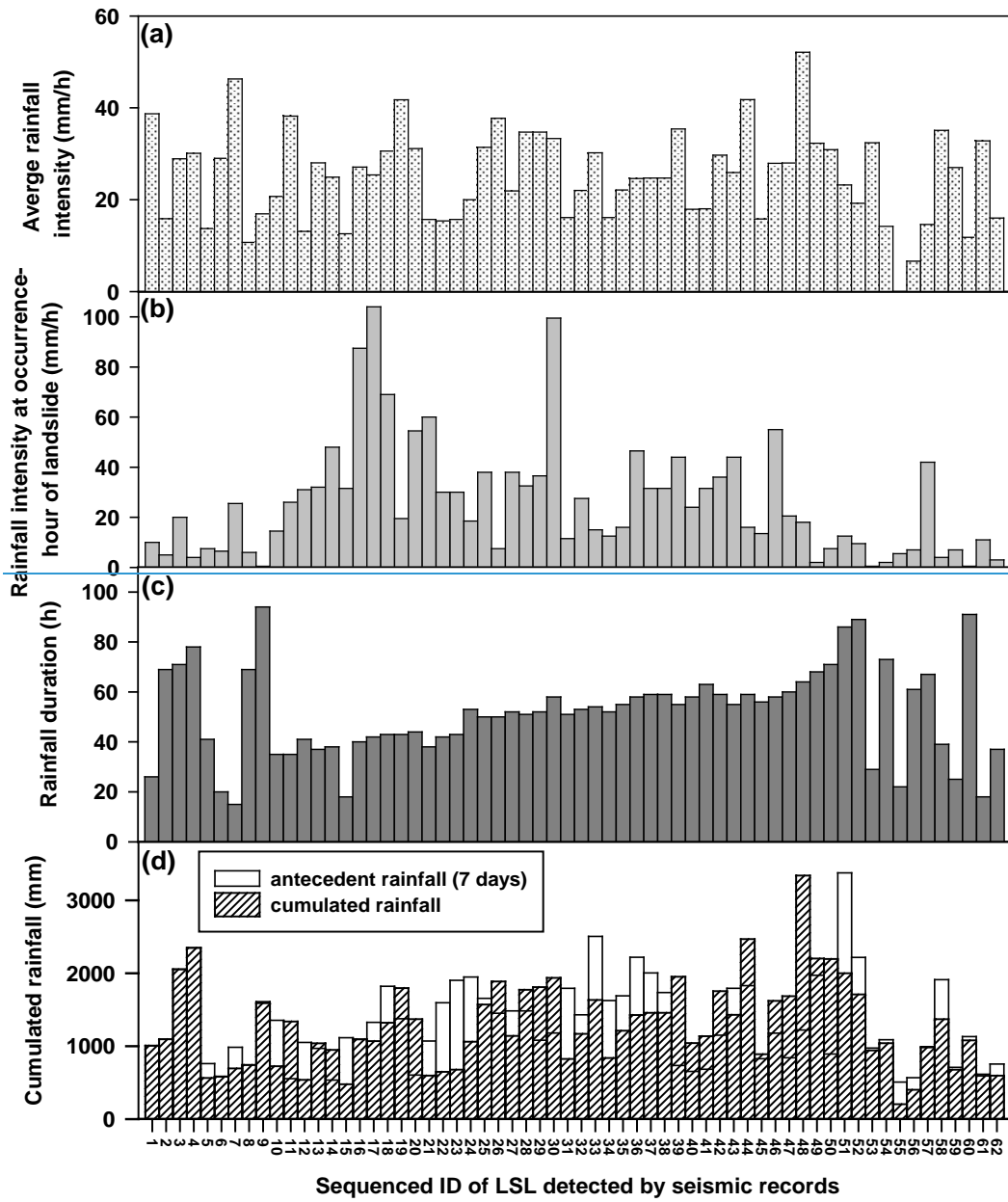


Figure 3: Characteristic triangle signature visible in a spectrogram within a time window starting at UTC 22:15 and ending at UTC 22:20 on August 8, 2009. (a) Original waveform and spectrogram of the vertical component at station YHNB. (b) Original waveform and spectrogram of the vertical component at station MASBSGSB. (c) Distribution of 15 detections of ground motion induced by the Xiaolin landslide and the location result. (d) The located point and the location of the Xiaolin landslide. The location error between the location result and the landslide site is about 1.5 km.



5 **Figure 4:** (a) Distribution map of **LSLs** (large landslides) from 2005 to 2014 and **SSLs** (small landslides) from 2006 to 2014. (b) The numerical distribution of slope gradients of **LSLs** (large) and **SSLs** (small landslides), presented in percentages. (c) The numerical

distribution of elevations of [LSL_{large}](#) and [SSL_{small landslides}](#), presented in percentages.



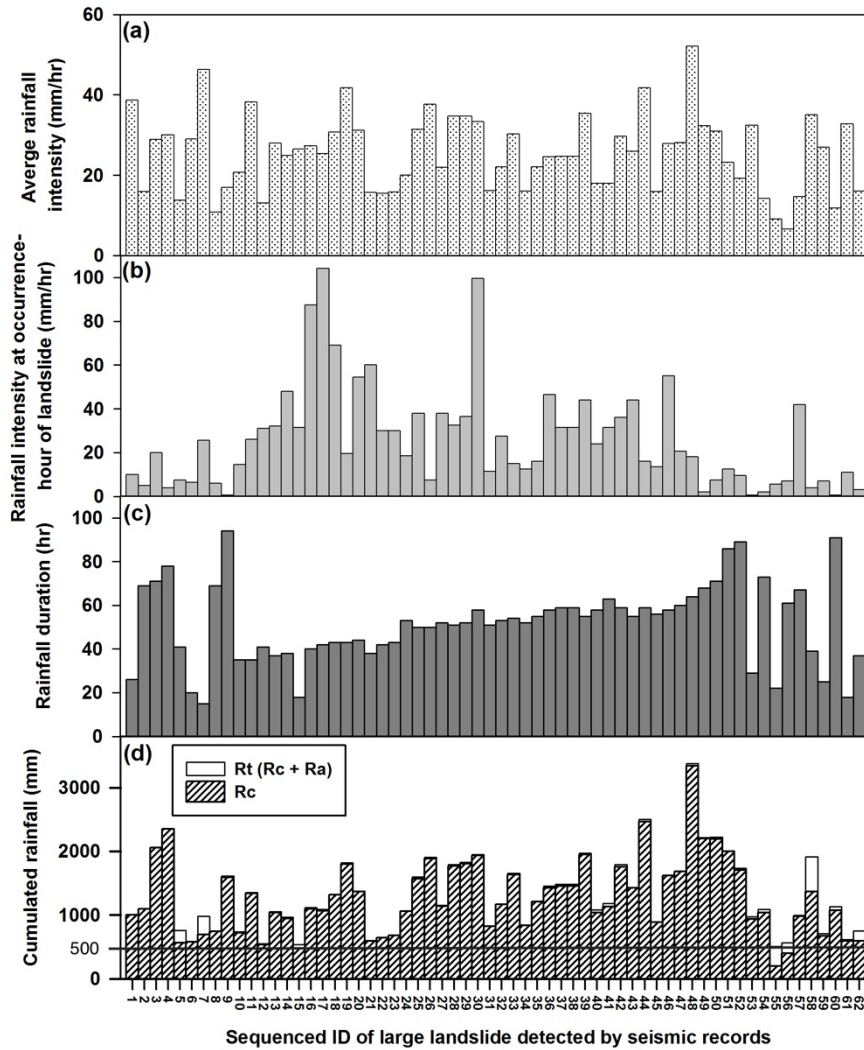
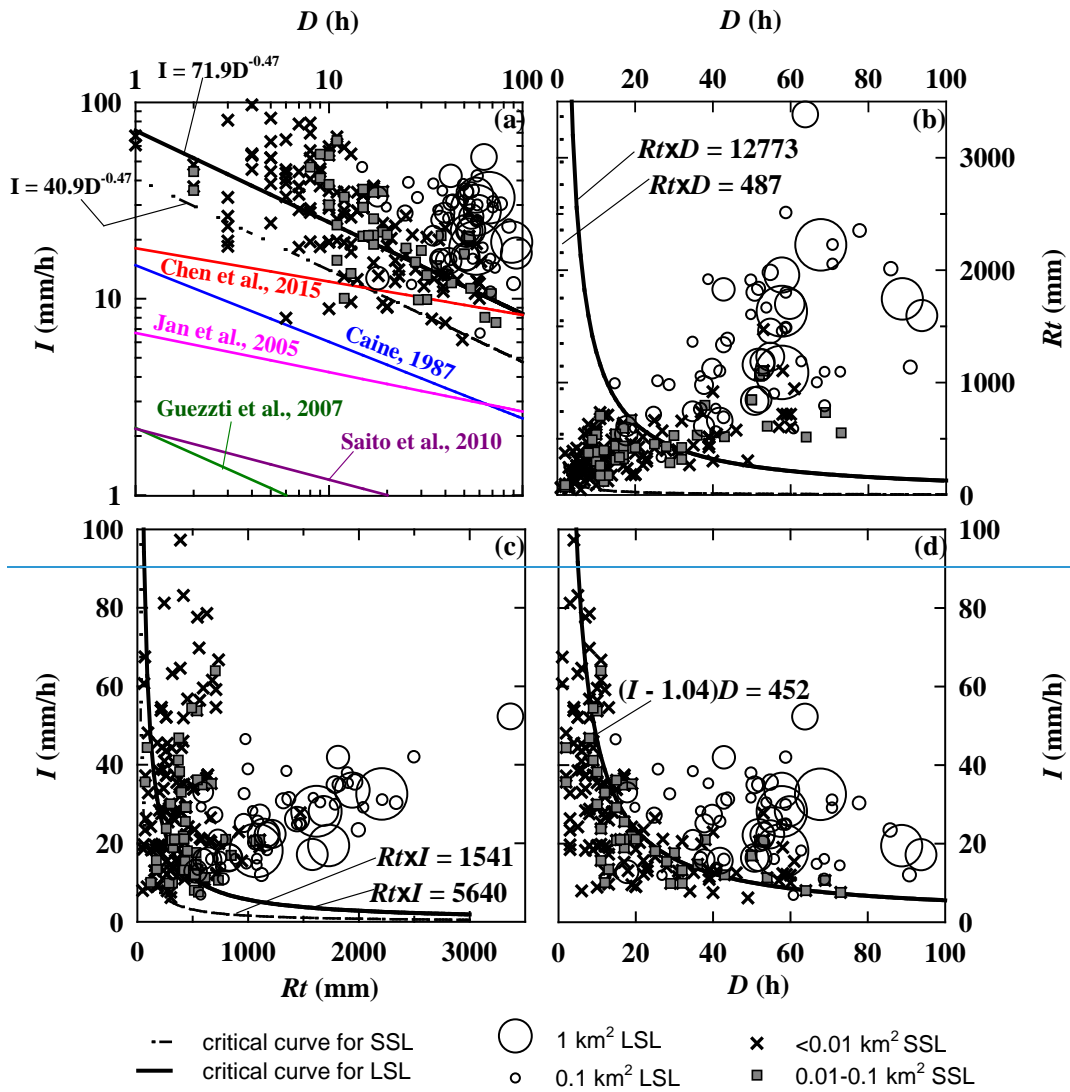


Fig.

Figure 5: Single-factor rainfall analysis. Each LSLlarge landslide is assigned an ID number in the figure. The ID numbers of LSLlarge landslides are displayed in chronological order. ID 1–4 are the LSLlarge landslides occurring in 2005; ID 5 is a LSLlarge landslide occurring in 2006; ID 6–9 are the LSLlarge landslides occurring in 2008; ID 10–52 are the LSLlarge landslides occurring in 2009; ID 53 is a LSLlarge landslide occurring in 2010; ID 54–56 are the LSLlarge landslides occurring in 2011; ID 57–60 are the LSLlarge landslides occurring in 2012; ID 61–62 are the LSLlarge landslides occurring in 2013. No LSLlarge landslides occurring in 2007 or 2014 were successfully paired with the seismic signal results. Most LSLlarge landslides occurred when rainfall duration exceeded 24 hours, cumulative rainfall exceeded 1000 mm, and rainfall intensity was less than 20 mm/h.



5

Fig.

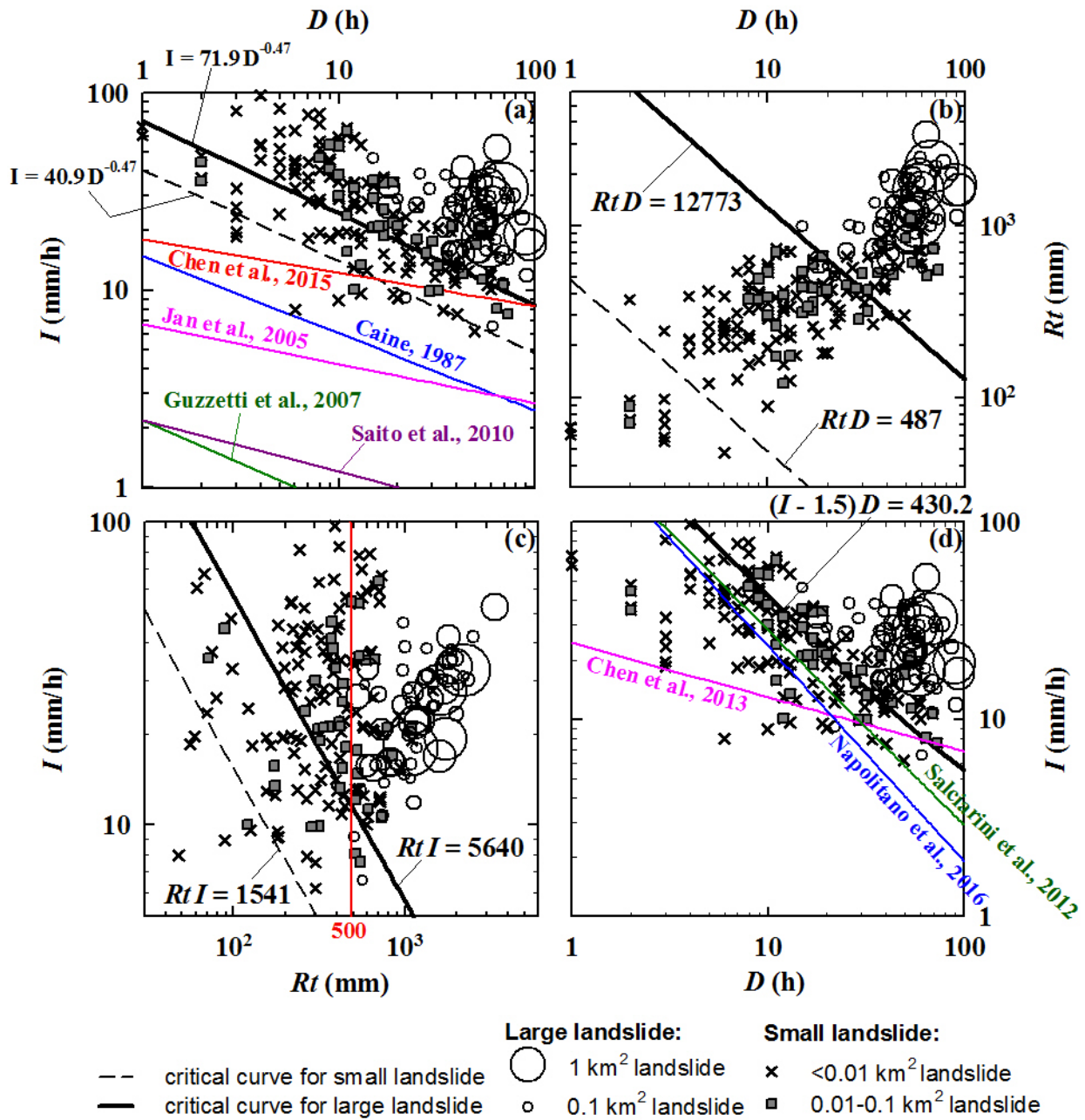


Figure 6: (a) I-D rainfall threshold. (b) Rt-D method rainfall threshold. (c) I-Rt-I method rainfall threshold. (d) Threshold of the critical volume/height of water model, $(I-1.5)D=430.2$.

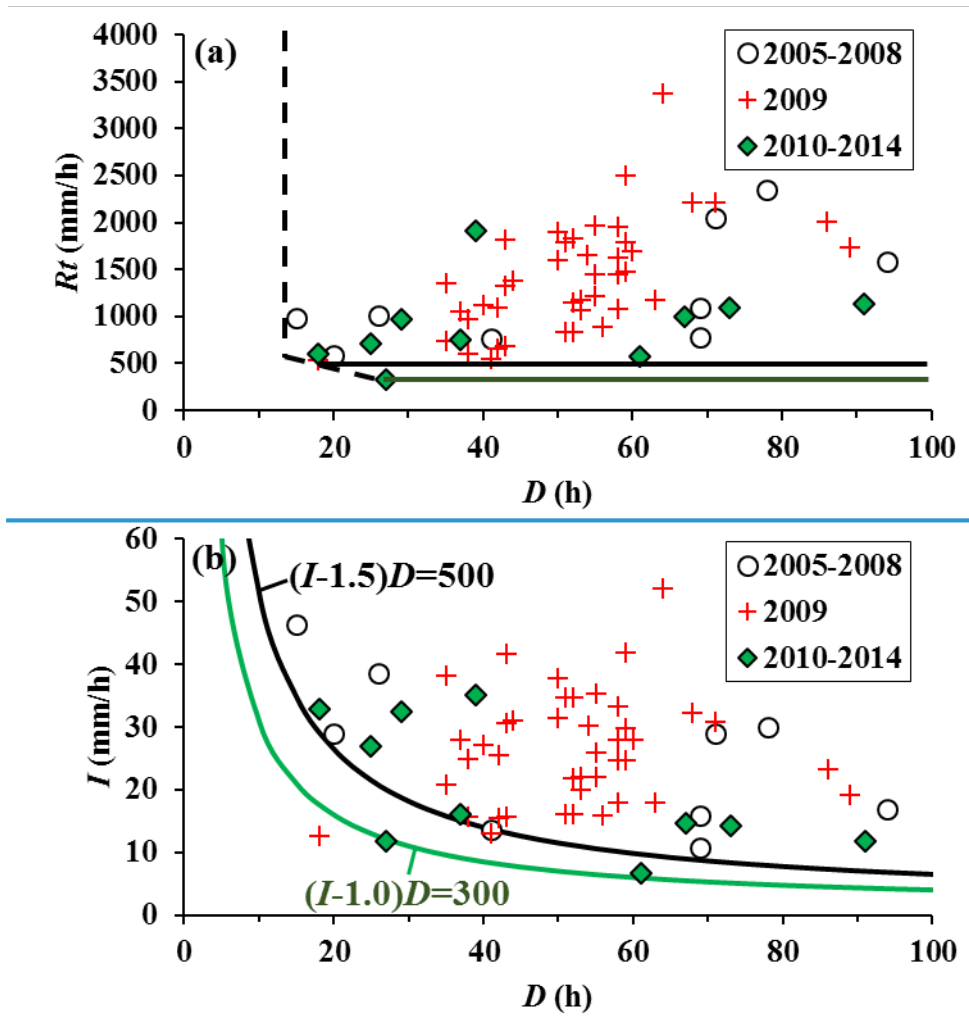


Fig. 7. (a) Variation of rainfall duration and cumulated rainfall. (b) Comparison of critical volume of water thresholds before and after 2009. The black solid line indicates the lower boundary of the 2005–2008 data. The green line indicates the lower boundary of the 2010–2014 data.

5

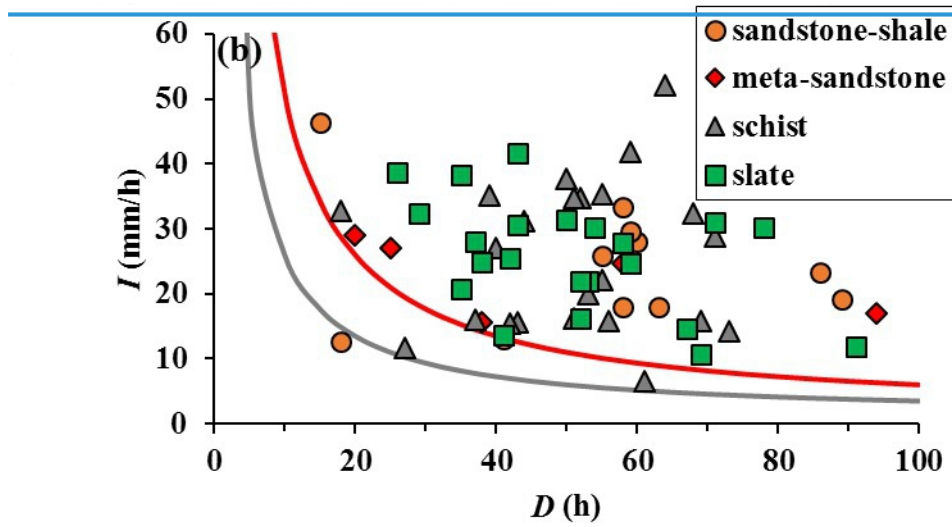
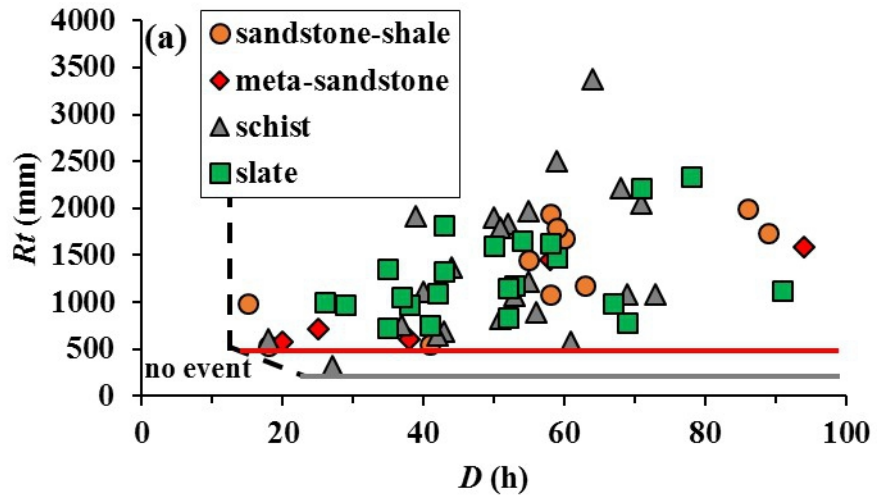


Fig. 8. Comparison of critical thresholds for different rock types. The grey line indicates the lower boundary of LSLs occurring on schist. The red line indicates the lower boundary of LSLs occurring on meta-sandstone.

5

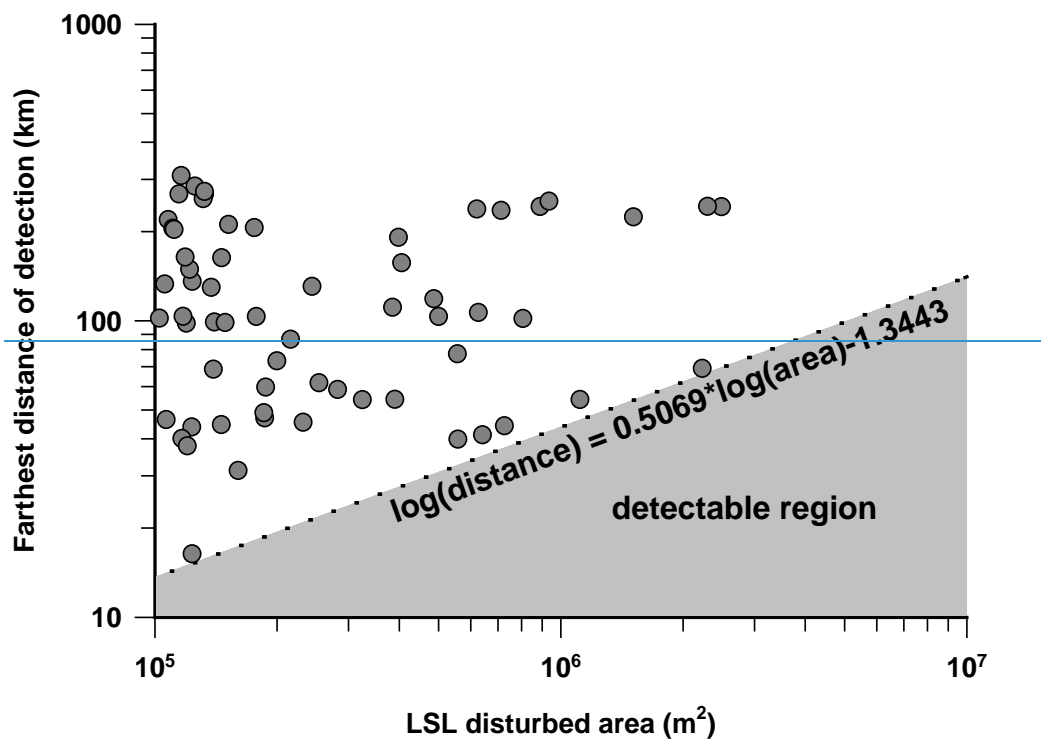


Fig. 9.

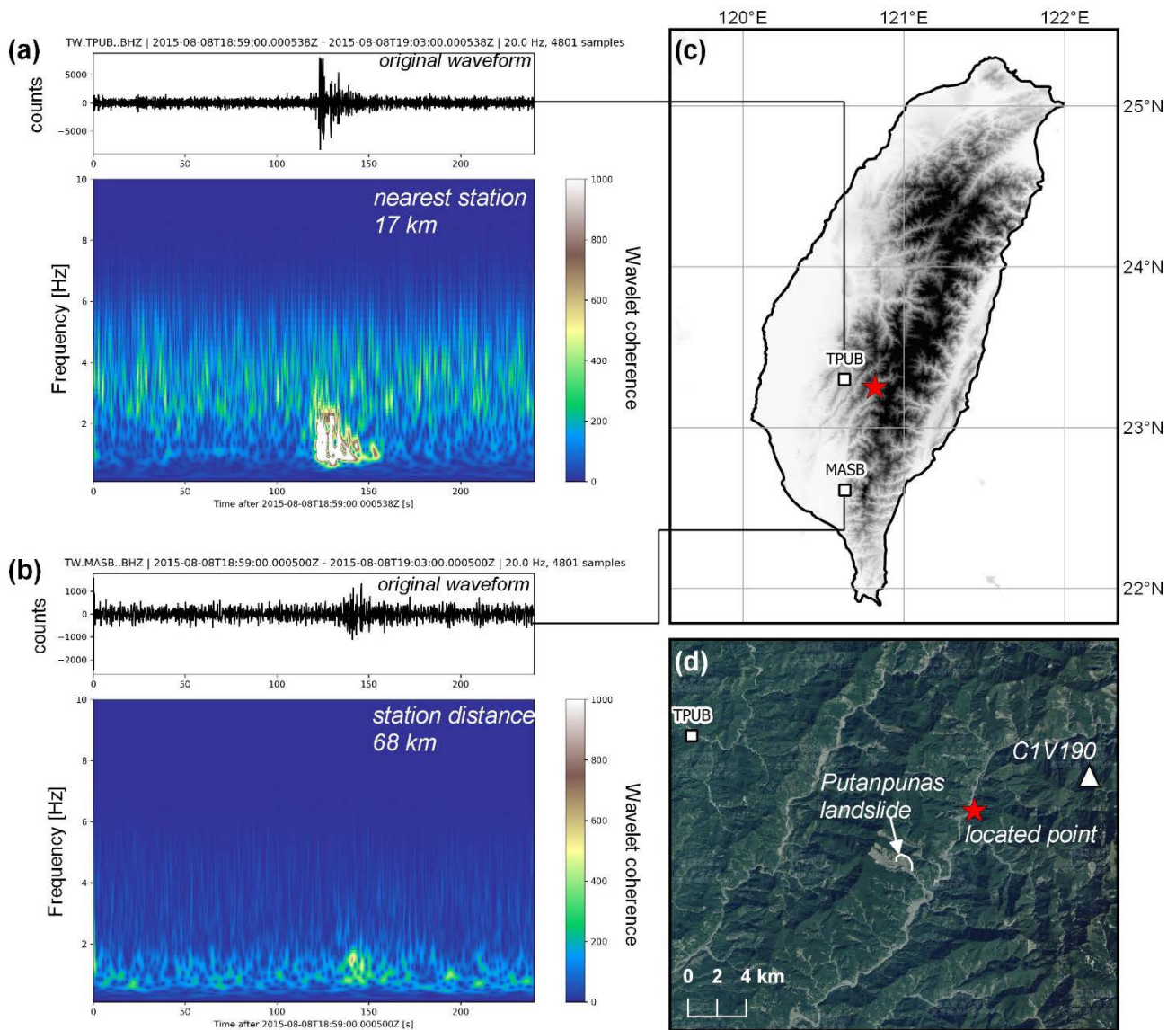


Figure 7: Characteristic triangle signature visible in a spectrogram within a time window starting at UTC 18:59 and ending at UTC 19:03 on August 8, 2015. (a) Original waveform and spectrogram of the vertical component at station TPUB. (b) Original waveform and spectrogram of the vertical component at station MASB. (c) Distribution of located point (red star) and these two seismic stations. (d) The located point and the landslide site. The distance error between the location result and the landslide site is 3.7 km.

5

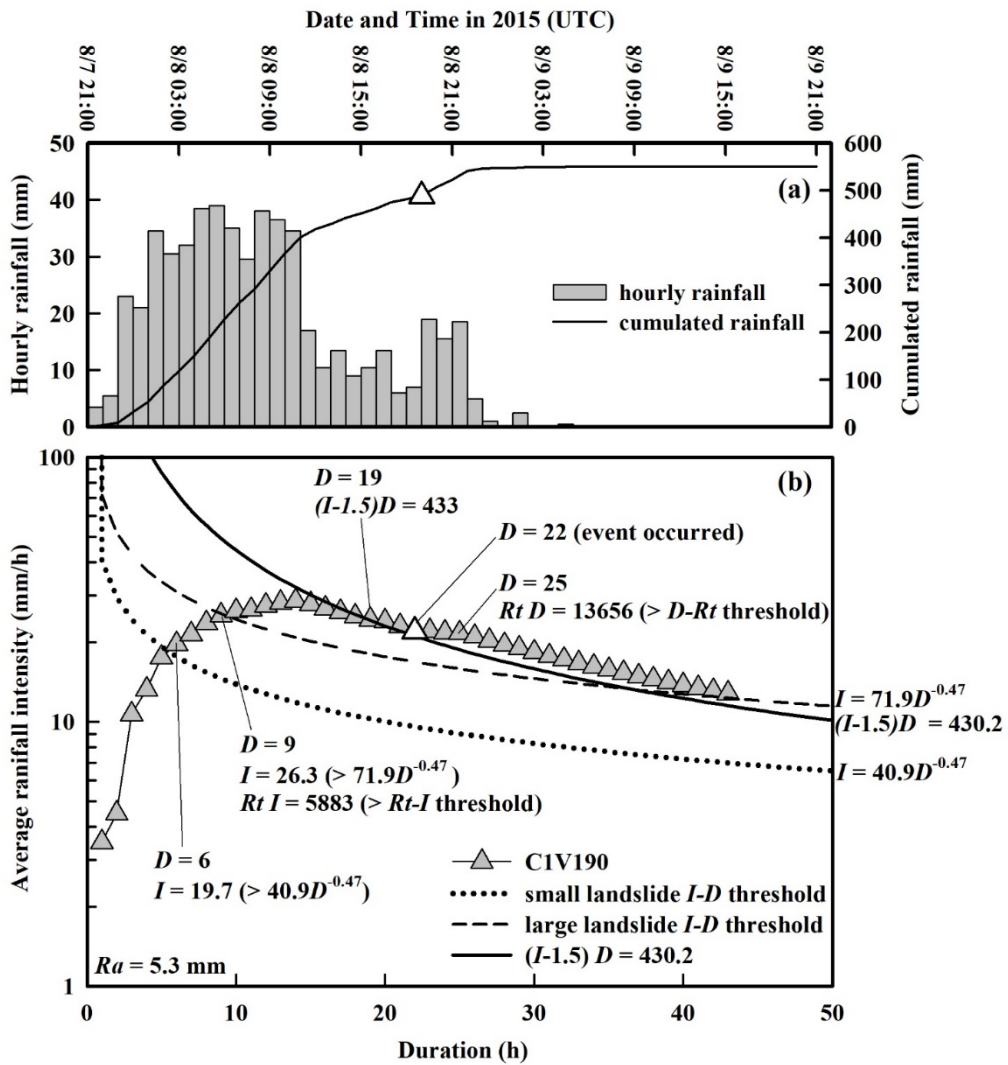


Figure 8: (a) Hourly and cumulated rainfall record by rainfall station CIV190. The white triangle showed the occurrence time of the large landslide occurring in 2015. (b) The rainfall threshold of the critical height of water model issued the early warning three hours before the landslide initiated (white triangle).

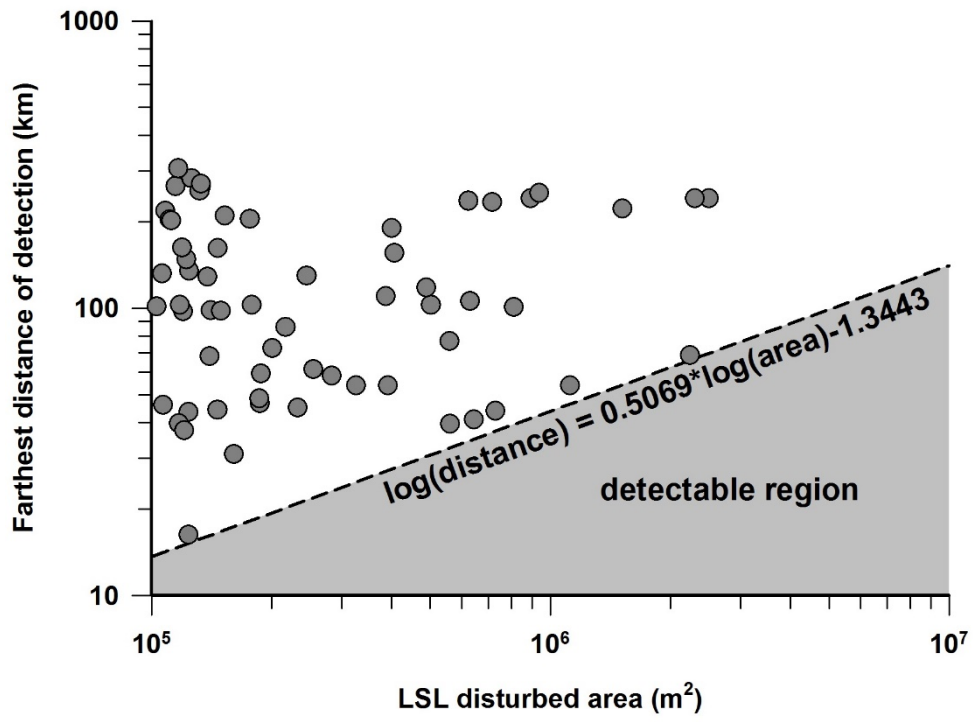


Figure 9: Maximum distance of landslide-signal detection as a function of landslide-disturbed area. For a given [LSL large landslide](#), the seismic signal should be visible at all stations plotted beneath the curve.